THE HONG KONG
POLYTECHNIC UNIVERSITY
香港理工大學
Pao Yue-kong Library
包玉剛圖書館

# Copyright Undertaking

This thesis is protected by copyright, with all rights reserved.

**By reading and using the thesis, the reader understands and agrees to the following terms:**

1. The reader will abide by the rules and legal ordinances governing copyright regarding the use of the thesis.

2. The reader will use the thesis for the purpose of research or private study only and not for distribution or further reproduction or any other purpose.

3. The reader agrees to indemnify and hold the University harmless from and against any loss, damage, cost, liability or expenses arising from copyright infringement or unauthorized usage.

# HELICAL COMPOSITE YARN ACTUATORS WITH A WIDE RANGE OF WORKING TEMPERATURE

## ZHANG ZIHENG

## PhD

**The Hong Kong Polytechnic University**

**2020**

**The Hong Kong Polytechnic University**

**Institute of Textiles and Clothing**

# HELICAL COMPOSITE YARN ACTUATORS WITH A WIDE RANGE OF WORKING TEMPERATURE

**ZHANG ZIHENG**

**A thesis submitted in partial fulfillment of the requirements for the degree of Doctor of Philosophy**

**January 2020**

# CERTIFICATE OF ORIGINALITY

I hereby declare that this thesis is my own work and that, to the best of my knowledge and belief, it reproduces no material previously published or written, nor material that has been accepted for the award of any other degree or diploma, except where due acknowledgement has been made in the text.

_____ (Signed)

_____ZHANG ZIHENG_____ (Name of student)

# Abstract

Actuators have been a significant field in recent years, owning to their wide applications, such as intelligent robots, prosthetic limbs for medical care, deformable textiles and energy harvesting systems. Different types of actuators are reviewed, including traditional electric actuator, flexible fluidic actuator, dielectric elastomer actuator, piezoelectric actuator, electrostrictive elastomer actuator, ionic actuator, shape memory alloy actuator and fiber-based coiled linear actuator. Traditional electric motor actuators and flexible fluidic actuator can achieve high strain, large energy density and high energy conversion efficiency, whereas the structures are so complicate and bulky that difficult to be miniatured. Dielectric elastomer actuators, piezoelectric actuators and electrostrictive elastomer actuators can realize high stress and response frequency, while the actuating voltages are too high to be applied in fields that require high safety. Ionic actuators can realize large strain, whereas the defects of low stress and stability cannot be neglected. Shape memory alloy actuators have significant advantage of high deformability, nevertheless the high hysteresis have restraint their efficient application. The fiber-based coiled linear actuators are particularly advantageous due to their good flexibility and actuating performance, e.g. high stress, strain and specific work, as well as low hysteresis and actuating voltage. However, the structures of most actuators have not been designed and controlled for performance, which were only determined by the selected materials rather than utilizing the proper mutual synergism of elements. Besides, the operation of actuators under low temperature have not been explored sufficiently. It can be seen that the inflexible structure design and limited range of

working temperature have restraint the performance and application of actuators.

Therefore, for widening the performance and application of current actuators, this study aims to fabricate novel helical composite yarn actuators (HCYAs), which possess simple/flexible/portable/programmable structure, low operating voltage, high strain, high stress, high energy density, fast response, long-time cyclability, wide working temperature range, low hysteresis, low cost and simple fabricating process. To achieve effective actuation among a wide range of working temperature for the HCYAs, the candidate materials in composite structure are supposed to possess different thermal expansion coefficient to each other for realizing significant anisotropy of composite yarn, resistance against extremely low and high temperature, as well as safety. Based on above consideration, polyimide (PI) and polydimethylsiloxane (PDMS) were selected from many fiber substrates and polymer matrixes to fabricate the composite yarn, owning to their temperature resistance, ductile physical property under extremely cold condition, different thermal expansion coefficient and biological safety. Influencing factors of fabricating composite yarn have been investigated for optimizing the morphology and property, e.g. concentration of coating solution, volume fraction of PDMS, coating method, filament number etc.

Afterwards, thermally powered PI/PDMS HCYAs based on composite structure were fabricated by super-twisting process, while the morphology of HCYAs have been optimized from filament number, coil level, coil type and heat-setting temperature. The

thermomechanical properties of HCYAs were then characterized in terms of isotonic, isometric and isothermal behaviors. In isotonic tests, the actuations can be influenced by heat-setting temperature, filament number, coiled level, load, volume fraction and low temperature condition. Lower heat-setting temperature and more filament number benefited higher volume fraction of PDMS matrix, thus further better actuating performance. Double-level coil HCYAs and single-double-mixed-level coil HCYAs could realize higher tensile actuation compared with the single-level coil HCYAs, owning to the level change during actuations. The typical 6*100f PI/PDMS HCYA can achieve tensile actuation of 20.7% under 1.2MPa among a wide temperature range from -50 °C to 160 °C, while high linearity ($R^2$=0.99927), competitive specific work (158.9J/kg, 4 times of natural muscle) and low hysteresis (6.7%) can be realized.

In isometric tests, filament number, coil level and extension rate showed most obvious influence on the actuation, i.e. increased load. More filament number enhanced the volume fraction of PDMS and further the effective actuation. Proper extension rate of sample in isometric tests prevented the compact touch of coils and sample fatigue, thus facilitating higher actuation. Typical 20% extended 6*100f PI/PDMS HCYA can realize nearly tripled stress (from 0.38 MPa to 1.07 MPa) among temperature change from 20 °C to 100 °C, with good cyclability and stability in long period time-delay experiments.

An unusual thermally-hardening thermomechanical property was found in the

isothermal tests. The relevant mechanism was analyzed through comparing the physical property of PI/PDMS HCYA, PET/PDMS HCYA and PET monofilament HCYA, as well as their components. The balance between diameter increase of spring-like anisotropic fiber (promote modulus) and molecular mobility increase in axial direction (reduce modulus) were verified as the dominant factor for the unusual behavior. This discovery paves a road to adjust the thermomechanical property of materials by designing composite structure rather than changing the materials themselves.

Finally, electrothermally powered HCYAs were fabricated by adding conductive layer, thus the actuators can be triggered conveniently by joule heating. The process of electroless deposition of copper and silver has been optimized from solution concentration, processing temperature, processing time, filament number, yarn state etc. The resistance, strength and evenness are used to assess the qualities of conductive composite yarns and electrothermally powered HCYAs. Functional devices adopting electrothermally powered HCYAs were fabricated for practical applications, such as electrothermally powered artificial muscle for robotic arm, actuating strips and actuating fabrics for smart compressive stockings. The combination methods and weaving/braiding processes are developed through optimizing relevant parameters, including tension, filament/yarn number, end-fixing method, texture design etc.

# Publications Arising from the Thesis

1. Refereed Journal

Z. Zhang, B. Zhu, R. Yin, Z. Peng, R. H. Baughman and X. Tao, "Programmable and thermally-hardening composite yarn actuator with a wide range of operating temperature," to be submitted.

2. Patent

X. Tao and Z. Zhang, "Multi-level-architecture multifiber composite yarn," Hong Kong, China Patent US2019/0316277A1, Oct. 17, 2019.

# Acknowledgements

During the study for a PhD degree in Institute of Textiles and Clothing of Hong Kong Polytechnic University, I have received large support from many people, to whom I would like to express my sincere gratitude here.

Firstly, greatest thanks go to my supervisor, Prof. Tao Xiaoming, who guide me to a novel scientific field and frontier which enlarge my vision and enrich my ideas enormously. She always gives valuable and feasible advices when I encounter problems or loss my research orientation. Moreover, her patience, passion, prudence and goodness greatly affect me and demonstrate that real scientist should focus on practical problem and be responsible to the society.

I would like to express my gratitude to The Hong Kong Polytechnic University for the financial support of postgraduate scholarship. Research facilities and technical support from all the departments are acknowledged with appreciation.

I would like to thank Dr Yin Rong, Dr Zhu Bo, Dr Yang Bao, Dr Song Jian and Mr Peng Zehua for the support in device modelling, thank Dr Zeng Wei, Dr Gong Jiangliang, Mr Liu Shirui, Li Jun, Wong Cheuk Hang, Ms Huang Xinxin, Ma Linlin, Yang Xingxing and Lin Shuping for the experimental advice and material supply, thank Dr Wang Fei, Mr Liu Jin, Ms Li Ying, Liu Su and Xiong Ying for the administrative and technical support. Appreciation also goes to the undergraduate assistants, Mr Yim Man Kei, Chan Tat Sang, Yagi Makoto, Zhang Minghe, Ms Ning Sen, Li Ka Wing, Ma Yunru and Lin Ni Yun. The completion of this thesis is attributed to all your help.

Special thanks to my family, their care and love have supplied continuous motivation for my scientific exploration.

# Table of Contents

CHAPTER 4    FABRICATION AND CHARACTERIZATION OF HELICAL

# List of Figures

# List of Tables

# Abbreviations

| | |
|---|---|
| CF | Carbon fiber |
| CNT | Carbon nanotube |
| COCe | Cyclic olefin copolymer elastomer |
| CTE | Coefficient of thermal expansion |
| DC | Direct current |
| DEA | Dielectric elastomer actuator |
| DMA | Dynamic Mechanical Analysis |
| EM | Electron microscope |
| FCLA | Fiber-based coiled linear actuator |
| HCYA | Helical composite yarn actuators |
| HDPE | High-density polyethylene |
| IPMC | Ionic polymer-metal composites |
| LCEA | Liquid crystal elastomer actuators |
| LLDPE | Linear-low density polyethylene |
| P(VDF-TrFE) | Poly(vinylidene fluoride-tetrafluoroethylene) |
| PA | Polyamide |
| PDMS | Poly(dimethylsiloxane) |
| PE | Polyethylene |
| PET | Polyethylene terephthalate |

| | |
|---|---|
| PI | Polyimide |
| PLA | Polylactic acid |
| PMN | $Pb[Mg_{1/3}Nb_{2/3}]O_3$ |
| PVDF | Poly(vinylidienefluoride) |
| PZN | $Pb[Zn_{1/3}Nb_{2/3}]O_3$ |
| PZT | $Pb[Zr_xTi_{1-x}]O_3$ |
| SEM | Scanning Electron Microscope |
| SMA | Shape memory alloy |
| TMA | Thermomechanical Analysis |

# CHAPTER 1
# INTRODUCTION

## 1.1 Background

Actuators are a type of materials and devices which can contract, expand, or rotate reversibly under external stimulus (e.g. voltage, current, temperature, pressure, light, chemical etc.)[1, 2]. This research field becomes more and more significant in recent years, owning to their wide applications, such as intelligent robots, prosthetic limbs for medical care, deformable textiles and energy harvesting systems. Based on different principle, actuators can be divided as traditional electric actuator, flexible fluidic actuator, dielectric elastomer actuator, piezoelectric actuator, ferroelectric actuator, ionic actuator, shape memory alloy actuator, coiled polymer actuator etc. Ideal actuator should possess simple/flexible/portable structure, low operating voltage, high strain, high stress, high energy density, fast response, long-time cyclability, a wide range of working temperature etc.

Traditional actuators, including electric motor actuators[3], pneumatic actuators[4], hydraulic actuators[5], can achieve high strain, large energy density and high energy conversion efficiency, whereas the structures are so complicate and bulky that difficult to be miniatured. Electric actuators, e.g. dielectric elastomer actuators[6, 7], piezoelectric actuators[8], electrostrictive elastomer actuators[6, 7], liquid crystal elastomer actuators [9], can realize high stress, specific work and response frequency,

while the actuating voltages are too high to be applied in wearable devices and other fields that require high safety. Ionic actuators, including gel actuators[10], polymer–metal composites actuators[11-13], conducting polymer actuators[6, 7, 14], can realize large strain, whereas the defects of low stress and stability cannot be neglected. Shape memory alloy actuators have significant advantage of high deformability, nevertheless the high hysteresis have restraint their efficient application[6, 9]. Detailed properties and performances of different actuators are reviewed in Chapter 2.

The fiber-based coiled linear actuators (FCLAs) are particularly advantageous due to their good flexibility and actuating performance. The earlier coiled actuators are commonly based on electromagnetic effect. In 1997, a muscle cell was invented, including many paralleled coiled electromagnetic actuators and an elastomeric substrate. The principle of this type of actuator lies on the contraction resulted from electromagnetic attraction between the wire coils. When there was a current going through the wire coil of the electromagnetic actuator, the produced magnetic field made the coils attract the adjacent ones, then the squeezed elastomeric substrate, as well as the length of actuator, could recover to the initial state after the current was off[15]. Later, another actuator was created utilizing magnetic rheopectic (MR) liquid, in which the magnetic polarization of MR liquid and resultant deformation are the core mechanism, leading to a high contraction force and lighter weight[16]. Nevertheless, some disadvantages exist in this type of electromagnetic driving actuator, such as complicate structure and difficulty of deployment due to high electric fields.

In recent years, thermally powered actuators have aroused more attentions. In 2012, actuators made by guest-infiltrated carbon nanotube (CNT) yarn (guests include paraffin wax, polyethylene glycol etc.) were reported and could be actuated by thermal, electrothermal, photothermal and chemical power[17, 18]. The actuator structures were relatively simpler than that of the electromagnetic actuators, meanwhile obtained higher power and more excellent cyclability. The varieties of driving powers facilitate the versatile applications in different conditions, and they were multifunctional when combined with numerous power sources and functional materials. However, the volume fraction of yarn/matrix was not effectively controlled, and the range of working temperature (30 °C～83 °C) was rather limited. Both shortcomings have impeded the maximization of the actuating performance of the actuator.　Moreover, the high cost of CNT yarn also impedes its wide application in large-scale industries.

For avoiding the shortcomings, low-cost thermally and electrothermally powered muscles were presented in 2014[19, 20], with nylon fishing line and sewing thread as the raw materials. The cost was largely reduced compared with that of CNT yarns while the tensile actuation and specific work were also competitive compared with the human muscle. However, the actuating temperatures have to be very high for obtaining large stroke.

In 2016, a new coiled fiber actuator made by linear-low density polyethylene (LLDPE)

were proposed[21], which could be driven in low temperature (< 60 °C) to reach strain of 10%. This novel application of traditional material paved a new road for low-temperature actuators, meanwhile it promoted the transferring of actuating materials from industrial application to domestic and wearable use. Nevertheless, like the actuator made by nylon fishing line mentioned above, the contracting stroke and actuating power remain limited owing to the fixed material component, thus the intrinsic properties of applied materials can only satisfy certain capacity requirement rather than desired power in a wide range.

Later on, strain-programmable spring-like artificial muscles were fabricated by bimorph fibers composed of PE and COCe through cold drawing process[22]. The composite actuators can lift weight of over 650 times of their own and can realize strain of 12% with temperature increase of only 10 °C in 2s. However, the effects of the percentage of components and the performance under extremely cold condition have not been reported.

The structures of the actuators previously reported have not been designed and adjusted for better performance, which were only determined by the selected materials rather than utilizing the proper mutual synergism of elements. Besides, the operation of actuators under low temperature have not been explored sufficiently. Therefore, for improving the performance and widening the application, a comprehensive and systematic study is needed to fabricate novel thermally powered actuators based on

composite yarn, which can be produced with low cost, fabricated with simple process, and controlled in structure for versatile functions.

## 1.2 Problem Statement

Though the previous fiber-based single-component thermally powered actuators can realize relatively high tensile actuation strokes and high energy density, their fixed intrinsic properties led to limited actuating performance. Some actuators with composite structure, e.g. carbon fiber/PDMS and PE/COCe FCLAs, have potentials to extend their performance through adjusting the percentage of each components, whereas the systematic material selection and the optimization of volume fraction of components have not been implemented.

Besides, as many fiber materials could become rigid and vulnerable under extremely cold environment, almost all the reported actuators only operate at or above the ambient temperature, whereas few studies focus on the low temperature working condition, which is also important for the device working in cold region, outer space etc. More materials should be selected and adopted to fabricate actuators that can be applied under wide ranges of temperature for versatile applications.

Fabricating electrothermally powered actuators through inserting metal plating process can make the actuators more controllable and convenient in practical application, e.g. robot, engineering materials, textile industry etc. However, the metal plating process

specifically for certain fibers has not been investigated and optimized sufficiently. Besides, the material selection, material arrangement and texture of smart actuating devices/textiles have not been explored. These vacancies should be filled for extending the applications of electrothermally powered actuators.

## 1.3 Objectives

The main objectives for this project are:

(1) To fabricate thermally powered actuators based on composite yarn, i.e. helical composite yarn actuators (HCYAs), which are of multiple functions for different applications, low cost to be produced by simple fabrication process, and have stable chemical and physical properties.

(2) To study the factors influencing the fabrication of thermally powered HCYAs, including number of filaments, volume fraction, concentration of coating solution etc.

(3) To design proper experimental sensing system for isotonic property test, especially under an extremely cold condition.

(4) To characterize the thermomechanical properties of the thermally powered HCYAs in isotonic, isometric and isothermal conditions.

(5) To investigate the actuating mechanism in terms of the relationships between the properties of each material and performance of HCYAs.

(6) To fabricate electrothermally powered actuators and devices for practical applications, e.g. electrothermally powered artificial muscle, strips and fabrics, followed by related property characterization.

## 1.4 Methodology

For conducting a comprehensive and systematic research on the HCYAs, the methodologies are listed as follows:

(1) A composite yarn will be designed as a fundamental element of HCYAs. The difference of thermal expansion in axial and radial direction should be large enough to realize effective tensile actuation when changing temperature. Proper fiber substrate (e.g. Polyimide, PET, Nylon) and polymer matrix (e.g. polydimethylsiloxane, epoxy) will be selected according to their strength, high/low temperature resistance, coefficient of thermal expansion etc.

(2) HCYAs will be fabricated by the composite yarn through super-twisting process. Influencing factors will be investigated in terms of volume fraction of polydimethylsiloxane (PDMS), fabricating load, filaments number etc. Gradient parameters will be set for each influencing factor for analyzing their effects on actuating performance.

(3) Thermomechanical characterization will be carried out, including isotonic,

isometric and isothermal behavior tests. Experimental set-up will be designed to be feasible for wide temperature range, precise displacement and temperature data, as well as data repeatability.

(4) The actuating mechanism will be analyzed according to the thermomechanical behavior. Related specifications of HCYAs will be measured for modelling calculation and performance analysis. The certificated actuating mechanism will be used for further prediction of HCYAs with different parameters.

(5) Metal plating process will be optimized to obtain effective electrothermally powered HCYAs, through adjusting relevant parameters, e.g. solution concentration, processing temperature, fiber state, filament number etc. Twisting, braiding and weaving process will be adopted for fabricating smart devices, e.g. electrothermally powered artificial muscle, strips and fabrics.

## 1.5 Project Significance

The significance of this project exists in both academic and industrial aspects. For the academic significance, this project explores the actuating mechanism of HCYAs systematically, as well as optimizes the corresponding fabrication process. These theoretical works further broaden the scientific boundary in the actuator field.

For the industrial significance, HCYAs investigated in this project are very promising and valuable for society due to their versatile functions. First, they can be applied to healthcare product, e.g. medical compressive stockings, compressive clothes for sports.

In addition, they can be made into actuating assemblies, such as artificial muscles for arms of robots, retractable yarn of smart curtain etc. Most importantly, the fields of application cover industries of textile, material, medical care, artificial intelligence and information technology, thus the development of this material will promote interdisciplinary innovation in numerous industries in the whole society.

## 1.6 Structure of the Thesis

The study on thermally/electrothermally powered HCYAs are elaborated in seven chapters. The structure of this thesis is arranged as follows:

(1)  Chapter 1 gives an introduction to this study, including a research background of linear thermally powered actuators, current problems need to be addressed, objectives for the systematic studies, available and reasonable methodologies, significance to science and society, as well as thesis structure arrangement.

(2) Chapter 2 encloses a literature review of state-of-art on the actuators of all species. Their advantages and disadvantages were analyzed in terms of properties, performances, actuating requirements, energy density, actuating ratio etc. More literatures related to fiber-based linear coiled thermally powered actuators are summarized as benchmarks for this study.

(3) Chapter 3 elaborates the fabrication of composite yarns, in terms of material selection, fabrication and characterization. Different polymers for fiber substrate and coating matrix were compared in terms of modulus, temperature resistance, thermal expansion and other properties. Influencing factors in fabricating process

were investigated for optimizing the composite yarns, e.g. concentration of coating solution, volume fraction of PDMS, coating method, filament number etc.

(4) Chapter 4 presents the fabrication and characterization of HCYAs. The effects of influencing factors for fabricating devices were revealed, including fabricating load, twist turnings, heat-setting tensions, heat-setting time etc. Besides, isotonic, isometric and isothermal behaviors are used to assess the thermomechanical performances of HCYAs.

(5) Chapter 5 improves the function of HCYAs by adding conductive layer, thus the prepared electrothermally powered HCYAs can be triggered conveniently by joule heating. The process of electroless deposition of copper and silver was optimized from solution concentration, processing temperature, processing time, filament number, yarn state etc. Proper load, twisting turnings, ply number and fixed method were all investigated for fabricating the actuators. The resistance, strength and evenness are used to assess the qualities of conductive composite yarns and electrothermally powered HCYAs.

(6) Chapter 6 further illustrates the fabrication process of functional devices adopting electrothermally powered HCYAs for practical applications, such as electrothermally powered artificial muscle for robotic arm, actuating strips and actuating fabrics for smart compressive stockings. The combination methods and weaving/braiding processes are developed through optimizing relevant parameters, including tension, filament/yarn number, end-fixing method, texture design etc.

(7) Chapter 7 provides conclusions of this study, while indicates the limitation of

current work and suggested improvement in future work.

## Reference

[1] S. M. Mirvakili, A. Pazukha, W. Sikkema, C. W. Sinclair, G. M. Spinks, R. H. Baughman, and J. D. W. Madden, "Niobium Nanowire Yarns and their Application as Artificial Muscles," *Advanced Functional Materials,* vol. 23, no. 35, pp. 4311-4316, 2013.

[2] S. M. Mirvakili and I. W. Hunter, "Artificial Muscles: Mechanisms, Applications, and Challenges," *Advanced Materials,* vol. 30, no. 6, Feb 2018.

[3] J. Kim and J. Chang, "A New Electromagnetic Linear Actuator for Quick Latching," *IEEE Transactions on Magnetics,* vol. 43, no. 4, pp. 1849-1852, 2007.

[4] F. Daerden and D. Lefeber, "Pneumatic artificial muscles: actuators for robotics and automation," *European journal of mechanical and environmental engineering,* vol. 47, no. 1, pp. 11-21, 2002.

[5] S. A. Morin, R. F. Shepherd, S. W. Kwok, A. A. Stokes, A. Nemiroski, and G. M. Whitesides, "Camouflage and Display for Soft Machines," *Science,* vol. 337, no. 6096, pp. 828-832, 2012.

[6] J. D. Madden, N. A. Vandesteeg, P. A. Anquetil, P. G. Madden, A. Takshi, R. Z. Pytel, S. R. Lafontaine, P. A. Wieringa, and I. W. Hunter, "Artificial muscle technology: physical principles and naval prospects," *IEEE Journal of oceanic engineering,* vol. 29, no. 3, pp. 706-728, 2004.

[7] T. Mirfakhrai, J. D. W. Madden, and R. H. Baughman, "Polymer artificial muscles," *Materials Today,* vol. 10, no. 4, pp. 30-38, 2007.

[8] J. Huber, N. Fleck, and M. Ashby, "The selection of mechanical actuators based on performance indices," *Proceedings of the Royal Society of London. Series A: Mathematical, physical and engineering sciences,* vol. 453, no. 1965, pp. 2185-2205, 1997.

[9] Z. Peng, "Study on thermally activated coiled linear actuators made from polymer fibers," Master, Institute of Textiles and Clothing, The Hong Kong Polytechnic University, Hong Kong, 2018.

[10] S. Schuhladen, F. Preller, R. Rix, S. Petsch, R. Zentel, and H. Zappe, "Iris‐Like Tunable Aperture Employing Liquid‐Crystal Elastomers," *Advanced Materials,* vol. 26, no. 42, pp. 7247-7251, 2014.

[11] M. Shahinpoor and K. J. Kim, "Ionic polymer-metal composites: I. Fundamentals," *Smart materials and structures,* vol. 10, no. 4, p. 819, 2001.

[12] S. Nemat-Nasser, "Micromechanics of actuation of ionic polymer-metal composites," *Journal of applied Physics,* vol. 92, no. 5, pp. 2899-2915, 2002.

[13] P. Ariano, D. Accardo, M. Lombardi, S. Bocchini, L. Draghi, L. De Nardo, and P. Fino, "Polymeric materials as artificial muscles: an overview," *Journal of applied biomaterials & functional materials,* vol. 13, no. 1, pp. 1-9, 2015.

[14] G. M. Spinks, V. Mottaghitalab, M. Bahrami‐Samani, P. G. Whitten, and G. G. Wallace, "Carbon‐nanotube‐reinforced polyaniline fibers for high‐strength artificial muscles," *Advanced Materials,* vol. 18, no. 5, pp. 637-640,

2006.

[15]    J. Chilver, "Artificial muscle," Canada Patent WO9727822 (A1), 1997.

[16]    L. Liao, H. Yang, X. Yang, and C. Yang, "Artificial muscle," China Patent CN1413562 (A) 2002.

[17]    M. D. Lima, N. Li, M. Jung de Andrade, S. Fang, J. Oh, G. M. Spinks, M. E. Kozlov, C. S. Haines, D. Suh, J. Foroughi, S. J. Kim, Y. Chen, T. Ware, M. K. Shin, L. D. Machado, A. F. Fonseca, J. D. Madden, W. E. Voit, D. S. Galvao, and R. H. Baughman, "Electrically, chemically, and photonically powered torsional and tensile actuation of hybrid carbon nanotube yarn muscles," *Science,* vol. 338, no. 6109, pp. 928-32, Nov 16 2012.

[18]    N. Li, C. S. Haines, M. D. Lima, M. Jung de Andrade, S. Fang, J. Oh, M. E. Kozlov, D. Suh, and R. H. Baughman, "Coiled and non-coiled nanofiber yarn torsional and tensile actuators," Patent US20150152852A1, 2015.

[19]    C. S. Haines, M. D. Lima, N. Li, G. M. Spinks, J. Foroughi, J. D. W. Madden, S. H. Kim, S. Fang, M. J. d. Andrade, F. Göktepe, Ö. Göktepe, S. M. Mirvakili, S. Naficy, X. Lepró, J. Oh, M. E. Kozlov, S. J. Kim, X. Xu, B. J. Swedlove, G. G. Wallace, and R. H. Baughman, "Artificial muscles from fishing line and sewing thread," *Science,* vol. 343, no. 6173, pp. 868-872, 2014.

[20]    N. Li, C. S. Haines, M. D. Lima, M. Jung de Andrade, S. Fang, J. Oh, M. E. Kozlov, F. Goktepe, O. Goktepe, D. Suh, and R. H. Baughman, "Coiled and non-coiled twisted nanofiber yarn and polymer fiber torsional and tensile actuators," Patent WO2014022667 (A2), 2014.

[21] M. Hiraoka, K. Nakamura, H. Arase, K. Asai, Y. Kaneko, S. W. John, K. Tagashira, and A. Omote, "Power-efficient low-temperature woven coiled fibre actuator for wearable applications," *Scientific Reports,* vol. 6, p. 36358, Nov 4 2016.

[22] M. Kanik, S. Orguc, G. Varnavides, J. Kim, T. Benavides, D. Gonzalez, T. Akintilo, C. C. Tasan, A. P. Chandrakasan, Y. Fink, and P. Anikeeva, "Strain-programmable fiber-based artificial muscle," *Science,* vol. 365, no. 6449, pp. 145–150, 2019.

# CHAPTER 2
# LITERITURE REVIEW

## 2.1 Introduction

Actuators have become a hotspot for researchers recently, due to their promising applications in many fields, e.g. robotics, sensors, energy harvesting, deformable textiles etc. With the development of actuators, the mainstream of requirement tends to be soft, safe, portable, efficient, energy-saving, eco-friendly and so on. To achieve a satisfactory actuator for certain application, many types could be taken into consideration. Main aspects of actuators include traditional actuators, electric actuators, ionic actuators, shape memory alloy (SMA) actuators and fiber-based coiled linear actuators (FCLAs). Their performances will be assessed in terms of strain, stress, specific work, energy density, power density, cyclability, temperature resistance, hysteresis, response time, safety etc.

In this chapter, different types of actuators will be reviewed, as well as the analysis of principles and advantages/disadvantages. As mentioned above in chapter 1, the FCLAs have attracted more attentions in scientific field than other types of actuators, owing to their obvious advantages in high stress, energy density and practical use, a comprehensive review is made on FCLAs in terms of materials, power sources and applications, while other types of actuators are also introduced explicitly.

## 2.2 Traditional actuators

### 2.2.1 Electromagnetic actuator

Electromagnetic actuators, e.g. electric motor and electric latch, are very attractive in traditional actuator technology, owing to their high energy density and efficiency. The electric motor can also achieve high torque under low speed, which facilitates the energy transmission and actuation. The ankle of humanoid robot ASIMO in a human size (54kg) could achieve 200W and 700W when walking and sprinting, respectively[1]. Except for the rotating actuation, the linear electromagnetic actuators are also important in practical industrial application, such as combustion engine. An electric latch with engine valve control system (Figure 2.1) can realize fast transition time and actuation while reduce the power consumption[2]. Obviously, the traditional electromagnetic actuators have advantages in terms of energy density, efficiency, response time etc, whereas their applying condition is restricted by the rigid structure and large scale, especially when flexibility and miniature have become a main requirement for actuators in recent years.
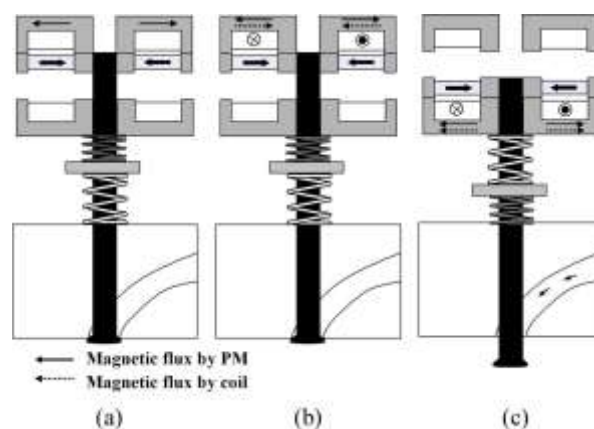


Figure 2. 1 Principle of operation of electric latch (a) upper end, (b) starting and (c) lower end.

## 2.2.2 Pneumatic actuator

Pneumatic actuators are usually actuated by pressurized air, which goes through the channels within the elastic body[3]. Different deformation can be obtained in different part due to the difference of thickness and modulus, thus the actuators can implement actions, e.g. grip, lift, twining etc. A resilient soft robot made by pneumatic actuator was presented by Harvard University in 2014 (Figure 2.2). This robot can hold load of 8kg when working under pressurized air of 138kPa[4]. A bio-spired robotic snake was also fabricated by the pneumatic actuator, this snake can realize forward locomotion through the generated anisotropic friction when actuated pneumatically[5]. The advantages of pneumatic actuators exist in their less inviscid and light weight, thus they are preferred than the hydraulic actuator[3]. However, the operation needs extra pressurized system which may bring inconvenience in many conditions, especially for the wearable and portable devices.
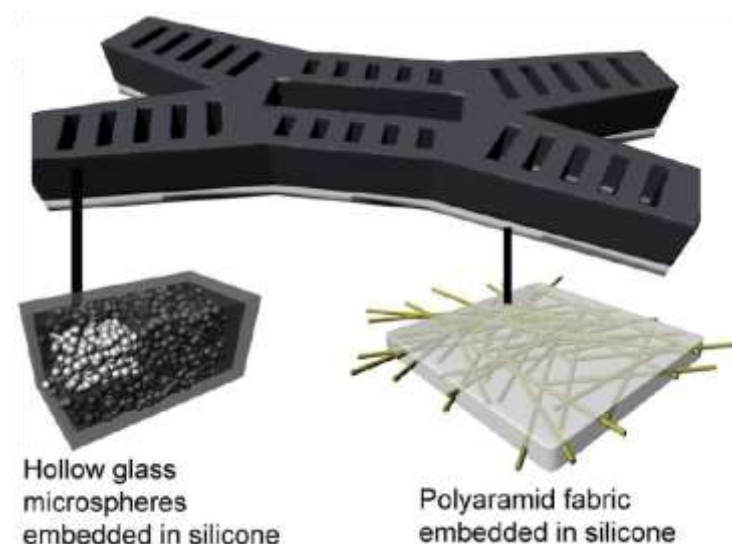


Figure 2. 2 Structure and component illustration of the resilient and untethered soft robot

### 2.2.3 Hydraulic actuator

Like pneumatic actuators, hydraulic actuators are also deformable and adaptable actuators, which are actuated by pressurized liquid going through the embedded channels in the elastic body[3]. An autonomous robotic fish was fabricated and actuated hydraulically to realize swimming in three dimensions. The embedded closed-circuit drive system facilitate the transmission and circulation of water, thus provides control of the caudal fin of the robotic fish[6]. For medical use, a soft robotic glove (Figure 2.3) was design with hydraulic actuator to help the grasp of handicapped hand. Under the pressure regulation of a close-loop controller, the hydraulic actuator could generate significant force to support the motion of fingers[7]. The advantages of hydraulic actuators lie in the large force compared with pneumatic ones, as well as the ability to be applied in untethered robotics under water, whereas the application in air can be restrained by extra water-supply system.



Figure 2. 3 Soft robotic glove made by hydraulic actuator for rehabilitation of handicapped hand

## 2.3 Electric actuator

### 2.3.1 Dielectric elastomer actuator

Dielectric elastomer actuator (DEA) composes of a central layer of dielectric elastomer and two compliant conductive electrode layers beside (Figure 2.4). The actuation happens when a voltage is exerted on the electrodes, thus the dielectric elastomer deforms with the generated electric field[8]. The maximum strain of DEA can reach up to 380% when a pre-strained acrylic was adopted as the dielectric elastomer[9]. Many materials can be applied into DEA, e.g. silicone, polyurethane, acrylic etc. Though the DEAs can achieve large strain and relatively fast response time, high voltage for actuation, as well as the stability under high voltage, impedes the wide application in flexible and wearable devices[8].
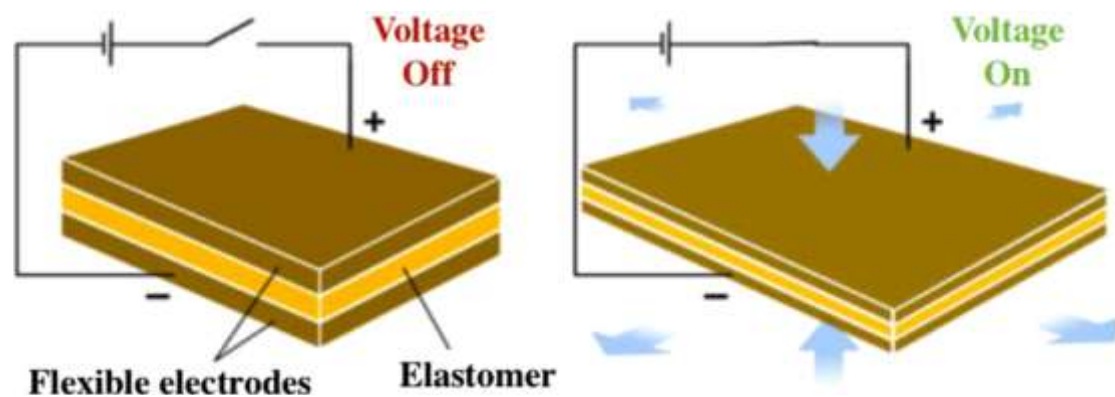


Figure 2. 4 The principle of dielectric elastomer actuator

### 2.3.2 Piezoelectric actuator

Piezoelectric actuator was made of piezoelectric materials, which can generate electric field when imposing mechanical stress across the materials and vice versa[10]. The

typical piezoelectric actuator was fabricated by PZT ($Pb[Zr_xTi_{1-x}]O_3$), the maximum

strain was only 0.5% while the excitation field was in a scale of MV/m (Figure2.5)[11].

Other piezoelectric materials, e.g. PMN ($Pb[Mg_{1/3}Nb_{2/3}]O_3$) and PZN

($Pb[Zn_{1/3}Nb_{2/3}]O_3$), could reach a bit higher strain of 0.6% and 1.7%, respectively,

under electric field of same scale as PZT[12]. Though the piezoelectric actuators have

very high efficiency of over 90% and large resonance frequency bandwidth (up to

10MHz), the low strain and high excitation field have held back their application in

wearable device. Instead, they can be applied in ultrasonic transducer, piezomotor and

energy-harvesting devices preferably[13].
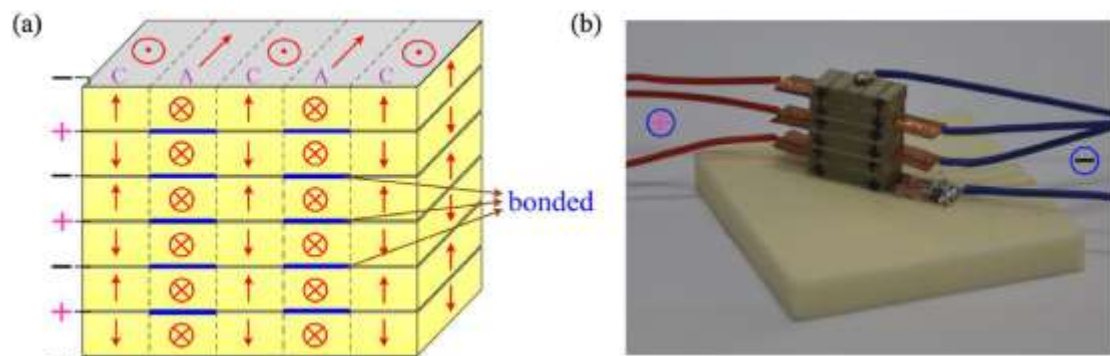


Figure 2. 5 A piezoelectric actuator made by six-layer PZT. (a) scheme (b) photograph

### 2.3.3 Electrostrictive elastomer actuator

Electrostrictive elastomer actuators are fabricated by electrostrictive copolymers,

wherein the poly(vinylidene fluoride-cotrifluoroethylene) (P(VDF-TrFE)),

electrostrictive graft elastomers (Figure 2.6) and P(VDF-TrFE)-based terpolymers are

well studied[12]. The actuation principle lies in the polar crystalline regions in the

copolymer, which can realign under sufficient electric field, thus causing dimensional

change of the actuators[14]. P(VDF-TrFE) actuator can reach strain of 10% under an

20

electric field of 9MV/m while high response frequency of 100kHz was achieved[15].

Compared with P(VDF-TrFE) copolymer actuators, electrostrictive graft elastomers

and P(VDF-TrFE)-based terpolymers obtained relatively lower strain of 4% and 7%, as

well as equivalent energy density of 0.46 and 1.1MJ/m$^3$[16, 17], respectively. One of

the limitations of electrostrictive elastomer actuator is the non-linear actuation behavior

(relationship between voltage and displacement), that make it complicate to be

controlled. Other limitations are same as the piezoelectric actuators, i.e. the relatively

low strain and high excitation voltage[12].
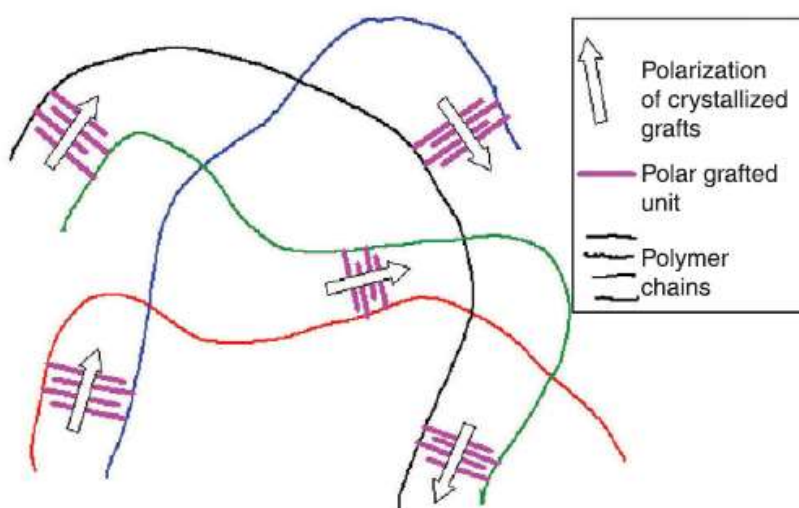


Figure 2. 6 Electrostrictive graft elastomer without electric field


## 2.3.4 Liquid crystal elastomer actuator

Liquid crystal can change orientation under appropriate electric field (Figure 2.7).

Utilizing this special property, liquid crystal elastomer actuators (LCEAs) can be

fabricated by grafting the liquid crystal molecular fragments onto polymer backbones

or sides chains[14]. LCEA can realize a relatively low strain of 4% under electric field

of 1.5MV/m[18]. As common LCEAs possess low modulus and low strain, the work density is rather low. To improve this, polymers with higher modulus could be adopted to prepare the LCEAs[19]. The defects of LCEAs exist in their low strain, high excitation voltage, low density, as well as lower response frequency compared with the piezoelectric actuators and electrostrictive actuators.
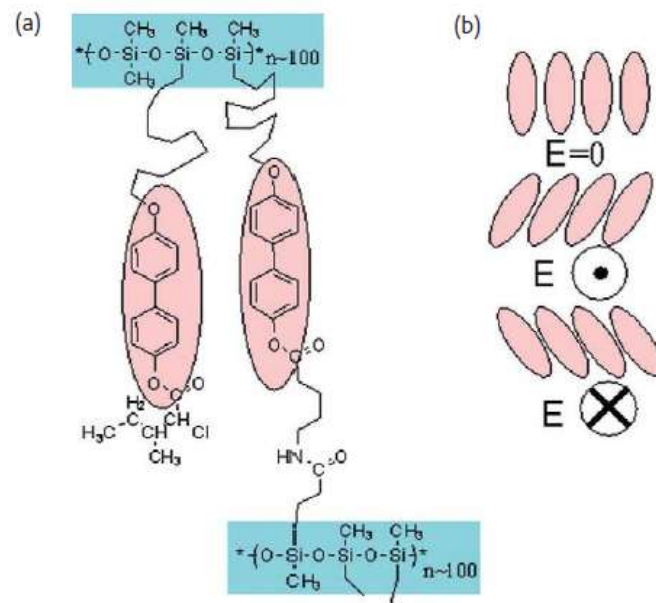


Figure 2. 7 Chemical structure of liquid crystal elastomer actuators (left) and actuation mechanism (right)

## 2.4 Ionic actuator

### 2.4.1 Stimuli-responsive gel actuator

The stimuli-responsive gel actuator is based on the polymer gel that can be responsive to temperature, pH, light, electricity etc. The principle is that chemical or physical changes happen in the polymer chain when certain stimuli is exerted. Taking the temperature-responsive gel actuator as an example (Figure 2.8), the gel composes of both hydrophilic and hydrophobic segments, when the temperature of the gel is lower

than the critical value, the hydrophilic segments domain the property, i.e. the gel swells in the solution. Alternatively, when the temperature of the gel is higher than the critical value, the hydrogen bonds between the hydrophilic segment and water are broken, thus the gel deswells[12]. The gel actuator can achieve strain of 90% under stress of 4MPa, as well as energy density of 460kJ/m$^3$[20]. For thin gel actuators, the response time can be less than one second while thicker gel actuators may take several minutes or hours to reach the maximum strain[21]. The merits of gel actuators are their good elasticity and extensibility, whereas the limitations of gel actuator are relatively slow response time compared with piezoelectric actuator, instable chemical property and performance decay over time[12].
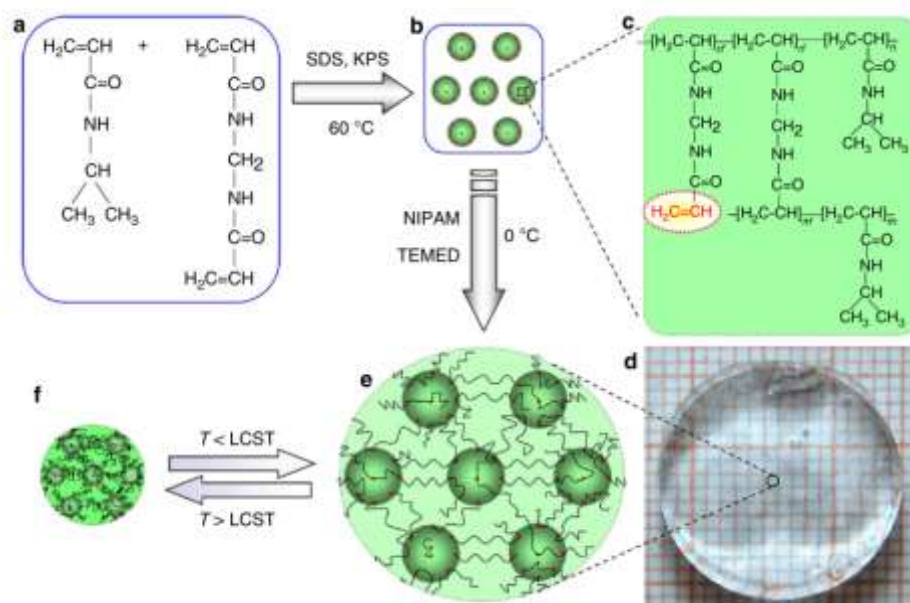


Figure 2. 8 Chemical structure and actuating mechanism of temperature-responsive gel actuator[21].

**2.4.2 Ionic polymer-metal composites (IPMC)**

IPMC actuator consists of an ionically conductive layer sandwiched between two conductive electrodes. The ionically conductive layers are generally made of perfluorinated polymers that contain ionic carboxylate and sulfonate groups, while the conductive electrodes can be gold, platinum, carbon nanotube, graphene etc[22]. For improving the cost effectiveness, ionic conductivity and environmental friendliness, sulfonated biopolymers (e.g. cellulose and chitosan) can be used to substitute the perfluorinated polymers as host materials. When imposing a voltage on the conductive electrode, the cation of electrolyte will move onto the cathode while the anions move to anode. As the cations possess larger volume than the anions, strain of cathode is much larger than anode, thus cause the bending of IPMC actuator due to asymmetric deformation[12]. An IPMC actuator was fabricated by polyacrylic acid and polyacrylonitrile copolymer as the gel host, ionic liquid and halloysite nanoclays as the electrolyte, as well as the gold nanocluster as the electrode (Figure 2.9). This actuator can be actuated by low voltage of 0.1~5V, with 76000 cycles of operation. Besides, the electrodes possess very low specific resistance of less than $100ohm/cm^2$ and high capacitance of mF/g scale[23]. The aqueous-electrolyte-based IPMCs are not stable in air while the ionic liquid-based IPMCs are stable in air but response slowly. As many types of actuators, IPMC actuators also bear a high cost to be commercialized.
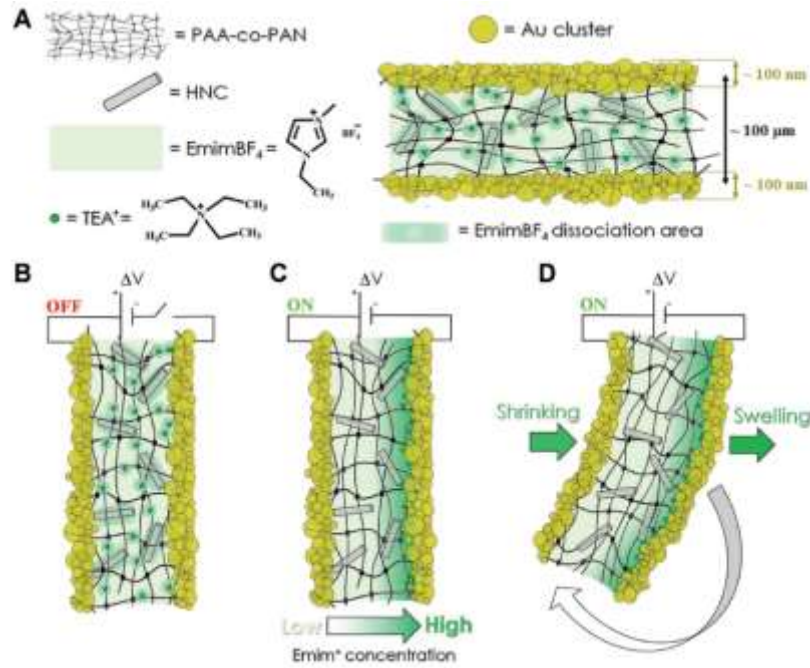
Figure 2. 9 The chemical structure and actuating mechanism of IPMC actuator

## 2.4.3 Conductive polymer actuator

Conductive polymer actuators are based on conductive polymers with monomer that can be chemically oxidized or reduced, e.g. pyrrole, thiophene, aniline etc. The structure can be bilayer (one passive layer and one active layer) or trilayer (one passive layer between two active layers). When an electric potential is imposed to the active layer, the ions of electrolyte will migrate onto the layer for neutralizing the generated charges (Figure 2.10), thus causing the expansion/contraction of each layer and the bending of the whole actuator[24]. A carbon-nanotube-reinforced polyaniline fiber was prepared through wet-spinning technique for artificial muscle. The addition of carbon nanotube significantly promotes the strength of the actuator (100MPa, i.e. 300 times of skeletal muscle) and strain (from 1.3% to 2%)[25]. Conductive polymer microactuator can achieve very high response frequency of kHz when ultrathin interpenetrating

polymer networks were adopted as the active layer through spin coating technique. The strain of this microactuator can reach up to 0.9% and generated force of µN scale[26]. One of the limitations of conductive polymer actuators is that fast response and large force cannot be obtained simultaneously, as higher thickness restricts the ion migrating time, whereas lower thickness only can offer tiny force. Another contradiction is that aqueous electrolyte have higher conductivity and faster charging ability but too small ion radius to obtain large strain and stress, while ionic liquid electrolyte have lower conductivity and slower charging ability but large ion radius to obtain better strain and stress[12].
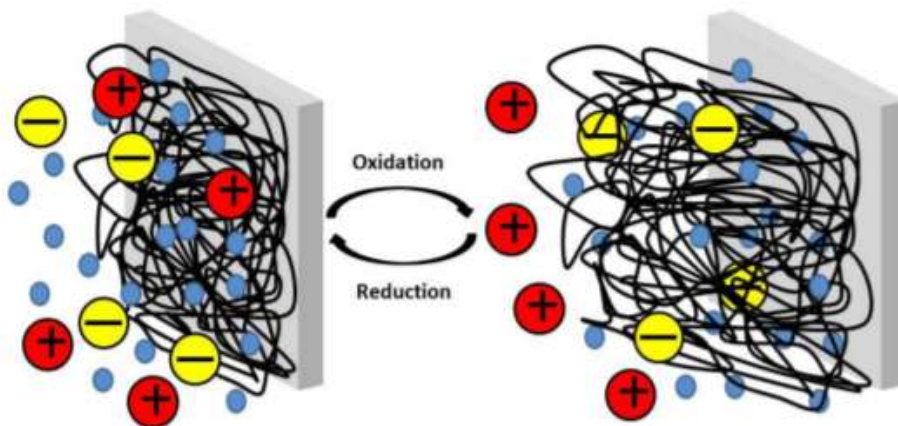


Figure 2. 10 Schematic illustration of actuating mechanism of conductive polymer actuator[24].

## 2.5 Shape memory alloy (SMA)

SMA is capable of recovering to original state when stimulated by heat, magnetic field etc. Utilizing this property, SMA actuators can achieve different deformations, e.g. bending, twisting, contracting, folding etc. SMAs include one-way SMA and two-ways SMA, wherein the one-way SMA can recover to its original state when the applied

stimulus is removed, and the two-way SMA can memorize the original states at both high temperature and low temperature. Fast torsional artificial muscles were fabricated by twisted shape memory NiTi alloy yarn which could achieve maximum torsional actuation of 16°/mm, speed of 10500 rpm and torque of 8 Nm/kg[27]. Another bending SMA actuator realized very fast actuation with bending frequency of 35Hz, through adopting multiple thin NiTi fiber which can dissipate the heat quickly. Coupling bending with twisting deformation, this actuator also realized a fast response frequency of 10Hz (Figure 2.11)[28]. The disadvantages of SMA actuators commonly exist in the high hysteresis that leading to a difficult control. Besides, the cyclability and the cost-efficiency need to be further improved[12].
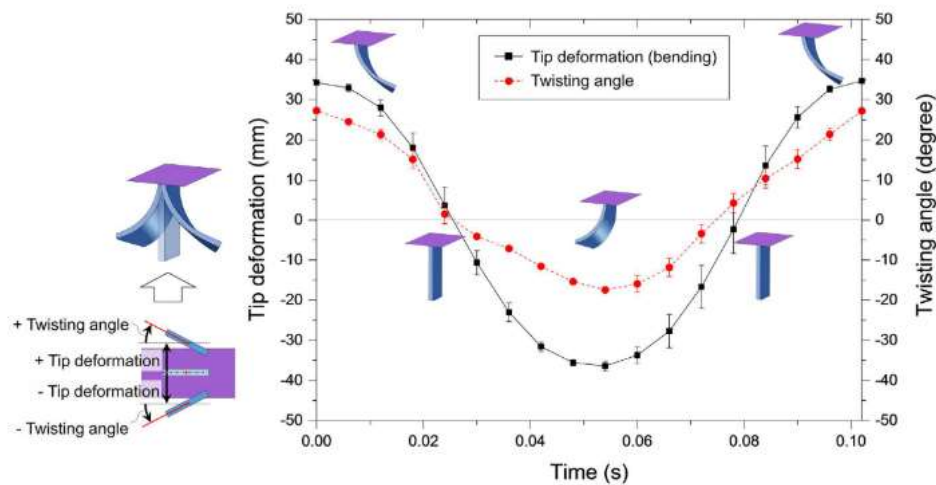


Figure 2. 11 SMA actuator with bending-twisting coupled mode

## 2.6 Fiber-based coiled linear actuators

### 2.6.1 Thermally powered actuators based on different materials

#### 2.6.1.1 Nylon

High strain and high stress are hardly to be obtained simultaneously for most actuators,

whereas fiber-based coiled linear actuators (FCLAs) are the exception. The first low-cost thermally powered FCLAs were presented by nylon fishing line (Figure 2.12)[29, 30]. After extreme twisting insertion, the coiled actuators can obtain a contraction of 49% and lift much heavier load than human muscle under the same condition. Though the work capacity was high enough, the working temperature range may be not wide enough as nylon always become crisp under extremely cold environment.
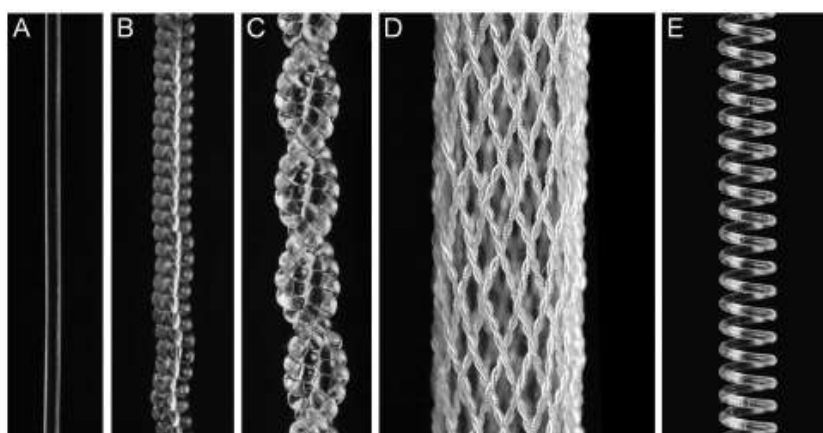


Figure 2. 12 Thermally powered muscles made by nylon sewing thread.

## 2.6.1.2 Polyethelene

In 2016, a new coiled fiber actuator was proposed by linear-low density polyethylene (LLDPE), which can be driven in low temperature and in favour of the use in wearable systems[31]. This novel application of traditional materials has paved a new road for low-temperature driving actuators, meanwhile promoted the transferring of actuating materials from industrial application to civil use. The only unsatisfactory point lies on the stability of LLDPE, as its structure changes readily with slight change of temperature, leading to uncontrollable deformation and fragile property.

**2.6.1.3 Poly(vinylidienefluoride) (PVDF)**

Pure PVDF-based coiled artificial muscles were fabricated by Melvinsson[32], finding that higher degree of crystallinity and molecular weight of the material facilitated better properties (Figure 2.13). This work has linked the internal chemical structure and chemical property of key materials with the practical characteristics of artificial muscle, which is a significant reference for the material selection, but the tensile actuations of all the fabricated samples were even lower than 1% and consequently the effect of practical application was deprived enormously.
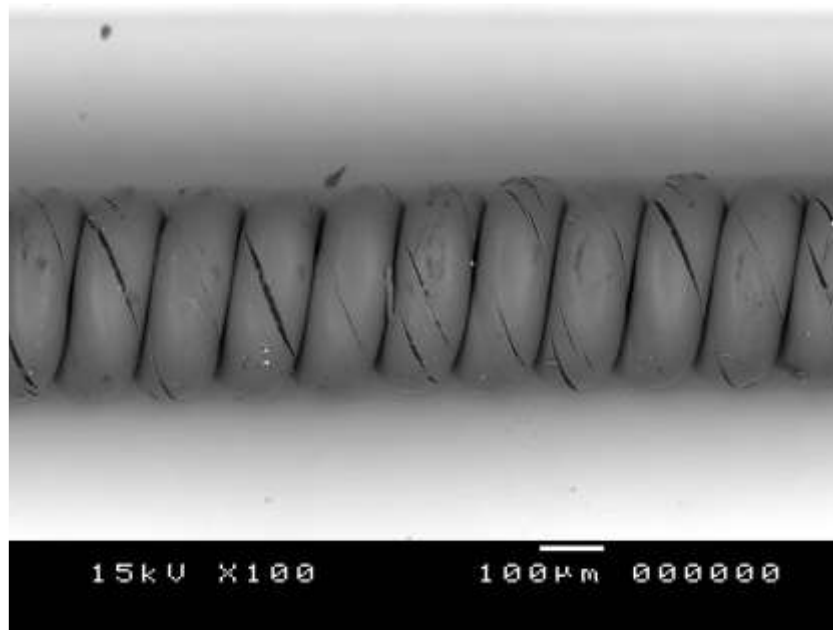


Figure 2. 13 PVDF-based coiled artificial muscles

**2.6.1.4 Polyethylene terephthalate (PET)**

PET is also a potential choice for artificial muscle material due to the satisfactory thermoplastic property. A twisted-coiled polymer fiber actuator was developed by surface-modified (silver-plating) PET yarn, providing a potential for the use in artificial muscle (Figure 2.14)[33]. It is known that PET is a low-cost common material with

high breaking strength and can be widely used in large-scale industry. However, the silver-plating process is a high-cost and polluting operation, which brings more disadvantages than benefits.
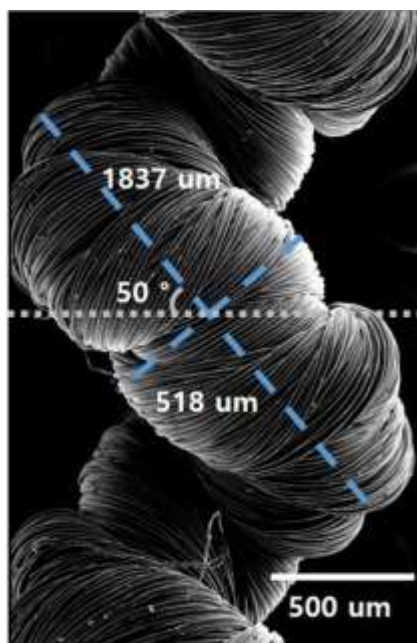


Figure 2. 14 Thermally powered actuator made silver-plating PET yarn

**2.6.1.5 Carbon nanotube (CNT)**

CNT yarns were guest-filled and twisted into artificial muscles by Lima, Li *et al* [34, 35] that provide high force and large tensile/torsional actuation (Figure 2.15). Besides, they can afford at least a million of torsional and tensile actuations when spinning a rotor (11500 revolutions/minute) or lifting load (3% contraction with frequency of 1200 cycles/minute). Nevertheless, this actuator has limited working temperature range due to the wax with low melting temperature as a guest, which depresses the actuating performance and adaptability.
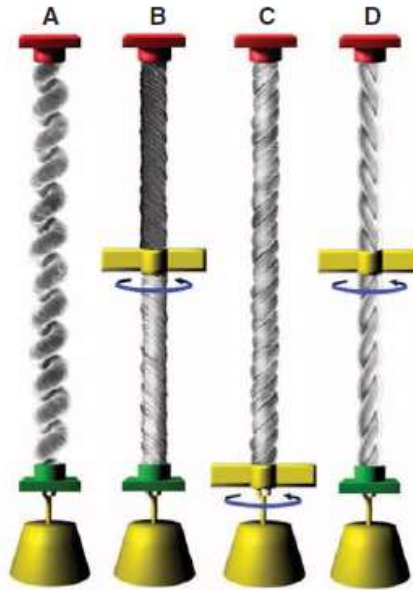
Figure 2. 15 Configurations of artificial muscles made by guest-infiltrated CNT yarn

**2.6.1.6 Composite fiber**

Compared with single-component fiber, composite fiber can be more flexible and adjustable to design actuators with satisfactory properties. A carbon/polydimethylsiloxane composite coiled actuator was fabricated to realize tensile strain of more than 25% under stress of 60MPa, as well as a high specific work of 758 J/kg (> 18 times of skeletal muscle)[36]. Another strain-programmable COCe/HDPE FCLAs with bimorph polymer structure (polyethylene and cyclic olefin copolymer elastomer) were reported that tensile strain and work capacity could be controlled by stretching with different strains (Figure 2.16)[37]. Nevertheless, volume fraction of each component of above actuators have not been adjusted for optimizing the performance. Also, few investigations are focused on the actuating effects of FCLAs under extremely cold condition (e.g. from -50 ℃ to room temperature).
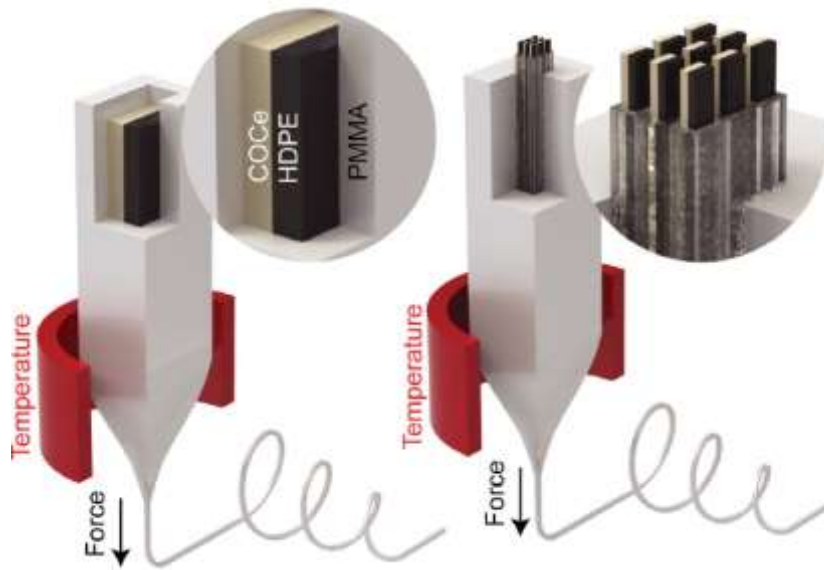
Figure 2. 16 COCe/HDPE composite strain-programmable coiled actuator

## 2.6.2 Power source of actuators

### 2.6.2.1 Physically thermal power source

Thermally powered actuators can be driven by many physical triggers, such as air-heating, electricity, hot water and so on. A hydrothermally powered artificial muscle was designed and analyzed by Wu et al[38], for actuating a biomimetic robotic hand. By switching the hot and cold water into spring-like coiled nylon muscle, contraction and extension of artificial finger were realized for handshake of robot. For characterizing the thermally-driven coiled nylon actuator, a test bench was fabricated through applying hot air flow as the power source, carrying out isometric test to observe the force actuation of the actuator (Figure 2.17)[39]. Another electrothermally powered actuator was reported by Zhang et al[40] for healing the structural-scale crack of ionomer composite. The carbon fiber-embedded coiled nylon actuator was resistively heated by DC power, in order to contract the actuator as well as melt the ionomer composite.

32
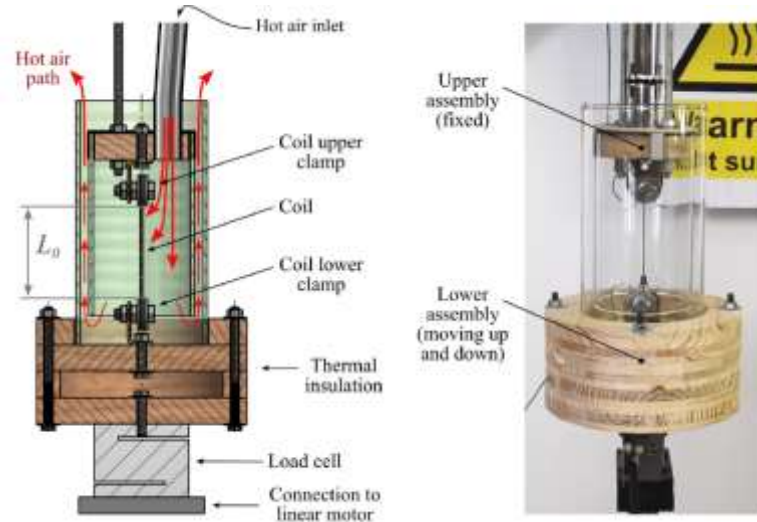
Figure 2. 17 Test bench for observing the force actuation of actuators

## 2.6.2.2 Chemical power source

A chemically-triggered torsional actuator was reported by Lima et al[34], which was fabricated by twisting palladium-containing nanotube sheet stack into a hydrogen-responsive intelligent muscle. Injecting 0.05-atm H2 into the testing vacuum chamber cause 1.5 paddle rotation of actuator in a few seconds, while full reversion happened after vacuum the hydrogen within a similar time. Alternatively, electrochemically powered CNT actuators were demonstrated by coating gel electrolyte on two-ply coiled yarn (Figure 2.18)[41]. This actuator provided tensile contraction of 16.5% and reached an energy conversion efficiency of 5.4%. Both of the properties were better than previous chemically powered muscle and thermally powered muscle.
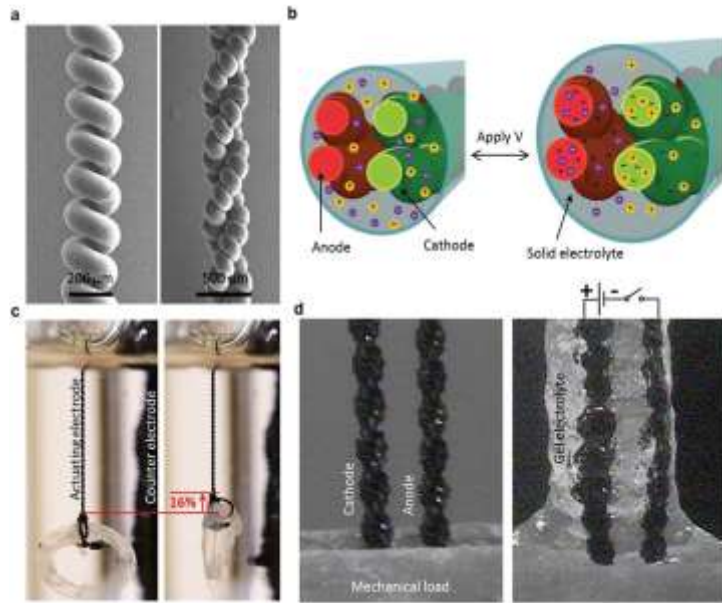
Figure 2. 18 Yarn structures and actuating mechanism of electrochemically powered CNT actuators

## 2.6.2.3 Biothermal power source

A CNT yarn was biscrolled into a biothermally powered torsional actuator by Lee et al (Figure 2.19), through entrapping an enzyme linked with thermally sensitive hydrogel. Once the enzyme combined with glucose, the released energy would cause the expansion of hydrogel, further inducing the rotation of torsional actuator. An equilibrated angle can be reached in no more than 2 min under normal temperature range from 25 °C to 37 °C[42].
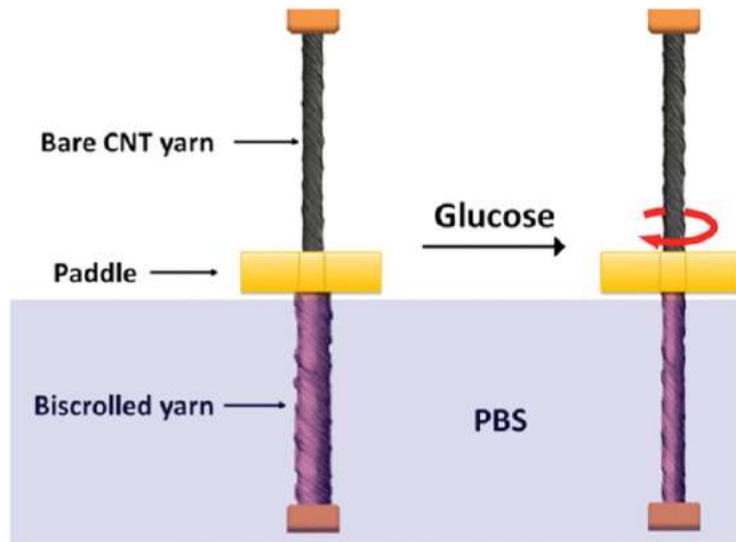
Figure 2. 19 Biothermally powered torsional actuator

## 2.6.3 Versatile applications of fiber-based coiled linear actuators

### 2.6.3.1 Artificial muscle

Artificial muscle is one of the most common application of thermally powered actuator. For example, the nylon yarn can be fabricated into artificial muscle by twisting insertion. In 2017, artificial muscle made by super-coiled conductive nylon sewing thread was exhibited, which offered strong mechanical power and were applied to the grab of robotic hand (Figure 2.20)[43]. The artificial muscle also had rather quick responses to the electrical irritation within only 30 milliseconds, which was much less than the normal actuating time of human muscle, thus obtaining better performance and enlarging applications in bionic field. However, the working temperature range of deployed materials was limited (below 100 ℃), as the maximum load of the coiled nylon sewing thread decreased rapidly when the yarn was overheated. The low heat resistance had restricted the further promotion in terms of actuating deformation.

Figure 2. 20 Robotic muscles made by conductive nylon sewing thread

## 2.6.3.2 Energy harvesting

Energy-harvesting apparatuses were developed by torsional and tensile thermally powered actuators made from common nylon or polyethylene fishing line, converting thermal energy into electrical energy (Figure 2.21)[44]. The torsional actuator was powered by hot/cold air to spin the magnetic rotor (maximum speed: 70000 rpm) for more than 300000 cycles. The tensile actuator can produce 1.4J of electrical energy every cycle when heated/cooled by water flow.
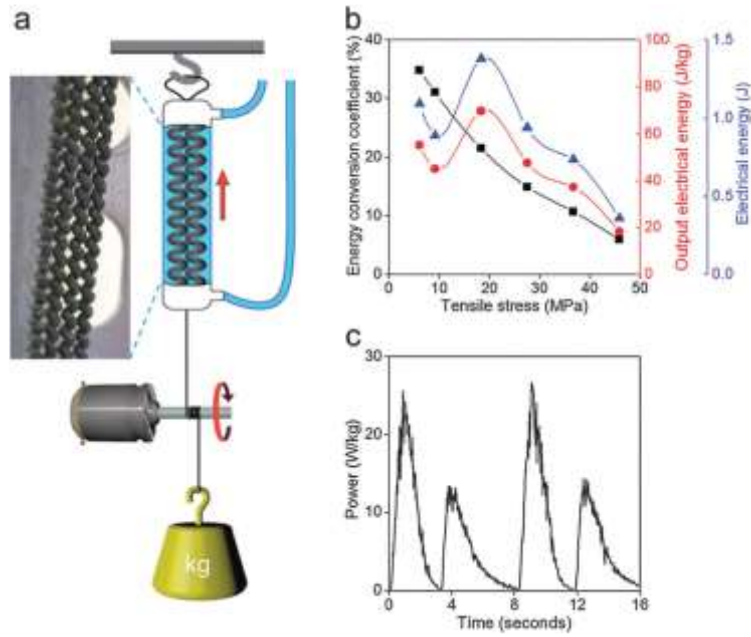
Figure 2. 21 Energy-harvesting apparatus made by tensile thermally powered actuator

Another CNT yarn energy harvesting apparatus was also demonstrated by Kim et al[45], wherein tensile/torsional mechanical energy was converted electrochemically into electrical energy (Figure 2.22). 250 watts/kg of electrical power can be generated by stretching the coiled yarns with a frequency of 30Hz.
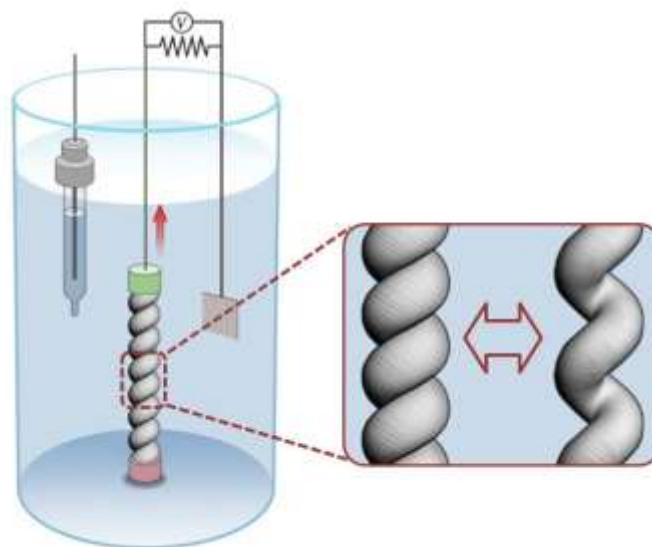


Figure 2. 22 Tensile electrochemical energy harvesting system

## 2.6.3.3 Sensor

A torsional actuator was fabricated as glucose sensor by two-end-tethered twisted nanogel-guested CNT yarn (Figure 2.23)[46]. The nanogel can swell/deswell with the binding/unbinding between the glucose-sensing material and glucose, thus cause the rotation of the torsional actuator. This bio-sensor can be applied to monitor the variation of glucose concentration with high sensitivity and short response time while no extra electrical power source needs to be supplied.
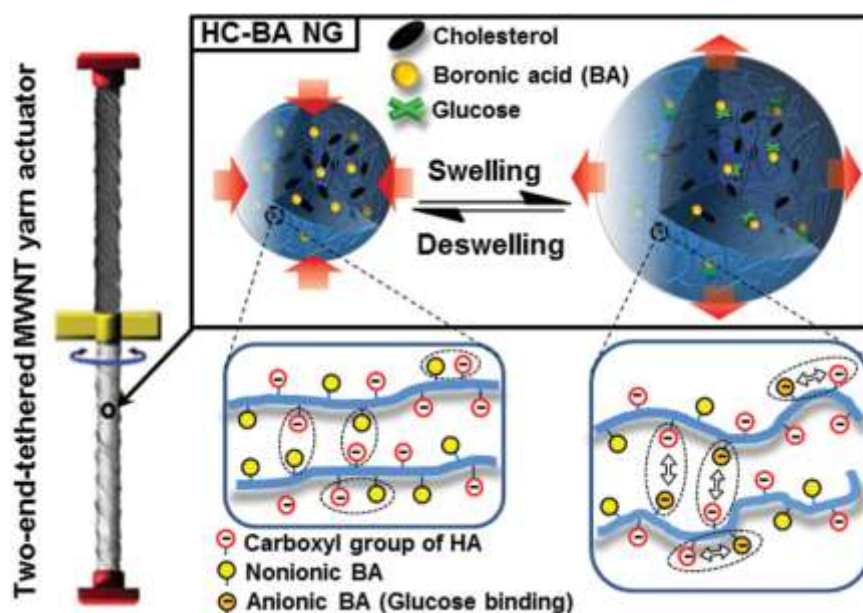


Figure 2. 23 Glucose sensor made by CNT yarn-based torsional actuator

## 2.6.3.4 Smart textile and cloths

Cotton yarns were twisted and coiled into spring-like actuators that can contract with moisture irritation.  A smart textile equipped with this moisture-driven actuator was demonstrated as a structure-adjustable garment that can open gaps for releasing sweat when humidity was high enough during sports (Figure 2.24A)[47]. The moisture-driven actuator was attached on the flaps which was closed without humidity. When perspiration and moisture came out, the actuator contracted and flaps opened for

alleviating body discomfort. Besides, similar application was demonstrated as smart sleeves made by moisture-driven coiled silk actuators (Figure 2.24C)[48]. The sleeves can shrink when humidity increase, owing to the contraction of moisture-driven actuators, while the sleeves expanded when the humidity decrease. The smart sleeves can be used for moisture/thermal management and skin comfort during physical sports.

Apart from application of actuator based on tensile actuation, torsional actuator can also be used in the smart textiles field. For example, a smart window was fabricated with moisture-driven torsional actuators based on twisted cotton yarn, which were knitted through 2cm-wide and 5cm-long fabrics (Figure 2.24B)[49]. In sunny day, the smart window kept open in the dry environment, while it closed in rainy day with high humidity, owing to the torsional actuations of the moisture-driven actuators that can rotate 5.6 times of their weight.
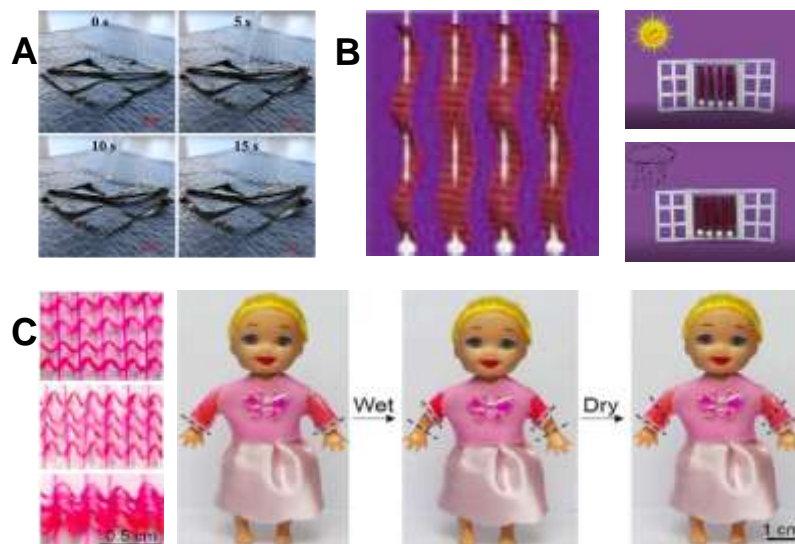


Figure 2.24 Application of fiber-based coiled linear actuators as smart textile and clothes. (A) Structure-adjustable garment (B) Smart window (C) Smart sleeves

**2.6.4 Fiber-based linear actuators with double level coils**

The twisted and coiled fiber or yarn can be further twisted into "supercoiled state" or called "double-level coil" state. For example, spandex@carbon nanotube fiber was twisted into supercoiled structure (Figure 2.25A) and applied as transmission line, artificial muscle etc[50]. The supercoiled structure imparts high stretchability (-800 ~1500 %) to the actuator, as well as effective actuation (-4.2%). By the same method, 8 strands of spandex fibers were super-twisted into $2^{nd}$-order coiled actuator (Figure 2.25C) and achieved maximum tensile actuation of 45% from ambient temperature to 130, as well as specific work of 1523 J/kg (40 times higher than natural muscle)[51].

Another similar type of actuator with double-level coil was prepared by twisting multiwalled carbon nanotubes fibers, prior to set to spring shape though thermo-hydro method (Figure 2.25B)[52]. The spring-like hierarchically arranged helical fibers were successfully applied as actuator and solvent sensor, due to high sensitivity to organic solvents, e.g. dichloromethane, acetone and ethanol. Maximum strain of 59% was achieved when the sample-to-solvent distance changed from 6 cm to 4 cm, and the performance can be kept for at least 50 cycles.
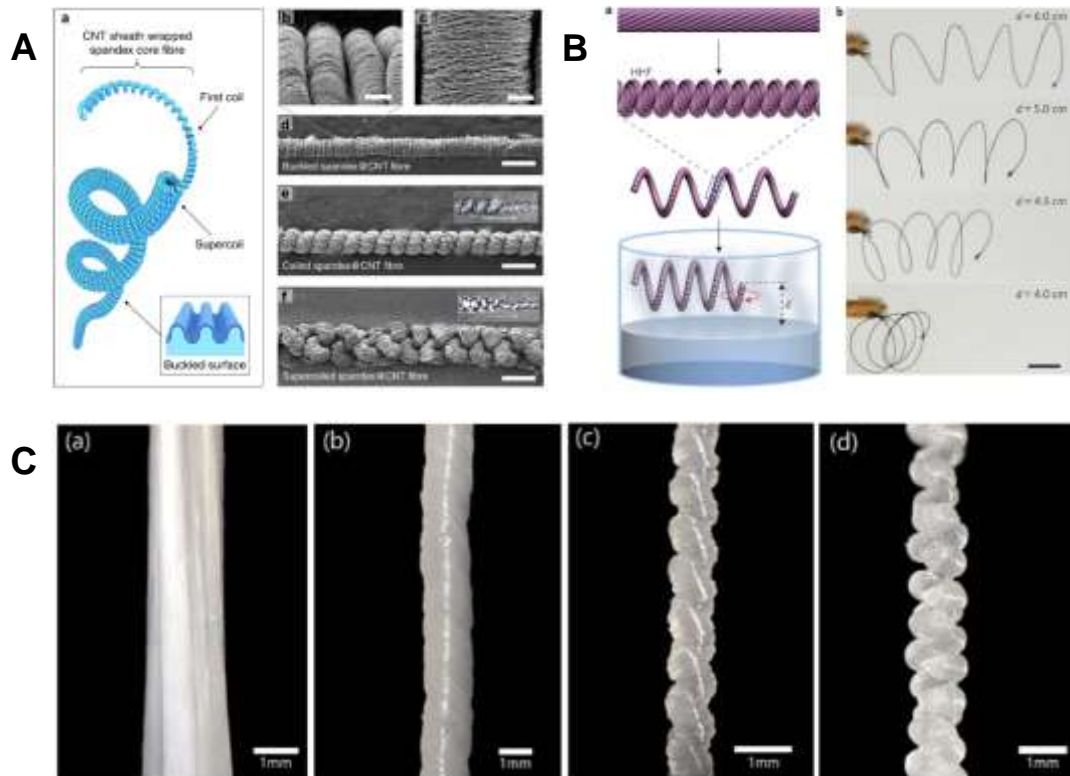
Figure 2.25 Fiber-based linear actuators with double level coils. (A) Supercoiled spandex@canbon nanotube fiber; (B) Hierarchically arranged helical fibers based on multiwalled carbon nanotubes; (C) Twisted and coiled soft actuator based on spandex fiber.

## 2.7 Summary

Various types of actuators have been reviewed, including traditional actuators, electric actuators, ionic actuators, shape memory alloy actuator and fiber-based coiled actuators. A comparison of those actuators is summarized in Table 2.1.

Table 2. 1 Properties and performances of different actuators and skeletal muscle

| Actuator | | Strain /% | Voltage /V | Specific work /J/kg | Stress /MPa | Ref. | Shortcoming |
|---|---|---|---|---|---|---|---|
| Traditional | Electric motor | 8.9 | 24 | - | - | [2] | Rigid |
| | Pneumatic actuator | 41.5 | - | - | 0.005 | [53] | Complex |
| | Hydraulic actuator | 24.0 | - | - | - | [54] | Complex |
| Electric | Dielectric elastomer | 10-380 | >1000 | ≈10-150 | - | [14, 55] | High voltage |
| | Piezoelectric | 3.5-7 | >1000 | - | 45 | [56] | High voltage; low strain |
| | Electrostrictive elastomer | 2.5-4 | - | ≈500 | | [14, 55] | Low strain |
| | Liquid crystal elastomer | < 10 | - | ≈20 | - | [57] | Low strain |
| Ionic | Gel | 50-100 | 2 | - | - | [58] | Low stress |
| | Polymer–metal composites | 3 | 1-5 | - | 3-30 | [59-61] | Low strain |
| | Conducting polymer | 2 | 2-10 | ≈325 | 5-34 | [14, 25, 55] | High cost; low strain |
| Shape memory alloy | | 6 | - | ≈100 | 1 | [55, 57] | High cost; high hysteresis |
| Coiled actuator | Nylon | 34 | - | 2480 | 83.6 | [29] | unadjustable structure |
| | CNT | 2.8 | 18.3 | - | 6.8 | [34] | How strain; high cost; not safe |
| | PE | 23 | - | 120k | 20 | [31] | unadjustable structure |
| | PET | 15.6 | 6 | - | 6.2 | [33] | unadjustable structure |
| | CF | 7.2 | 7.5 | 758 | 60 | [36] | uncontrollable volume fraction |
| | PE/COCe | 11.8 | - | - | 0.07 | [37] | uncontrollable volume fraction |
| Skeletal Muscles | | 20-40 | - | 38.6 | 0.1-0.35 | [29, 55] | - |

NOTE: ms is milliseconds; RT is room temperature.

Traditional actuators have relatively larger energy density whereas the structures are complex, bulky and not prone to be miniatured. Electric actuators are apt to achieve high response frequency and stress, while the excitation voltages are rather high. Ionic actuators can realize large strain, but both the stress and stability are low. Shape memory alloy actuators possess high deformability whereas the hysteresis is too high.

Comparing to above types of actuators, fiber-based coiled actuators have obvious advantages in multiple aspects, including flexible and simple structure, high stress, high strain, high energy density, low voltage to actuate, low hysteresis, low cost etc. The fiber-based coiled actuators can be fabricated by many types of fiber/yarn, e.g. PA, CNT, PE, PET etc. Each of fiber/yarn has specifically advantageous performance in certain aspects, whereas there was few flexible and precise performance design for actuators. Various power sources have been applied to trigger the actuators, including air-heating, hydrothermal, electrothermal, chemically thermal, biothermal power etc, wherein few investigations are focused on the performance of actuators under extremely cold condition. More works should be done in the material selection, structure control and design, process optimization and systematic research on actuating mechanism.

# References

[1]     J. D. Madden, "Mobile robots: motor challenges and materials solutions," *Science,* vol. 318, no. 5853, pp. 1094-1097, 2007.

[2]     J. Kim and J. Chang, "A New Electromagnetic Linear Actuator for Quick Latching," *IEEE Transactions on Magnetics,* vol. 43, no. 4, pp. 1849-1852, 2007.

[3]     C. Lee, M. Kim, Y. J. Kim, N. Hong, S. Ryu, H. J. Kim, and S. Kim, "Soft robot review," *International Journal of Control, Automation and Systems,* vol. 15, no. 1, pp. 3-15, 2017.

[4]     M. T. Tolley, R. F. Shepherd, B. Mosadegh, K. C. Galloway, M. Wehner, M. Karpelson, R. J. Wood, and G. M. Whitesides, "A Resilient, Untethered Soft Robot," *Soft Robotics,* vol. 1, no. 3, pp. 213-223, 2014.

[5]     C. D. Onal and D. Rus, "Autonomous undulatory serpentine locomotion utilizing body dynamics of a fluidic soft robot," *Bioinspiration & Biomimetics,* vol. 8, no. 2, p. 026003, Jun 2013.

[6]     R. K. Katzschmann, A. D. Marchese, and D. Rus, "Hydraulic autonomous soft robotic fish for 3D swimming," in *Experimental Robotics*, 2016, pp. 405-420: Springer.

[7]     P. Polygerinos, Z. Wang, K. C. Galloway, R. J. Wood, and C. J. Walsh, "Soft robotic glove for combined assistance and at-home rehabilitation," *Robotics and Autonomous Systems,* vol. 73, pp. 135-143, 2015.

[8]     D. Chen and Q. Pei, "Electronic Muscles and Skins: A Review of Soft Sensors

and Actuators," *Chemical Reviews,* vol. 117, no. 17, pp. 11239-11268, Sep 13 2017.

[9]     P. Brochu and Q. Pei, "Advances in dielectric elastomers for actuators and artificial muscles," *Macromolecular rapid communications,* vol. 31, no. 1, pp. 10-36, 2010.

[10]    S. C. Lee, I. K. Kwon, and K. Park, "Hydrogels for delivery of bioactive agents: a historical perspective," *Advanced drug delivery reviews,* vol. 65, no. 1, pp. 17-20, 2013.

[11]    Q. Wang and F. Li, "A low-working-field (2 kV/mm), large-strain (>0.5%) piezoelectric multilayer actuator based on periodically orthogonal poled PZT ceramics," *Sensors and Actuators A: Physical,* vol. 272, pp. 212-216, 2018.

[12]    S. M. Mirvakili and I. W. Hunter, "Artificial Muscles: Mechanisms, Applications, and Challenges," *Advanced Materials,* vol. 30, no. 6, Feb 2018.

[13]    S. Xu, B. J. Hansen, and Z. L. Wang, "Piezoelectric-nanowire-enabled power source for driving wireless microelectronics," *Nature communications,* vol. 1, p. 93, 2010.

[14]    T. Mirfakhrai, J. D. W. Madden, and R. H. Baughman, "Polymer artificial muscles," *Materials Today,* vol. 10, no. 4, pp. 30-38, 2007.

[15]    R. Casalini and C. Roland, "Highly electrostrictive poly (vinylidene fluoride–trifluoroethylene) networks," *Applied Physics Letters,* vol. 79, no. 16, pp. 2627-2629, 2001.

[16]    J. Su, J. S. Harrison, and T. L. S. Clair, "Electrostrictive graft elastomers," ed:

Google Patents, 2003.

[17]   C. Huang, R. Klein, F. Xia, H. Li, Q. Zhang, F. Bauer, and Z. Cheng, "Poly (vinylidene fluoride-trifluoroethylene) based high performance electroactive polymers," *IEEE Transactions on Dielectrics and Electrical Insulation,* vol. 11, no. 2, pp. 299-311, 2004.

[18]   W. Lehmann, H. Skupin, C. Tolksdorf, E. Gebhard, R. Zentel, P. Krüger, M. Lösche, and F. Kremer, "Giant lateral electrostriction in ferroelectric liquid-crystalline elastomers," *Nature,* vol. 410, no. 6827, p. 447, 2001.

[19]   C. Huang, Q. Zhang, and A. Jákli, "Nematic Anisotropic Liquid‐Crystal Gels—Self‐Assembled Nanocomposites with High Electromechanical Response," *Advanced Functional Materials,* vol. 13, no. 7, pp. 525-529, 2003.

[20]   K. Deligkaris, T. S. Tadele, W. Olthuis, and A. van den Berg, "Hydrogel-based devices for biomedical applications," *Sensors and Actuators B: Chemical,* vol. 147, no. 2, pp. 765-774, 2010.

[21]   L.-W. Xia, R. Xie, X.-J. Ju, W. Wang, Q. Chen, and L.-Y. Chu, "Nano-structured smart hydrogels with rapid response and high elasticity," *Nature communications,* vol. 4, p. 2226, 2013.

[22]   J. Kim, S. H. Bae, M. Kotal, T. Stalbaum, K. J. Kim, and I. K. Oh, "Soft but Powerful Artificial Muscles Based on 3D Graphene–CNT–Ni Heteronanostructures," *Small,* vol. 13, no. 31, p. 1701314, 2017.

[23]   Y. Yan, T. Santaniello, L. G. Bettini, C. Minnai, A. Bellacicca, R. Porotti, I. Denti, G. Faraone, M. Merlini, and C. Lenardi, "Electroactive ionic soft

actuators with monolithically integrated gold nanocomposite electrodes," *Advanced Materials,* vol. 29, no. 23, p. 1606109, 2017.

[24] J. Arias-Pardilla, T. F. Otero, J. G. Martínez, and Y. A. Ismail, "Biomimetic Sensing–Actuators Based on Conducting Polymers," in *Aspects on Fundaments and Applications of Conducting Polymers*: Intechopen, 2012.

[25] G. M. Spinks, V. Mottaghitalab, M. Bahrami‐Samani, P. G. Whitten, and G. G. Wallace, "Carbon‐nanotube‐reinforced polyaniline fibers for high‐strength artificial muscles," *Advanced Materials,* vol. 18, no. 5, pp. 637-640, 2006.

[26] A. Maziz, C. Plesse, C. Soyer, C. Chevrot, D. Teyssié, E. Cattan, and F. Vidal, "Demonstrating kHz frequency actuation for conducting polymer microactuators," *Advanced Functional Materials,* vol. 24, no. 30, pp. 4851-4859, 2014.

[27] S. M. Mirvakili and I. W. Hunter, "Fast Torsional Artificial Muscles from NiTi Twisted Yarns," *ACS applied materials & interfaces,* vol. 9, no. 19, pp. 16321-16326, 2017.

[28] S.-H. Song, J.-Y. Lee, H. Rodrigue, I.-S. Choi, Y. J. Kang, and S.-H. Ahn, "35 Hz shape memory alloy actuator with bending-twisting mode," *Scientific reports,* vol. 6, p. 21118, 2016.

[29] C. S. Haines, M. D. Lima, N. Li, G. M. Spinks, J. Foroughi, J. D. W. Madden, S. H. Kim, S. Fang, M. J. d. Andrade, F. Göktepe, Ö. Göktepe, S. M. Mirvakili, S. Naficy, X. Lepró, J. Oh, M. E. Kozlov, S. J. Kim, X. Xu, B. J. Swedlove, G.

G. Wallace, and R. H. Baughman, "Artificial muscles from fishing line and sewing thread," *Science,* vol. 343, no. 6173, pp. 868-872, 2014.

[30]   N. Li, C. S. Haines, M. D. Lima, M. Jung de Andrade, S. Fang, J. Oh, M. E. Kozlov, F. Goktepe, O. Goktepe, D. Suh, and R. H. Baughman, "Coiled and non-coiled twisted nanofiber yarn and polymer fiber torsional and tensile actuators," Patent WO2014022667 (A2), 2014.

[31]   M. Hiraoka, K. Nakamura, H. Arase, K. Asai, Y. Kaneko, S. W. John, K. Tagashira, and A. Omote, "Power-efficient low-temperature woven coiled fibre actuator for wearable applications," *Scientific Reports,* vol. 6, p. 36358, Nov 4 2016.

[32]   R. Melvinsson, "Textile actuator fibers," Master, The Swedish School of Textiles, University of Boras, Sweden, 2015.

[33]   J. Park, J. W. Yoo, H. W. Seo, Y. Lee, J. Suhr, H. Moon, J. C. Koo, H. R. Choi, R. Hunt, K. J. Kim, S. H. Kim, and J.-D. Nam, "Electrically controllable twisted-coiled artificial muscle actuators using surface-modified polyester fibers," *Smart Materials and Structures,* vol. 26, no. 3, p. 035048, 2017.

[34]   M. D. Lima, N. Li, M. Jung de Andrade, S. Fang, J. Oh, G. M. Spinks, M. E. Kozlov, C. S. Haines, D. Suh, J. Foroughi, S. J. Kim, Y. Chen, T. Ware, M. K. Shin, L. D. Machado, A. F. Fonseca, J. D. Madden, W. E. Voit, D. S. Galvao, and R. H. Baughman, "Electrically, chemically, and photonically powered torsional and tensile actuation of hybrid carbon nanotube yarn muscles," *Science,* vol. 338, no. 6109, pp. 928-32, Nov 16 2012.

[35]     N. Li, C. S. Haines, M. D. Lima, M. Jung de Andrade, S. Fang, J. Oh, M. E. Kozlov, D. Suh, and R. H. Baughman, "Coiled and non-coiled nanofiber yarn torsional and tensile actuators," Patent US20150152852A1, 2015.

[36]     C. Lamuta, S. Messelot, and S. Tawfick, "Theory of the tensile actuation of fiber reinforced coiled muscles," *Smart Materials and Structures,* vol. 27, no. 5, 2018.

[37]     M. Kanik, S. Orguc, G. Varnavides, J. Kim, T. Benavides, D. Gonzalez, T. Akintilo, C. C. Tasan, A. P. Chandrakasan, Y. Fink, and P. Anikeeva, "Strain-programmable fiber-based artificial muscle," *Science,* vol. 365, no. 6449, pp. 145–150, 2019.

[38]     L. Wu, M. Jung de Andrade, R. S. Rome, C. Haines, M. D. Lima, R. H. Baughman, and Y. Tadesse, "Nylon-muscle-actuated robotic finger," vol. 9431, p. 94310I, 2015.

[39]     A. Cherubini, G. Moretti, R. Vertechy, and M. Fontana, "Experimental characterization of thermally-activated artificial muscles based on coiled nylon fishing lines," *AIP Advances,* vol. 5, no. 6, p. 067158, 2015.

[40]     P. Zhang, U. Ayaugbokor, S. Ibekwe, D. Jerro, S.-S. Pang, P. Mensah, and G. Li, "Healing of polymeric artificial muscle reinforced ionomer composite by resistive heating," *Journal of Applied Polymer Science,* vol. 133, no. 28, 2016.

[41]     J. A. ScienceLee, N. Li, C. S. Haines, K. J. Kim, X. Lepro, R. Ovalle-Robles, S. J. Kim, and R. H. Baughman, "Electrochemically Powered, Energy-Conserving Carbon Nanotube Artificial Muscles," *Advanced Materials,* vol. 29, no. 31, Aug 2017.

[42] S. H. Lee, T. H. Kim, M. D. Lima, R. H. Baughman, and S. J. Kim, "Biothermal sensing of a torsional artificial muscle," *Nanoscale,* vol. 8, no. 6, pp. 3248-53, Feb 14 2016.

[43] M. C. Yip and G. Niemeyer, "High-Performance Robotic Muscles from Conductive Nylon Sewing Thread," in *Proceedings of 2015 IEEE International Conference on Robotics and Automation*, Washington State Convention Center, 2015, pp. 2313-2318: IEEE.

[44] S. H. Kim, M. D. Lima, M. E. Kozlov, C. S. Haines, G. M. Spinks, S. Aziz, C. Choi, H. J. Sim, X. Wang, H. Lu, D. Qian, J. D. W. Madden, R. H. Baughman, and S. J. Kim, "Harvesting temperature fluctuations as electrical energy using torsional and tensile polymer muscles," *Energy & Environmental Science,* vol. 8, no. 11, pp. 3336-3344, 2015.

[45] S. H. Kim, C. S. Haines, N. Li, K. J. Kim, T. J. Mun, C. Choi, J. Di, Y. J. Oh, J. P. Oviedo, J. Bykova, S. Fang, N. Jiang, Z. Liu, R. Wang, P. Kumar, R. Qiao, S. Priya, K. Cho, M. Kim, M. S. Lucas, L. F. Drummy, B. Maruyama, D. Y. Lee, X. Lepró, E. Gao, D. Albarq, R. Ovalle-Robles, S. J. Kim, and R. H. Baughman, "Harvesting electrical energy from carbon nanotube yarn twist," *Science,* vol. 357, no. 6353, pp. 773-778, 2017.

[46] J. Lee, S. Ko, C. H. Kwon, M. D. Lima, R. H. Baughman, and S. J. Kim, "Carbon Nanotube Yarn-Based Glucose Sensing Artificial Muscle," *Small,* vol. 12, no. 15, pp. 2085-91, Apr 2016.

[47] X. Yang, W. Wang, and M. Miao, "Moisture-Responsive Natural Fiber Coil-

Structured Artificial Muscles," *ACS Appl Mater Interfaces,* vol. 10, no. 38, pp. 32256-32264, Sep 26 2018.

[48]   T. Jia, Y. Wang, Y. Dou, Y. Li, M. Jung de Andrade, R. Wang, S. Fang, J. Li, Z. Yu, R. Qiao, Z. Liu, Y. Cheng, Y. Su, M. Minary‑Jolandan, R. H. Baughman, D. Qian, and Z. Liu, "Moisture Sensitive Smart Yarns and Textiles from Self‑Balanced Silk Fiber Muscles," *Advanced Functional Materials,* vol. 29, no. 18, 2019.

[49]   Y. Li, X. Leng, J. Sun, X. Zhou, W. Wu, H. Chen, and Z. Liu, "Moisture-sensitive torsional cotton artificial muscle and textile," *Chinese Physics B,* vol. 29, no. 4, 2020.

[50]   W. Son, S. Chun, J. M. Lee, Y. Lee, J. Park, D. Suh, D. W. Lee, H. Jung, Y. J. Kim, Y. Kim, S. M. Jeong, S. K. Lim, and C. Choi, "Highly twisted supercoils for superelastic multi-functional fibres," *Nature Communications,* vol. 10, no. 1, p. 426, Jan 25 2019.

[51]   S. Y. Yang, K. H. Cho, Y. Kim, M.-G. Song, H. S. Jung, J. W. Yoo, H. Moon, J. C. Koo, J.-d. Nam, and H. R. Choi, "High performance twisted and coiled soft actuator with spandex fiber for artificial muscles," *Smart Materials and Structures,* vol. 26, no. 10, 2017.

[52]   P. Chen, Y. Xu, S. He, X. Sun, S. Pan, J. Deng, D. Chen, and H. Peng, "Hierarchically arranged helical fibre actuators driven by solvents and vapours," *Nature nanotechnology,* vol. 10, no. 12, p. 1077, 2015.

[53]   F. Daerden and D. Lefeber, "Pneumatic artificial muscles: actuators for robotics

and automation," *European journal of mechanical and environmental engineering,* vol. 47, no. 1, pp. 11-21, 2002.

[54]    S. A. Morin, R. F. Shepherd, S. W. Kwok, A. A. Stokes, A. Nemiroski, and G. M. Whitesides, "Camouflage and Display for Soft Machines," *Science,* vol. 337, no. 6096, pp. 828-832, 2012.

[55]    J. D. Madden, N. A. Vandesteeg, P. A. Anquetil, P. G. Madden, A. Takshi, R. Z. Pytel, S. R. Lafontaine, P. A. Wieringa, and I. W. Hunter, "Artificial muscle technology: physical principles and naval prospects," *IEEE Journal of oceanic engineering,* vol. 29, no. 3, pp. 706-728, 2004.

[56]    J. Huber, N. Fleck, and M. Ashby, "The selection of mechanical actuators based on performance indices," *Proceedings of the Royal Society of London. Series A: Mathematical, physical and engineering sciences,* vol. 453, no. 1965, pp. 2185-2205, 1997.

[57]    Z. Peng, "Study on thermally activated coiled linear actuators made from polymer fibers," Master, Institute of Textiles and Clothing, The Hong Kong Polytechnic University, Hong Kong, 2018.

[58]    S. Schuhladen, F. Preller, R. Rix, S. Petsch, R. Zentel, and H. Zappe, "Iris‐Like Tunable Aperture Employing Liquid‐Crystal Elastomers," *Advanced Materials,* vol. 26, no. 42, pp. 7247-7251, 2014.

[59]    M. Shahinpoor and K. J. Kim, "Ionic polymer-metal composites: I. Fundamentals," *Smart materials and structures,* vol. 10, no. 4, p. 819, 2001.

[60]    S. Nemat-Nasser, "Micromechanics of actuation of ionic polymer-metal

composites," *Journal of applied Physics,* vol. 92, no. 5, pp. 2899-2915, 2002.

[61]	P. Ariano, D. Accardo, M. Lombardi, S. Bocchini, L. Draghi, L. De Nardo, and

P. Fino, "Polymeric materials as artificial muscles: an overview," *Journal of*

*applied biomaterials & functional materials,* vol. 13, no. 1, pp. 1-9, 2015.

# CHAPTER 3
# FABRICATION AND CHARACTERIZATION OF PI/PDMS COMPOSITE YARNS

## 3.1 Introduction

Fiber-based coiled linear actuators (FCLAs) have been a significant research field in recent years, owning to their wide applications, such as artificial muscle[1], intelligent robots[2, 3], prosthetic limbs for medical care[4], deformable textile[4] and energy harvesting[5]. As illustrated in Chapter 2, compared with many other types of actuators, FCLAs have obvious advantages in multiple aspects, including flexible and simple structure, high stress, high strain, high energy density, low voltage to actuate, low hysteresis, low cost etc. The basic actuating principle lies in the anisotropic property of the fiber, in which the expansion/contraction in radial direction is largely different from that in axial direction during temperature increase/decrease[4], solvent-absorption/desorption[6, 7] etc. Appropriate composite structure design of FCLAs can magnify the anisotropy, thus achieving better actuating performance. However, many FCLAs are made from single-component fibers, so the contracting stroke and actuating power are limited by the fixed material component, thus the intrinsic properties of used materials can only satisfy certain capacity requirement rather than desired power in a wide range. Other FCLAs with composite structure can be programmable and

controllable to achieve different spring index, tensile strain and work capacity[8, 9], whereas volume fraction of each component have not been adjusted for optimizing the performance. Besides, few investigations are focused on the actuating effects of FCLAs under extremely cold condition (e.g. from -50 °C to room temperature).

Therefore, in this chapter, preliminary studies will be carried out for fabricating programmable helical composite yarn actuators (HCYAs) with wide working temperature range. First, a series of polymers or carbon materials will be investigated and compared for selecting proper fiber substrates and polymer matrix that can achieve high anisotropy and chemical/physical stability. Many other factors will be also taken into consideration, including temperature-resistance, ductile/brittle transition temperature, thermal expansion and safety property. Secondly, appropriate coating processes will be explored to fabricate composite yarns that can meet the aimed requirements (high evenness, high anisotropy, high chemical/physical stability, ductile under wide temperature range, safe). Finally, the morphology and thermomechanical properties of the prepared composite yarns will be tested and analyzed. The works about composite yarn in this chapter will pave a fundamental road for fabricating high-performance HCYAs which will be described in the following chapters.

## 3.2 Experimental

### 3.2.1 Materials

Polyimide (PI) filament yarn of 200D/100f  (Suplon® ， Aoshen, China), i.e.

monofilaments of 2.1dtex (a diameter of 11 μm), was used as host material of the composite yarn. Polydimethylsiloxane (PDMS) liquid silicone rubber (ELASTOSIL® LR 7665 AB, Wacker, Germany) was selected as polymer matrix to offer an expansion in radial direction of the composite yarn. Ethyl acetate (ACS Grade, ANAQUA, Hong Kong) was adopted to dilute PDMS for lowering down the viscosity and coating the PI filament yarn evenly. Polyester (PET) filament yarn of 150D (Dhoma, China) was also applied to fabricate PET/PDMS composite yarn for investigating the actuating mechanism.

### 3.2.2 Fabrication of PI/PDMS composite yarns

### 3.2.2.1 Padding method

PI yarn was cut into segments with a length of 50cm (filament number: 3*100f, 6*100f or 9*100f), then were dipped into PDMS/ethyl acetate solution (w:w=1:2 or 1:4), followed by getting through a padder, in which the gap between two rollers was controlled by a digital level at 0.03mm, 0.1mm or 0.2mm for PI filament of 3*100f, 6*100f or 9*100f, respectively (Figure 3.1). After dipping and padding once or several times, the PDMS-coated PI yarns were vulcanized at 80 °C for 3h before PI/PDMS composite yarns were achieved.
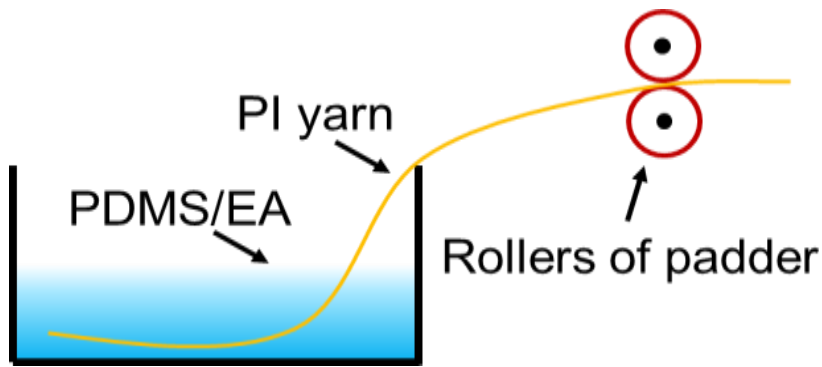
Figure 3. 1 Processing system of padding method.

### 3.2.2.2 Dip-coating method

PI yarn segments mentioned above were soaked into PDMS/ethyl acetate solution for a period (3min~3h), then elevated gradually by motor with a speed of about 15cm/min to realize even coating (Figure 3.2). Afterwards, the coated PI yarn segments were vulcanized by the same parameter as above.
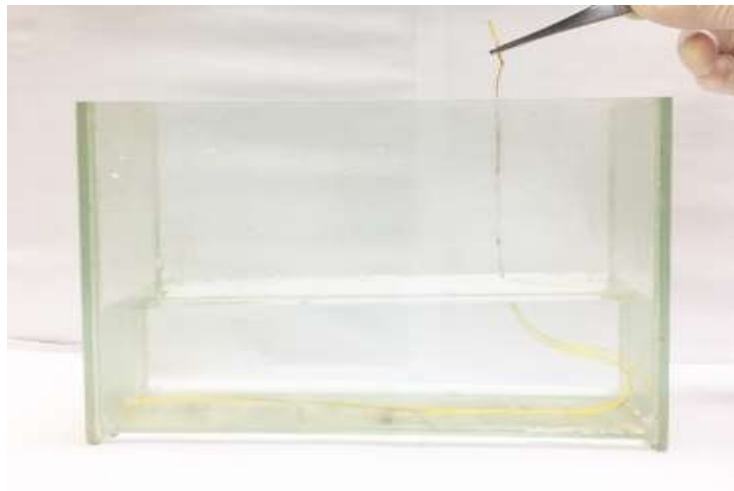


Figure 3. 2 Processing system of dip-coating method

### 3.2.2.3 Glass board method

Glass board method was a coating process completed on a glass board rather than in the glass jar mentioned above. This method can achieve a high PDMS volume fraction of over 80%. The concrete steps were as follows:

a. Cut 30cm long segment of the PI yarn, then draw out the monofilaments.

b. Wind the monofilaments to metal framework, which two ends were winded by the double-sided tape (Figure 3.3A).

c. Coat the fixed monofilaments with PDMS/ethyl acetate solution (1:2) on the glass board, then vulcanize PDMS at 150 °C for 30min. Repeat this step for 2 times (Figure 3.3B).

d. Combine seven coated monofilaments into a yarn, which was then dipped into PDMS/ethyl acetate solution (1:5) without tension and vulcanized at 90 °C for one night (Figure 3.3C).

e. Cool down in ambient air.
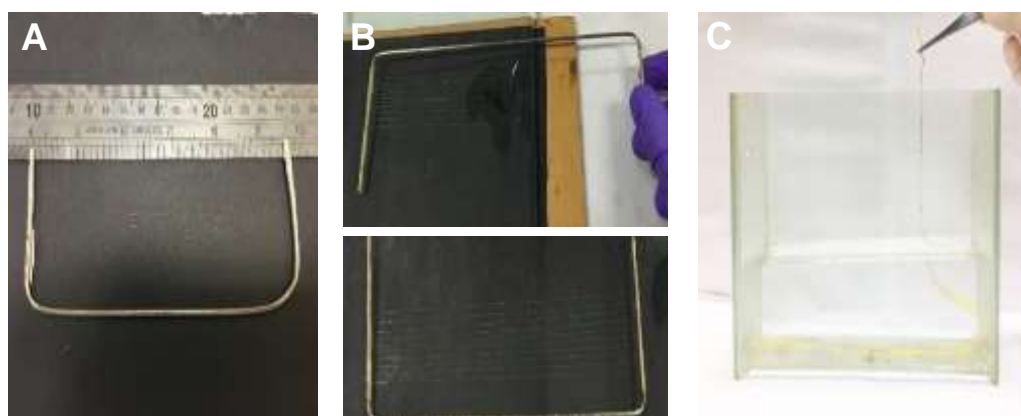


Figure 3. 3 Process of glass board method. (A) Wind the monofilaments to metal framework (B) Dip-coating monofilaments with tension (C) Dip-coating the yarn made by combined and coated monofilament without tension

### 3.2.2.4 Nozzle-coating method

Nozzle-coating method means coating a monofilament by drawing it through a narrow nozzle (Figure 3.4) which can achieve a high PDMS volume fraction. However,

intermittent bead may form due to high surface tension between PI and PDMS. The steps were as follows:

a. Get syringe half-filled with PDMS.

b. Insert an iron wire (200um) which is winded by PI monofilament.

c. Fix a nozzle (400um) on the head of syringe.

d. Draw iron wire out of nozzle for coating PI monofilament
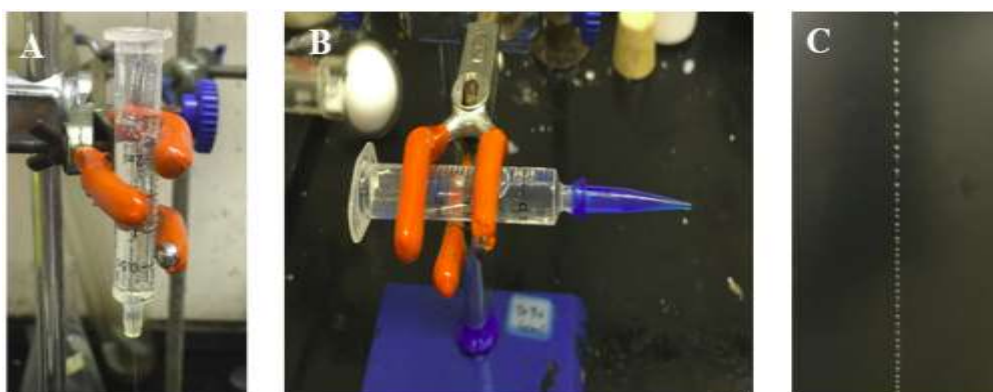


Figure 3. 4 Process of nozzle-coating method. (A) Iron wire/PI monofilament goes through syringe half-filled with PDMS (B) Draw iron wire out of nozzle for coating PI monofilament (C) PDMS bead forms gradually after coating

**3.2.2.5 Capillary method**

Capillary method took the advantages of vacuum and capillary to fabricate PI/PDMS composite fiber or yarn with a very high PDMS volume fraction of almost 100% (Figure 3.5). The explicit steps were as follows:

a. Make the PI monofilament go through the capillary.

b. Pump PDMS into capillary.

c. Vulcanize PDMS in ambient temperature for 2 days.

d. Break capillary by boiling water, utilizing the expansion of PDMS.

e. Take the PDMS/PI string out of capillary.
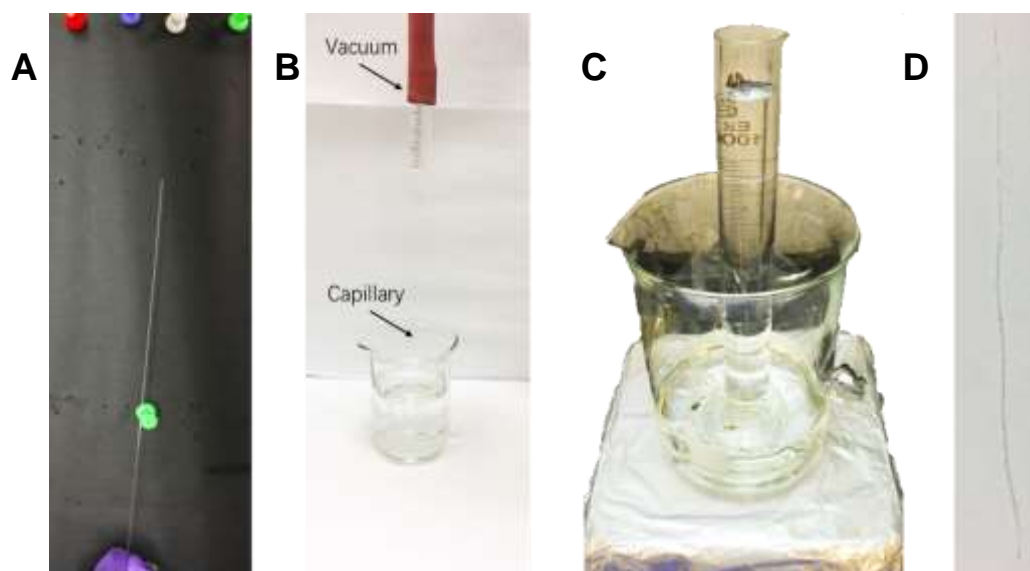


Figure 3. 5 Process of capillary method (A) Make PI monofilament go through the capillary (B) Pump PDMS into capillary (C) Boil water to break capillary due to expansion of PDMS (D) Take the PI/PDMS string out of capillary

### 3.2.3 Characterization of PI/PDMS composite yarns

### 3.2.3.1 Morphology

Electron microscope (Leica M165 C or DFC290 HD) and scanning electron microscope (Hitachi TM3000) were adopted to measure the surface morphology, diameter and cross section of PI/PDMS composite yarn or PI monofilament.

### 3.2.3.2 Volume fraction

The volume fraction of PDMS in PI/PDMS composite yarn was calculated by following formula:

$$\text{Volume fraction (\%)} = \frac{\frac{m(\text{composite}) - m(\text{PI})}{\rho(\text{PDMS})}}{\frac{m(\text{composite}) - m(\text{PI})}{\rho(\text{PDMS})} + \frac{m(\text{PI})}{\rho(\text{PI})}} \times 100\%$$

wherein the mass of composite yarn was measured by electronic balance (Sartorius, 0.01mg resolution) while that of PI yarn was measured by linear density test machine (Mesdan lab, CT022, Italy). The densities of PDMS and PI were obtained by observing the volume change when immersing certain amount of sample into cylinder containing water.

### 3.2.3.3 Thermomechanical properties

Coefficient of thermal expansion of PI fiber or PI/PDMS composite yarn was determined by TMA (METTLER TOLEDO, TMA/SDTA 1+) in tension/compression mode for axial/radial direction and modulus of PI/PDMS composite yarn was tested by DMA (METTLER TOLEDO, DMA 1) through the same mode as above.

## 3.3 Results and discussions

### 3.3.1 Material selection

As stated in the introduction part, in order to fabricate programmable HCYAs with wide working temperature range, the potential qualified composite yarn should own high evenness, high anisotropy, high chemical/physical stability, ductility under wide

temperature range, safety and relatively low cost. A series of candidate materials are summarized in Table 3.1. It can be seen that nylon, PET and polyethylene (PE) have relatively lower melting temperature, compared with other fiber materials (i.e. Carbon nanotube (CNT) yarn, carbon fiber (CF) and polyimide (PI) yarn), while the ductile/brittle transition temperatures are relatively higher than that of CNT yarn and PI yarn. Therefore, the working temperature ranges of nylon, PET and PE will be narrower than those of CNT yarn and PI yarn. CF can bear high temperature whereas the brittle property in radial direction restricts its machinability in super-twisting process of HCYA. CNT yarn has high temperature stability and conductivity, but the cost is relatively high currently. Therefore, PI is the best choice to be a fiber substrate for the composite yarn.

Besides, polydimethylsiloxane (PDMS) has larger coefficient of thermal expansion (CTE) than epoxy and paraffin, which facilitates higher radial thermal expansion of composite yarn, while possessing high biocompatibility and chemical stability. Therefore, PDMS can be selected as the matrix of the composite yarn and process of fabricating PI/PDMS composite yarns become the first step towards satisfied HCYAs.

Table 3. 1 Properties of potential materials for fabricating HCYA[10, 11]

| Material | $T_g$/°C | $T_m$/°C | Ductile/Brittle Transition Temperature/°C | safety | Coefficient of thermal expansion /$10^{-6}$°C$^{-1}$ |
|---|---|---|---|---|---|
| Nylon | 60 | 230 | -65 | Y | 50-90 |
| PET | 78 | 265 | -40 | Y | 59.4 |
| Polyethylene | -110 | 141 | -70 | Y | 108-200 |
| Carbon nanotube | >2000 | >2000 | <-195 | - | 19-21 |
| Carbon fiber | >2000 | >2000 | Always brittle in radial direction | Y | <2 |
| Polyimide | 410 | >500 | -270 | Y | 30-60 |
| Polydimethylsiloxane | - | - | - | Y | 776 |
| Epoxy | - | - | - | - | 45-65 |
| Paraffin | - | 37 | - | - | 106-408 |

**3.3.2 Influence factors on volume fraction of PI/PDMS composite yarns**

**3.3.2.1 Concentration of PDMS/ethyl acetate solution**

The concentration of PDMS/ethyl acetate coating solution showed obvious influence on the PDMS volume fraction in the PI/PDMS composite yarns. It can be seen from Table 3.2 that the volume fractions grow proportionately with the increase of percentage of PDMS in the coating solution for both dip-coating and padding method, i.e. the double of concentrations cause the approximate double of volume fractions.

Table 3. 2 Effect of concentration of PDMS/ethyl acetate solution

| No. | Concentration of PDMS/ethyl acetate solution | Coating method | Filament number | Volume Fraction (%) |
|-----|------------------------------------------------|----------------|-----------------|---------------------|
| 1 | 1:9 | Dip-coat once | 100 | 5.7 |
| 2 | 1:5 | Dip-coat once | 100 | 9.5 |
| 3 | 1:4 | Dip-coat once | 100 | 10.7 |
| 4 | 1:4 | Pad once | 9*100 | 26.8 |
| 5 | 1:2 | Pad once | 9*100 | 59.0 |

**3.3.2.2 Filament number of PI yarn**

Table 3.3 exhibits the variation of volume fraction when the coating processes were carried out under different filament number, coating solution concentration and coating method. It can be seen that no matter which coating solution concentration and coating method are selected, the volume fraction shows increasing trend with more filament number. A possible explanation for this might be that more filament number can supply larger interspace for the infiltration of PDMS/ethyl acetate coating solution into PI yarns, thus resulting more deposition of PDMS on PI yarn.

Table 3. 3 Effect of filament number on volume fraction

|  | Concentration of PDMS/ethyl acetate solution | Coating method | Filament number | Volume Fraction (%) |
|---|---|---|---|---|
| 1 | 1:4 | Dip-coat once | 100 | 10.7 |
| 2 | 1:4 | Dip-coat once | 2*100 | 16.2 |
| 3 | 1:4 | Dip-coat once | 3*100 | 17.2 |
| 4 | 1:4 | Dip-coat once | 6*100 | 19.8 |
| 5 | 1:4 | Dip-coat once | 9*100 | 22 |
| 6 | 1:4 | Pad once | 3*100 | 21 |
| 7 | 1:4 | Pad once | 6*100 | 24.1 |
| 8 | 1:4 | Pad once | 9*100 | 26.8 |
| 9 | 1:2 | Pad once | 3*100 | 31.1 |
| 10 | 1:2 | Pad once | 6*100 | 46.0 |
| 11 | 1:2 | Pad once | 9*100 | 59.0 |

**3.3.2.3 Padding times**

In order to investigate the effect of padding time on volume fraction during padding process, 9*100f PI yarns were padded by 1:2 PDMS/ethyl acetate solution for different treating times (Table 3.4). It can be seen that the PDMS volume fraction goes up remarkably along with the padding time. Therefore, the volume fraction can be readily controlled by padding times. Besides, high volume fraction of 78.5% can be realized with padding four times, which may contribute to high tensile actuations for thermally powered actuators.

Table 3. 4 Effect of padding times on volume fraction

| No. | Concentration of PDMS/ethyl acetate solution | Coating method | Filament number | Volume Fraction (%) |
|-----|-----|-----|-----|-----|
| 1 | 1:2 | Pad once | 9*100 | 59.0 |
| 2 | 1:2 | Pad 2 times | 9*100 | 67.1 |
| 3 | 1:2 | Pad 3 times | 9*100 | 71.3 |
| 4 | 1:2 | Pad 4 times | 9*100 | 78.5 |

### 3.3.3 Influencing factors on morphology of PI/PDMS composite yarns

### 3.3.3.1 Concentration



Figure 3. 6 PI/PDMS composite yarns coated by PDMS/ethyl acetate solution of different concentrations (from left to right: 1:4, 1:2, 1:1 and 2:1)

30f PI yarns were dip-coated by PDMS/ethyl acetate solution of different concentrations, i.e. 1:4, 1:2, 1:1 and 2:1, as shown in Figure 3.6. The higher concentration of coating solution leads to uneven coating and intermittent PDMS beads, which may affect the fabrication and performance of thermally powered actuator. The formation of PDMS beads are mainly due to high surface tension between PDMS/ethyl acetate solution and polyimide yarn, as polyimide yarn (hydrophobic) and PDMS/ethyl acetate solution (hydrophilic) have relatively large different in surface energy. The percentage of 1:4 and 1:2 seems proper concentrations for coating as almost no unevenness appears through the whole PI yarns.

### 3.3.3.2 Coating times
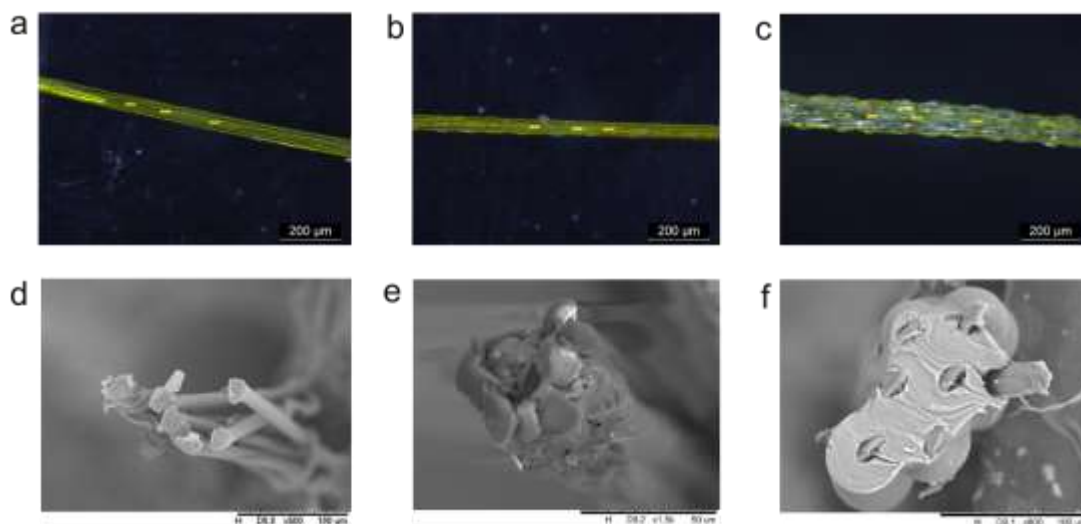


Figure 3. 7 Side view and cross section of 7f PI/PDMS composite yarn coated (a)(d) 1 time, (b)(e) 3 times and (c)(f) 5 times

Figure 3.7 illustrates the side view and cross section of 7f PI/PDMS composite yarn

dip-coated 1, 3 and 5 times. In dip-coating method, more coating times can contribute to higher volume fraction of PDMS in composite yarn. The volume fraction increases sharply from 3 times to 5 times, probably due to enlargement of interspace among the PI monofilaments after the deposition of PDMS, thus more coating solution can be absorbed through capillary effect. Besides, too many coating times may cause unevenness on the surface of composite yarn because of surface tension, so 3 times could be an appropriate choice as both relatively high volume fraction and evenness could be obtained. Finally, it can be seen that seven monofilaments cannot form a hexagonal cross-section after coating, implying that a round cross-section cannot be obtained as few coated monofilaments assign randomly in radial direction, even if this is reasonable theoretically.

### 3.3.3.3 Filament number
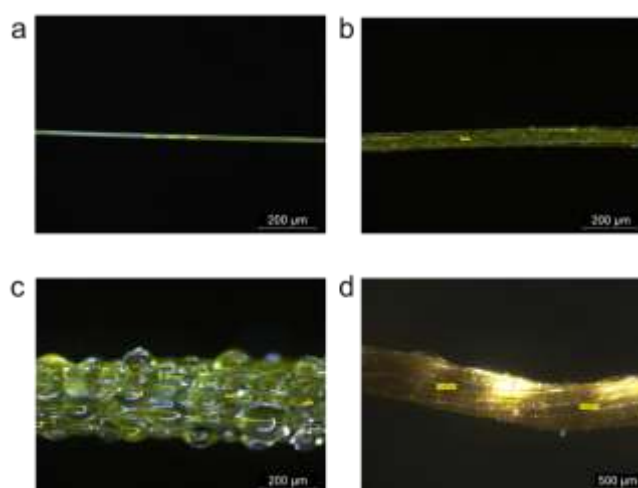


Figure 3. 8 PI/PDMS composite yarn of different filament number. (a) monofilament dip-coated once ($V_f$=5.0%) (b) 8f composite yarn dip-coated once ($V_f$=9.7%) (c) 20f composite yarn dip-coated 3 times ($V_f$=88.3%) (d) 300f composite yarn dip-coated once ($V_f$=17.2%)

Figure 3.8 presents the morphology of PI/PDMS composite yarns of different filament number. It can be seen that both the monofilament and 8f composite yarn have even coating surface, whereas the PDMS volume fractions were less than 10%, thus effective actuation may not be realized. In order to raise the volume fraction, more coating times are adopted for 20f composite yarn, nevertheless the surface became rough consequently. 300f composite yarn exhibits an advantageous state with both relatively even surface and higher volume fraction. Therefore, 300f composite yarn can be used to fabricate thermally powered actuator for obtaining effective actuation.

### 3.3.3.4 Vacuum, pressing, padding gap and stretching

During the fabricating process, many parameters may affect the morphology of PI/PDMS composite yarn, e.g. vacuum vulcanization, squeezing for sufficient penetrating of coating solution, padding gap for controlling quantity of coating solution and even appearance, tension for preventing the aggregation of coating solution to the middle part of yarn etc.

Table 3.5 presents the appearance of PI/PDMS composite yarn fabricated under vacuum vulcanization and other different parameters. It is found that the squeeze in first padding slightly improves the evenness of PI/PDMS composite yarns padded between a gap of 260μm and keep the state of the samples padded between a gap of 170μm. The evenness of samples padded between gap of 170μm is better than that of samples padded between gap of 260μm. The narrower gap reduces the pick-up of

coating solution, thus avoiding the unevenness caused by overflow and migration of coating solution. The applied tension during vulcanization facilitates the evenness of samples, especially for the samples padded between gap of 170μm, as loose state of samples leads to the migration of coating solution to middle part under gravity while tension restrains the migration. To sum up, squeeze in the first padding, narrower gap and tension during vulcanization are advantage for the evenness of PI/PDMS composite yarns.
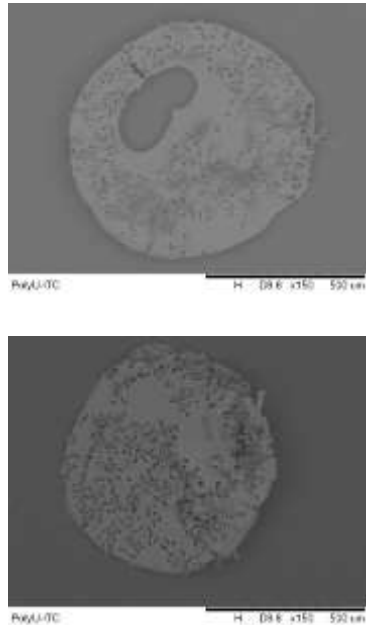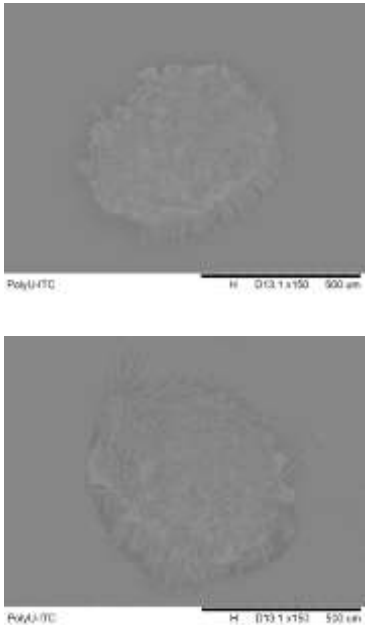
Table 3. 5 Fabrication parameter of each PI/PDMS sample and their image

| Sample No. | Squeeze in padding | Padding gap (μm) | Tension | Photo |
|---|---|---|---|---|
| 1 | ✔ | 260 | ✔ | No bubble, little uneven |
| 2 | ✔ | 170 | ✔ | No bubble, even |
| 3 | ✔ | 260 | ✘ | Bubble, little uneven |
| 4 | ✔ | 170 | ✘ | Bubble, uneven |
| 5 | ✘ | 260 | ✔ | Bubble, very uneven |
| 6 | ✘ | 170 | ✔ | No bubble, even |
| 7 | ✘ | 260 | ✘ | Bubble, very uneven |
| 8 | ✘ | 170 | ✘ | Bubble, uneven |

Note: The PI/PDMS composite yarns were vulcanized under vacuum condition.

Vulcanization under vacuum condition or non-vacuum condition can cause different state in the internal part of the PI/PDMS composite yarn. Cross sections of both are shown in Table 3.6.

Table 3. 6 SEM image of the cross sections of PI/PDMS composite yarn samples vulcanized under vacuum and non-vacuum environment

| | Sample 1: Non-vacuum | Sample 2: Vacuum |
|---|---|---|
| Yarn Diameter | Larger | Smaller |
| Space Inside the Yarn Core | ✔ | ✗ |
| Evenness | Lower | Higher |
| Roundness in Cross Sectional Shape | Higher | Lower |
| Compactness | Lower | Higher |
| PDMS Containment | More | Less |
| SEM Images |  |  |

It can be seen that the PI/PDMS composite yarn vulcanized under non-vacuum condition can achieve higher PDMS-containment, yarn diameter and roundness

whereas the evenness and compactness of yarn distribution are lower than that of samples vulcanized under vacuum condition. The bubble in the composite yarn could potentially affect the even force of prepared HCYA while offer higher thermal expansion in the radial direction of composite yarn, as well as higher actuation of HCYA, owning to higher thermal expansion of air than PDMS. In the practical test, it is found that HCYAs that made by samples vulcanized under non-vacuum condition has higher actuation than the samples vulcanized under vacuum condition. This phenomenon certificates that PDMS-containment is a more important factor than the evenness of composite yarn.

The distribution of PI monofilaments in PDMS matrix is depicted in Table 4.2. The monofilaments appear to be randomly arranged in the matrix, i.e. some parts have higher PI aggregating density while other parts have more percentage of PDMS. For achieving better performance of thermally powered actuator, some measures should be taken to avert uneven distribution, e.g. taking more soaking time when dipping the PI yarn into coating solution, keeping a proper tension to maintain smooth surface etc.

**3.3.4 Thermomechanical properties of PI/PDMS composite yarns and their components**

The coefficient of thermal expansion (CTE) and modulus of PI filament, PDMS strip and PI/PDMS composite yarn are shown in Table 3.7. PI filament has a minus CTE

value which means that it contracts when heating, whereas PDMS strip has a large positive CTE, which facilitates the significant radial expansion of PI/PDMS composite yarn. Because of the large difference between axial CTE and radial CTE of composite yarn, the tensile actuation can be realized through this anisotropic property[4]. There are many types of polyimide with different coefficient of thermal expansion, which can affect the anisotropy of yarn or composite yarn. Generally speaking, the higher thermal expansion in the radial direction or the lower thermal expansion in the axial direction for the polyimide yarns, the better anisotropy they can possess, thus further faciliating more effective tensile actuations of helical composite yarn actuators when heated.

Besides, the composite yarn has a moderate modulus between that of PI filament and PDMS strip, allowing it offers enough strength as well as expansive property simultaneously, thereby feasible for the fabrication of thermally powered actuator.

Table 3. 7 Thermomechanical properties of composite yarns and their components

| Item | PI filament | PDMS strip (0.41*1*12.5mm) | PI/PDMS 3*100f composite |
|---|---|---|---|
| CTE | $-29.19*10^{-6}$ (45-220°C，100f, axial, tension mode) | $776*10^{-6}$ (-25-230°C, tension mode) | $424*10^{-6}$ (50-180°C, radial, compression mode) |
| Modulus /MPa | 1150.8~7787 (50-150°C, 1f, axial, tension mode) | 2~0.2 (100~180°C, tension mode) | 110.0~36.8 (60~180°C, radial, compression mode) |

## 3.4 Summary

In order to lay a foundation for fabricating programmable HCYAs with wide working temperature range, composite yarns were designed in terms of material selection, coating process, vulcanizing method, followed by characterization of morphologies and thermomechanical properties.

Firstly, the properties of many candidate materials were compared for selecting proper fiber substrate (Nylon, PET, polyethylene, carbon nanotube, carbon fiber and polyimide) and matrix (Polydimethylsiloxane, epoxy, paraffin), then polyimide and Polydimethylsiloxane were designated as the optimal fiber substrate and matrix, respectively.

Secondly, the fabricating processes, including coating processes and vulcanizing processes, were investigated and optimized in terms of coating method, concentration of coating solution, padding times, filament number, tension, coating gap, pre-squeeze and vacuum vulcanization. The typical processing parameters were: padding method, PDMS: ethyl acetate=1:2, padding 3 times, 6*100 filaments, without tension, 260μm coating gap, pre-squeeze and non-vacuum vulcanization.

Thirdly, the morphologies of PI/PDMS composite yarns were characterized by electronic microscope and SEM, while the thermomechanical properties were characterized by TMA and DMA. Many factors can affect the morphology, e.g. coating

time, concentration, filament number, tension and coating gap. To achieve better evenness, it was necessary to adopt appropriate level for above parameters. Besides, modulus of composite yarns exhibited their enough strength and expansive property to fabricate HCYAs while the CTEs of PI/PDMS composite yarns validated their high anisotropy that facilitated the effective actuations of HCYAs.

# References

[1]     M. D. Lima, N. Li, M. Jung de Andrade, S. Fang, J. Oh, G. M. Spinks, M. E. Kozlov, C. S. Haines, D. Suh, J. Foroughi, S. J. Kim, Y. Chen, T. Ware, M. K. Shin, L. D. Machado, A. F. Fonseca, J. D. Madden, W. E. Voit, D. S. Galvao, and R. H. Baughman, "Electrically, chemically, and photonically powered torsional and tensile actuation of hybrid carbon nanotube yarn muscles," *Science,* vol. 338, no. 6109, pp. 928-32, Nov 16 2012.

[2]     L. Wu, M. J. de Andrade, T. Brahme, Y. Tadesse, and R. H. Baughman, "A deformable robot with tensegrity structure using nylon artificial muscle," in *Proceedings of SPIE*, 2016, vol. 9799, p. 97993K.

[3]     M. C. Yip and G. Niemeyer, "High-Performance Robotic Muscles from Conductive Nylon Sewing Thread," in *Proceedings of 2015 IEEE International Conference on Robotics and Automation*, Washington State Convention Center, 2015, pp. 2313-2318: IEEE.

[4]     C. S. Haines, M. D. Lima, N. Li, G. M. Spinks, J. Foroughi, J. D. W. Madden, S. H. Kim, S. Fang, M. J. d. Andrade, F. Göktepe, Ö. Göktepe, S. M. Mirvakili,

S. Naficy, X. Lepró, J. Oh, M. E. Kozlov, S. J. Kim, X. Xu, B. J. Swedlove, G. G. Wallace, and R. H. Baughman, "Artificial muscles from fishing line and sewing thread," *Science,* vol. 343, no. 6173, pp. 868-872, 2014.

[5]     S. H. Kim, C. S. Haines, N. Li, K. J. Kim, T. J. Mun, C. Choi, J. Di, Y. J. Oh, J. P. Oviedo, J. Bykova, S. Fang, N. Jiang, Z. Liu, R. Wang, P. Kumar, R. Qiao, S. Priya, K. Cho, M. Kim, M. S. Lucas, L. F. Drummy, B. Maruyama, D. Y. Lee, X. Lepró, E. Gao, D. Albarq, R. Ovalle-Robles, S. J. Kim, and R. H. Baughman, "Harvesting electrical energy from carbon nanotube yarn twist," *Science,* vol. 357, no. 6353, pp. 773-778, 2017.

[6]     P. Chen, Y. Xu, S. He, X. Sun, S. Pan, J. Deng, D. Chen, and H. Peng, "Hierarchically arranged helical fibre actuators driven by solvents and vapours," *Nature Nanotechnology,* vol. 10, no. 12, pp. 1077-83, Dec 2015.

[7]     M. D. Lima, M. W. Hussain, G. M. Spinks, S. Naficy, D. Hagenasr, J. S. Bykova, D. Tolly, and R. H. Baughman, "Efficient, Absorption-Powered Artificial Muscles Based on Carbon Nanotube Hybrid Yarns," *Small,* vol. 11, no. 26, pp. 3113-8, Jul 2015.

[8]     C. Lamuta, S. Messelot, and S. Tawfick, "Theory of the tensile actuation of fiber reinforced coiled muscles," *Smart Materials and Structures,* vol. 27, no. 5, 2018.

[9]     M. Kanik, S. Orguc, G. Varnavides, J. Kim, T. Benavides, D. Gonzalez, T. Akintilo, C. C. Tasan, A. P. Chandrakasan, Y. Fink, and P. Anikeeva, "Strain-programmable fiber-based artificial muscle," *Science,* vol. 365, no. 6449, pp. 145–150, 2019.

[10]    T. E. Toolbox. (2019). *Coefficients of Linear Thermal Expansion*. Available: https://www.engineeringtoolbox.com/linear-expansion-coefficients-d_95.html

[11]    Omnexus. (2019). *Ductile/Brittle Transition Temperature*. Available: https://omnexus.specialchem.com/polymer-properties/properties/ductile-brittle-transition-temperature

# CHAPTER 4
# FABRICATION AND CHARACTERIZATION OF HELICAL COMPOSITE YARN ACTUATORS

## 4.1 Introduction

After PI and PDMS were selected as the fiber substrate and polymer matrix, to fabricate composite yarns after comprehensively analyzing the properties of many candidate materials, this chapter further moves on to the fabrication and characterization of helical composite yarn actuators (HCYAs). First, PI/PDMS HCYAs are fabricated by the as-prepared anisotropic PI/PDMS composite yarns, through super-twisting process with the application of twisting number sensor. Secondly, the morphologies of PI/PDMS HCYAs are characterized and analyzed in terms of filament number, coil level, coil type, heat-setting temperature. Finally, thermomechanical properties of HCYAs are investigated in terms of isotonic behavior (keep the load and test tensile actuation when changing temperature), isometric behavior (keep the tensile actuation and test load when changing temperature) and isothermal behavior (keep the temperature and test load when changing tensile actuation).

## 4.2 Experimental

### 4.2.1 Fabrication of thermally powered actuators

Thermally powered actuators were fabricated by an experimental setup as Figure 4.1. The two ends of PI/PDMS composite yarns were nipped by small drill chucks, then one end of the nipped composite yarn was fixed into the hole of the stirring head of stirrer (IKA RW 20) while another end was stretched by a proper load and prevented from rolling by a metal pin. Magnetic induced counter (GQGH, HB961, China) was used to test the twisting number by sensing the movement of a magnet stuck on the stirring head. The composite yarns were twisted until forming single-level coil state or double-level coil state (formed due to further twisting to single-level coil) (Figure 4.2).



Figure 4. 1 Experimental setup for fabricating thermally powered actuator

Figure 4. 2 Single-level coil state (left) and double-level coil state (right)

### 4.2.2 Characterization of thermally powered actuators

### 4.2.2.1 Morphology

Electron microscope (Leica M165 C) was applied to measure the surface morphology, diameters, spring index and bias angles of thermally powered actuators. Spring index are calculated by the following equation:

$$Spring\ index = \frac{D - d}{d}$$

wherein $D$ is the diameter of thermally powered HCYA and $d$ is the diameter of PI/PDMS composite yarn.

### 4.2.2.2 Thermomechanical properties

Thermomechanical properties of thermally powered actuators were assessed in terms of isotonic, isometric and isothermal test, wherein load frame (Instron 5566) equipped with a heating oven was used to carry out isotonic, isometric and isothermal tests in the temperature range from 20 °C to 200 °C, whereas climate chamber (Votsch, C7-600, Germany) was applied to implement isotonic tests from -50 °C~100 °C. The real-time

data of temperature and displacement were collected by temperature sensor (Asmik, MIK-ST500, China) and displacement sensor (Wen sheng wuxi, MYDJ-O, China) (Figure 4.3), respectively.
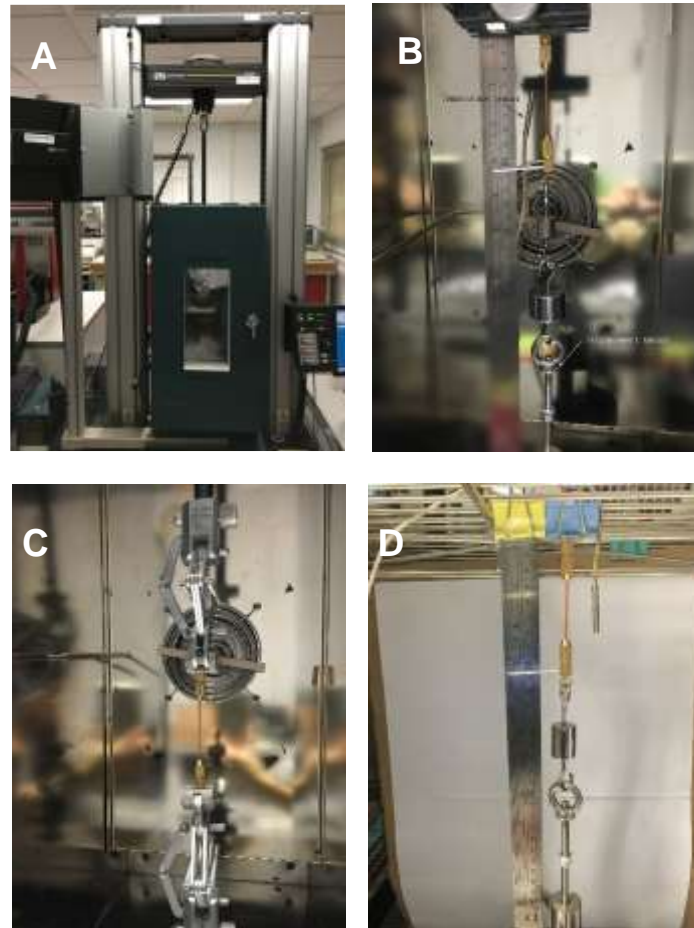


Figure 4. 3 Thermomechanical test system. (A) Instron 5566 equipped with oven (B) Isotonic test system in Instron 5566 (C) Isometric and isothermal test system in Instron 5566 (D) Isotonic test system in climate chamber

## 4.3 Results and discussions

### 4.3.1 Fabrication of HCYAs

#### 4.3.1.1 Twisting curve
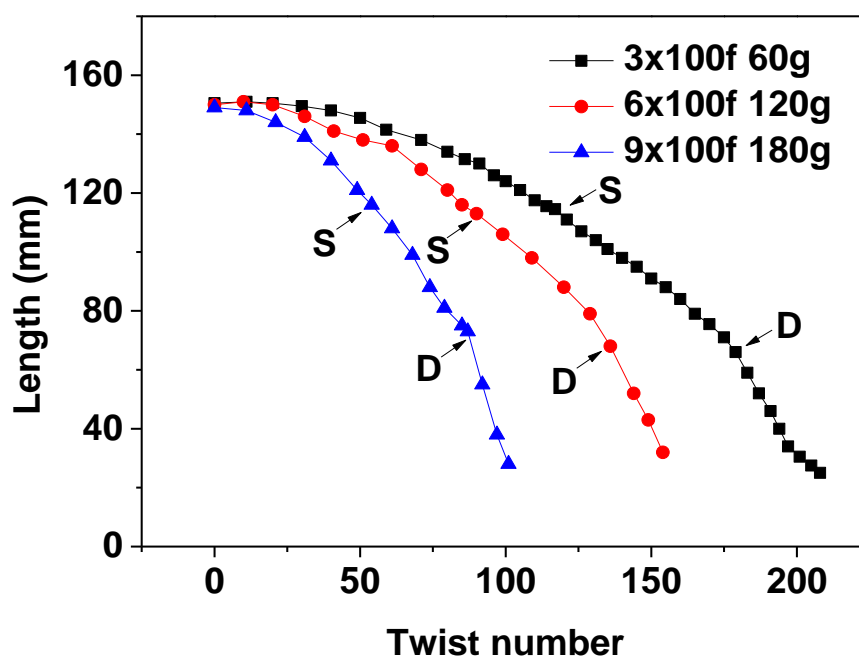


Figure 4. 4 Twist curve of PI/PDMS composite yarns (S: Single coils appear; D: Double

coils appear)

The composite yarns of 3*100f, 6*100f and 9*100f were twisted under stretching loads

of 60g, 120g and 180g, respectively. The longitudinal change was measured as the twist

number increased (Figure 4.4). The shortening speeds of twisted composite yarns was

faster when single-level coils formed and even faster when double-level coils formed.

The composite yarn with more filament number needs more twist number to form fully

single-level or double-level coil state.

## 4.3.1.2 Forming condition of single & double coils

Table 4. 1 Forming condition of single-level & double-level coils

| Load (g) | 3*100f uncoated | | 3*100f coated | | 6*100f coated | | 9*100f coated | |
|---|---|---|---|---|---|---|---|---|
| | single | double | single | double | single | double | single | double |
| 0.9 | N | N | / | / | / | / | / | / |
| 1.9 | Y | N | / | / | / | / | / | / |
| 8.7 | Y | N | <u>Y</u> | <u>Y</u> | <u>Y</u> | N | <u>Y</u> | N |
| 18.7 | Y | N | Y | Y | Y | <u>Y</u> | Y | N |
| 28.7 | Y | N | Y | Y | / | / | / | / |
| 68.7 | / | / | Y | Y | / | / | / | / |
| 78.7 | / | / | Y | Y (break) | / | / | / | / |
| 108.7 | Y | Break | Y | Y (break) | Y | Y (break) | Y | N |
| 118.7 | / | / | / | / | / | / | Y | <u>Y</u> |
| 208.7 | / | / | / | / | / | / | Y | Y |
| 408.7 | / | / | / | / | / | / | Break | / |

Note: Y means that the full coils can be realized to complete a HCYA. N means the coil cannot form. "Break" means the yarn was broken as the load was too heavy.

Referring to twist composite yarn into single-level or double-level coil thermally powered actuator, weak stretching force may not achieve effective and stable coil state, whereas too strong stretching force may break the yarn. Therefore, selecting proper loads for twisting the yarns is very important for fabricating actuators. The forming conditions of single-level and double-level coils are shown in Table 4.1. It can be seen that 8.7g is enough to form single-level coils for all the types of yarns, i.e. 3*100f uncoated, 3*100f coated, 6*100f coated and 9*100f coated yarn, while these yarns do not break under the load of 108.7g. However, formation of double-level coil requires heavier load for 6*100f and 9*100f composite yarn, as light load cannot keep the linear state, only leading to randomly twine by the yarn itself. Considering that lighter stretching load facilitates the fabrication of actuators of low bias angle, which may have higher potential to obtain larger tensile actuation, the proper load for each composite yarn should be the one corresponding to the "underlined Y" in the table.

### 4.3.2 Morphology



Figure 4. 5 Each state of sample for fabricating an PI/PDMS HCYA. (A) 100f PI yarn (B) 6*100f PDMS-coated PI yarn (C) 6*100f PI/PDMS HCYA

The PI/PDMS HCYAs were fabricated though combination of 100f PI filament yarn, PDMS coating for obtaining PI/PDMS composite yarn and super-twisting process for achieving a spring-like structure that PI/PDMS HCYAs should have. The morphology of each state, including yarn, composite yarn and HCYA, are shown in Figure 4.5. The raw material, i.e. 200D/100f PI yarn (Figure 4.5A), was loose and even. Six 200D/100f PI yarns were combined and coated by PDMS. After the vulcanization, solid bulky PI/PDMS composite yarn was formed with smooth, lustrous and even surface (Figure 4.5B), which was twisted and further coiled into thermally powered HCYA subsequently (Figure 4.5C). Many factors can influence the morphology of the HCYAs, e.g. filament number, coil level, coil type and heat-setting temperature.

### 4.3.2.1 Filament number

Table 4.2 gives the features of single-level and double-level coiled thermally powered actuators, fabricated by different coating method and filament number. There are generally three trends. First, uneven surface becomes much serious when filament number increases. Secondly, single-level actuators have smoother surface than the double-level actuators. Thirdly, padding method can achieve better appearance for actuators than dip-coating method, owning to well-controlled PDMS amount on every part when filament yarn goes through the gap between two rollers.

Table 4. 2 Single-level and double level thermally powered HCYAs of different filament number

| Coating method | Single | Double |
|---|---|---|
| 3*100f<br><br>dip coat 1:4 |  |  |
| 6*100f<br><br>dip coat 1:4 |  |  |
| 9*100f<br><br>dip coat 1:4 |  |  |
| 9*100f<br><br>Padding 1:2 |  |  |

### 4.3.2.2 Coil level



Figure 4. 6 Thermally powered HCYAs of different coil levels. (A) HCYA with single-level coil (B) HCYA with single-double-mixed-level coil (C) HCYA with double-level coil
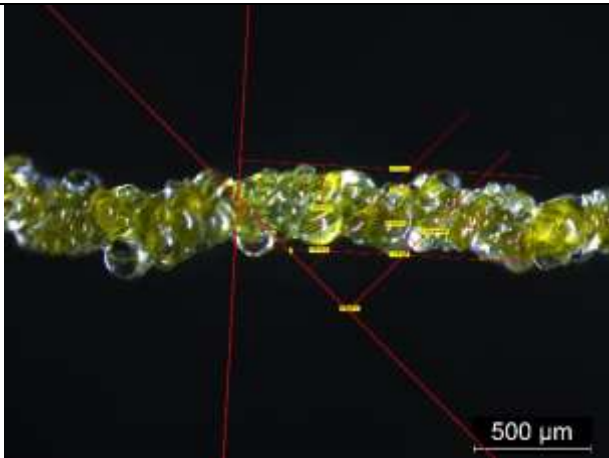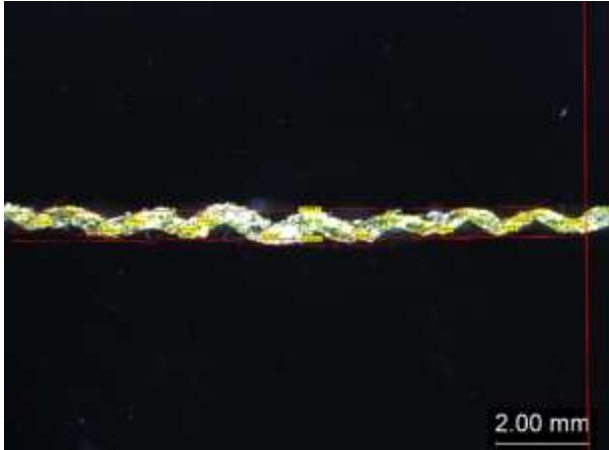
The morphologies of thermally powered actuators (600f, Pad-coating, 1:2) with three types of coil level (single level coil, single-double mixed level, double level coil) are shown in Figure 4.6. Through consistent twisting, single-level coil actuator (Figure 4.6A) becomes single-double-mixed-level coil one (Figure 4.6B), until fully buckled into double-level coil actuator (Figure 4.6C). From Figure 4.6, it can be seen that single-level coil actuator possesses larger bias angle (i.e. the angle between radial direction of HCYA and tilted coil) than double-level coil part. Besides, the single-double-mixed-level coil actuator has potential to achieve high tensile actuation, as the phase change from single-level to double-level coil can offer significant longitudinal change.

### 4.3.2.3 Coil type

The features of thermally powered actuators (20f composite yarn) coiled by twisting and coiled around mandrel are presented in Table 4.3, together with corresponding spring index and bias angle. The actuator coiled around mandrel has higher value of

87

spring index than the one coiled by twisting, implying its lower rigidity and higher deformability. Besides, the actuator coiled by twisting possess smaller initial bias angle than the one coiled around mandrel, showing its potential of higher tensile actuation.

Table 4. 3 Coil by twisting and coil around mandrel
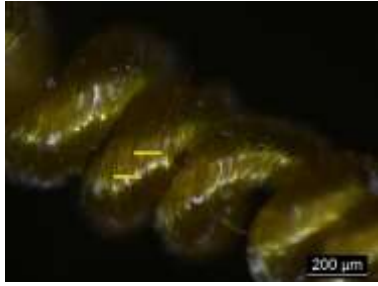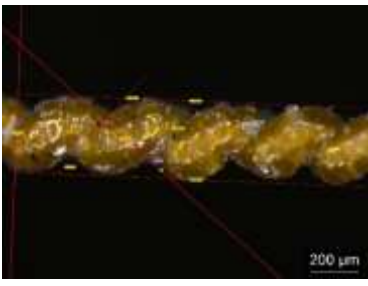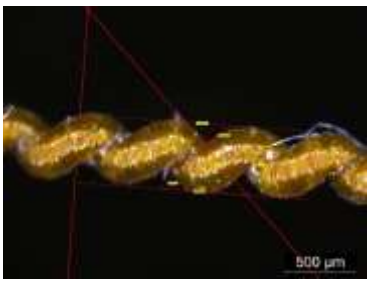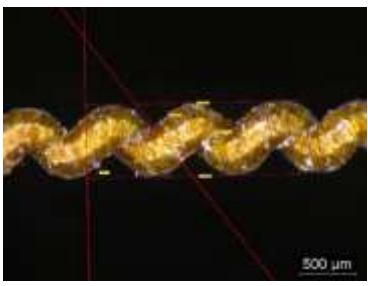
| Coil type | | Spring index | Bias angle |
|---|---|---|---|
| Single level coil |  | 0.60 | 43.0 |
| Coil around mandrel |  | 1.08 | 60.6 |

### 4.3.2.4 Temperature

PI has a very high grass transition temperature of over 350 °C. In order to fabricate thermally powered actuators with stable state by eliminating internal stress of PI fiber, following high-temperature heat-setting treatment should be implemented to the

twisted and buckled composite yarn (Table 4.4). Though treating at 380 °C can obtain

stable state for actuators, it shows that PDMS crack appears on the surface, which may

lead to inefficiency of actuation. Moreover, the bias angles are enlarged a lot comparing

380 °C treatment to 150 °C treatment, thus affecting the potential of higher tensile

actuation. Therefore, overheat-setting can reduce the actuating performance of

thermally powered actuator, whereas low-temperature or even no heating setting may

maintain the effective actuating ability.

Table 4. 4 Single-level coil actuators heat-set under different temperature

| Heat-set temperature | 150 °C | 380 °C |
|---|---|---|
| 90f |  |  |
| 180f |  |  |
| 270f |  |  |

## 4.3.3 Isotonic behavior
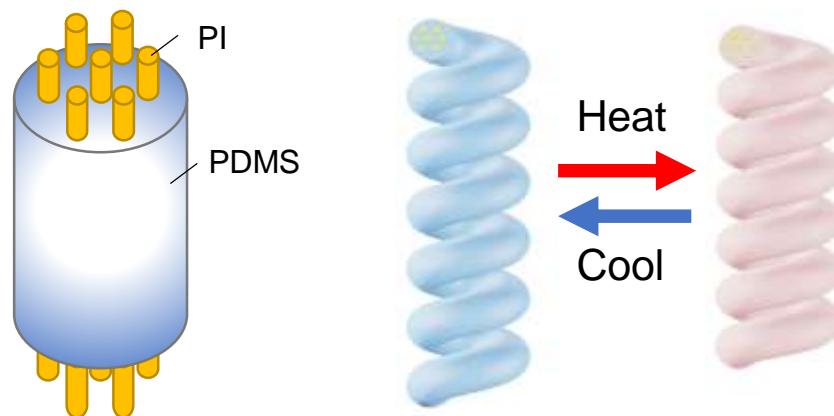


Figure 4. 7 Schematic illustration of composite yarns and thermally powered HCYA

The basic actuating principle lies in the anisotropic thermal and mechanical properties of the fiber, where the expansion/contraction in the radial direction is largely different from that in the axial direction during temperature change[1], therefore the HCYAs can be designed and fabricated by PI/PDMS composite yarns that possess high coefficient of thermal expansion (CTE) in radial direction, as well as low CTE in axial direction. Contraction will happen when the HCYAs are heated while extension will start when the samples are cooling down (Figure 4.7). In this isotonic test process, the load remains constant while the tensile actuations changes with temperature. The actuations are affected by many factors, including heat-setting temperature, filament number, coiled level, load, volume fraction and low temperature condition.

**4.3.3.1 Heat-setting temperature**
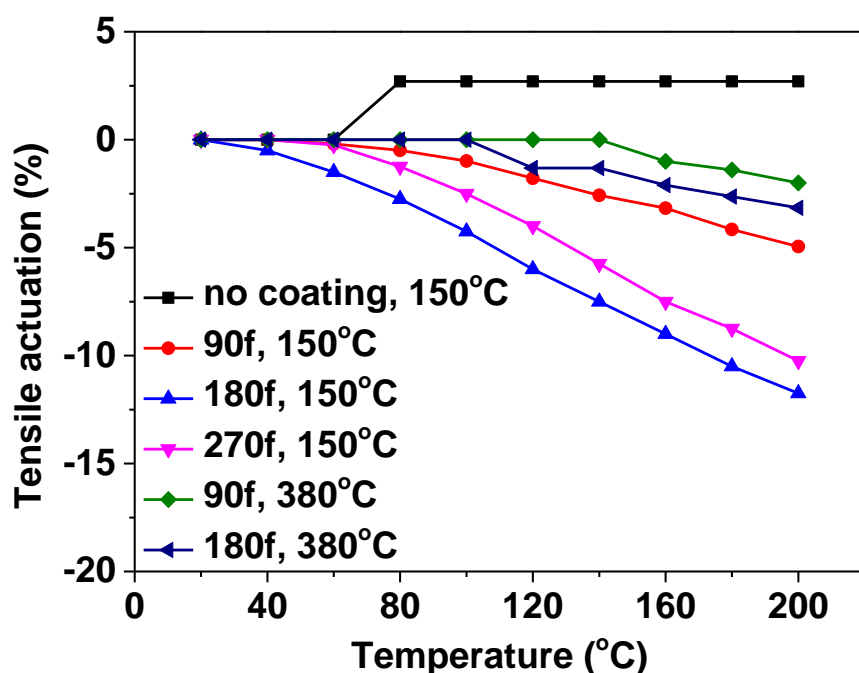


Figure 4. 8 Tensile actuation of thermally powered actuators heat-set under different

temperature

In order to fabricate thermally powered actuators with relatively stable state (less

untwisting), heat-settings under different temperatures (150 °C, 380 °C) were carried

out for actuators of different filament number (90f, 180f, 270f). Afterwards, their tensile

actuation performances were characterized by isotonic test under temperature ranging

from 20 °C to 200 °C (Figure 4.8). It can be seen that uncoated thermally powered

HCYA cannot be actuated as there is no large expansion in radial direction of PI yarn

in this temperature range, which is far below the $T_g$ of PI. Conversely, all the actuators

with PDMS coating can be thermally activated to different extent, wherein those heat-

set under 150 °C achieves higher tensile actuation than those heat-set under 380 °C.

The explanation for this result is that the PDMS coating has been wrecked by high temperature, thereby the radial expansion is reduced enormously, and the efficiency of actuation became low down. The 180f actuators seems have higher tensile actuation than those of less or more filament number, due to the less PDMS volume fraction in those of less filament number and the compact between adjacent bold coil of actuators of more filament number.

Table 4. 5 Specific work of thermally powered HCYA

| No. | Coated yarn weight (mg) | Muscle weight (mg) | Load weight (g) | Specific work (20-200°C) (J/kg) | Specific work (20-120°C) (J/kg) |
|---|---|---|---|---|---|
| No.1 (no coating, 90f, 150°C) | 2.96 | 1.97 | 9.15 | — | — |
| No.2 (90f, 150°C) | 4.35 | 2.90 | 9.16 | 77.35 | 27.85 |
| No.3 (180f, 150°C) | 10.42 | 6.95 | 9.15 | 60.68 | 30.98 |
| No.4 (270f, 150°C) | 17.28 | 11.52 | 9.15 | 31.92 | 12.46 |
| No.5 (90f, 380°C) | 4.35 | 2.59 | 10.94 | 41.39 | 0.00 |
| No.6 (180f, 380°C) | 10.42 | 6.09 | 10.94 | 21.13 | 8.80 |
| Nylon fishing line muscle[1] (1f, 220°C) | — | — | — | — | 2480 |
| Natural muscle[1] | — | — | — | — | 38.60 |

For assessing the efficiency of thermally powered actuators, specific works were

calculated through the value of tensile lifting work divided by the weight of each actuator. Table 4.5 shows that the actuators heat-set under 150 °C have higher value of specific work than those heat-set under 380 °C due to complete PDMS coating as illustrated above. Though the 180f actuator heat-set under 150 °C has more than twice tensile actuation as high as the 90f actuator, the values of their specific works (i.e. 30.98 J/kg and 27.85 J/kg) are very close to each other, which are similar to the specific work of natural muscle. However, their specific work are not competitive enough compared with that of artificial muscle made by nylon single fiber.

The diameters of composite yarn and HCYA were characterized by electronic microscope and then spring index of actuators were calculated accordingly. As shown in Table 4.6, the thermally powered HCYA with PDMS coating has larger spring index than the one without PDMS coating, while the values are almost the same for 90f, 180f and 270f actuator, indicating their similar rigidity and deformability.

Table 4. 6 Spring index of thermally powered actuators

| No. | Yarn diameter (mm) | Actuator diameter (mm) | Spring index |
|---|---|---|---|
| No.1 (no coating, 90f, 150°C) | 0.1988 | 0.4309 | 1.17 |
| No.2 (90f, 150°C) | 0.2659 | 0.6350 | 1.39 |
| No.3 (180f, 150°C) | 0.3568 | 0.8479 | 1.38 |
| No.4 (270f, 150°C) | 0.4389 | 1.0579 | 1.41 |

### 4.3.3.2 Filament number and coil level

After completing the fabrication of the thermally powered actuators of different filament number and coil level, the actuators were extended to proper length for tensile actuating test. Afterwards, the tensile actuation was calculated by longitudinal change divided by initial length, while the specific work capacity was calculated by specific work divided by temperature change.

As shown in Table 4.7, double-level coil actuators need heavier load to fabricate and actuate than single-level coil actuators, while loads for actuation are commonly heavier than loads for fabrication. Exceptionally, for the single-double-mixed-level coil actuator, load for actuation is lighter than the load for fabrication, since heavy load facilitates the formation of double-level coil state while light load is advantageous for the transition from single-level coil to double-level coil state, thereby increasing the tensile actuation rate.

Besides, the control of extension rate is an important part for obtaining large tensile actuation, as low extension rate may lead to the compaction of adjacent coils when heating while high extension rate may burden the actuator and reduce the actuation rate. Tensile actuation rate is usually less than the extension rate, whereas the 3*100f single-level coil actuator had the contrary result, indicating the occurrence of compaction between adjacent coils of HCYA.

Also, it can be seen from Figure 4.9~4.11 that all the actuators can achieve effective tensile actuation rate of over 10%, while the single-double-mixed-level coil actuator reaches extraordinary tensile actuation rate of 47.1% due to coil level transition (single to double level). When the coil level changes from single-level coil to double-level coil, the length of sample can be shortened sharply. For example, the length of 3*100f single-level coil actuator decreases from 66 mm to 25 mm when it is twisted into double-level coil actuator, with a length reduction of 62.1% (Figure 4.4). Besides, the corresponding specific work capacity is larger than that of all the single-level coil actuators. Double-level coil actuators possess higher specific work capacity than the single-level coil actuators, which is attributed to the fact that partial double-level coil changes to single-level state when adding load for actuation, then single-level coil returns to double-level state after heating.
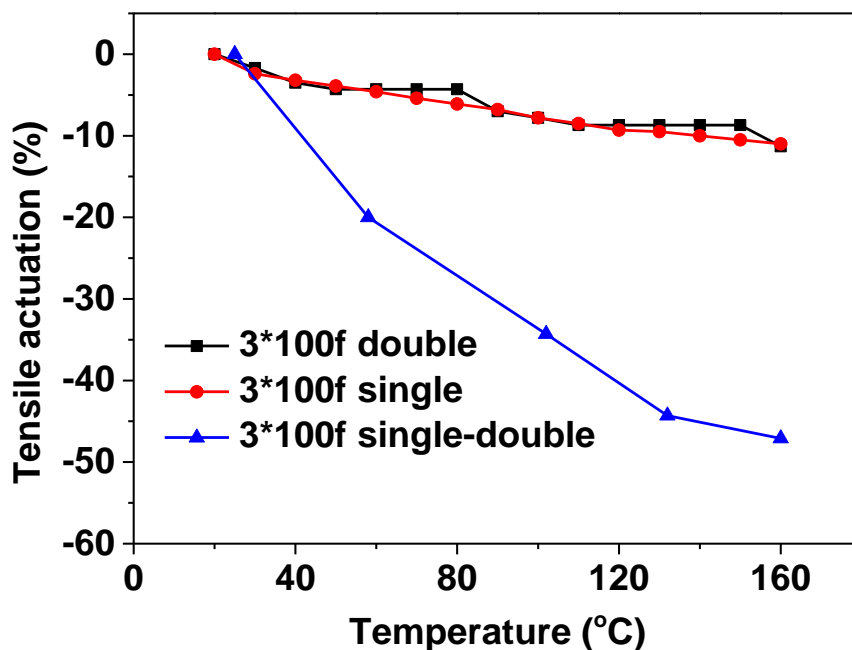


Figure 4. 9 Tensile actuation of 3*100f thermally powered actuators
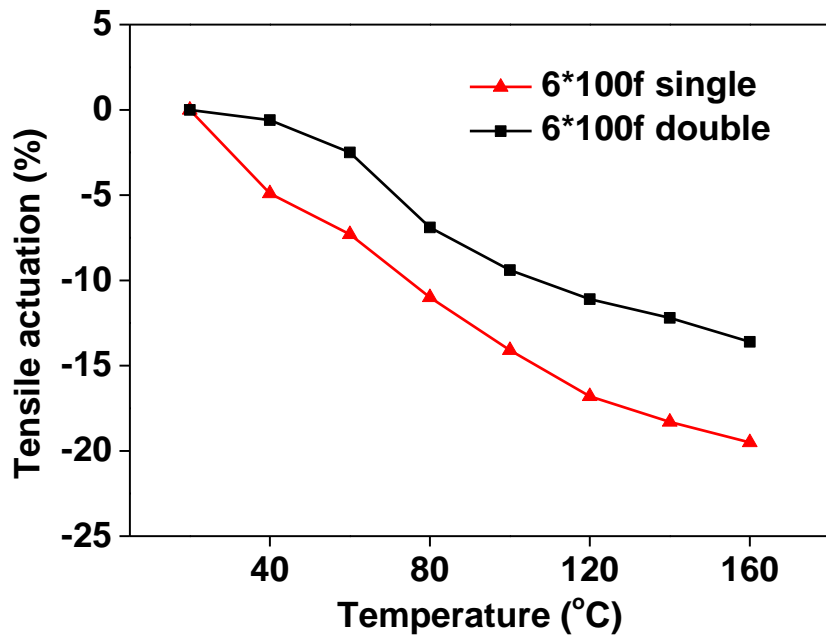
Figure 4. 10 Tensile actuation of 6*100f thermally powered actuators
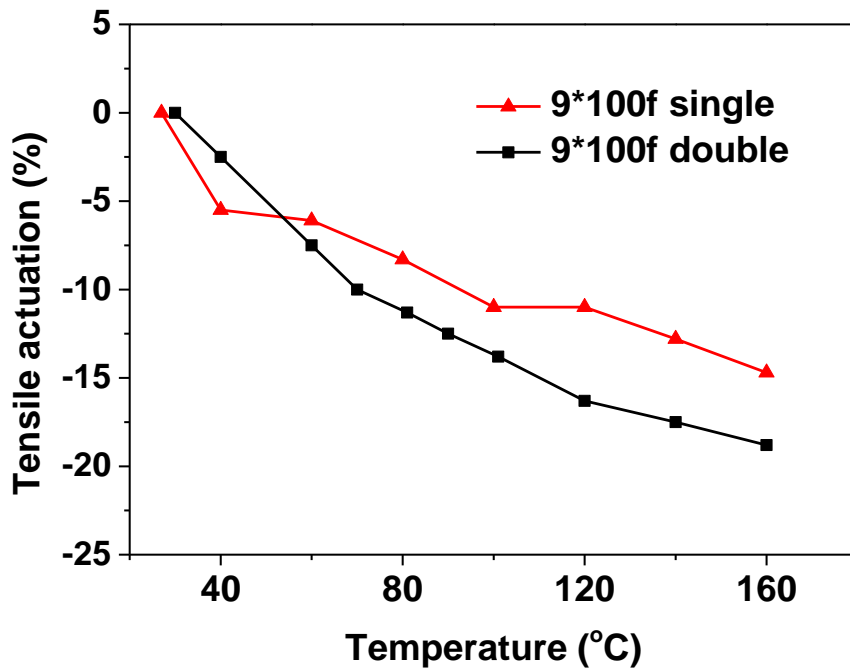


Figure 4. 11 Tensile actuation of 9*100f thermally powered actuators

Table 4. 7 Tensile actuation and specific work capacity of thermally powered actuators of different filament number and coil level

| PI/PDMS actuators heated from 20~30°C to 160°C | | Loads for fabrication /g (length /mm) | Loads for actuation /g (length /mm) | Extension rate/% | Tensile actuation rate /% | Specific work capacity /J/(kg·°C) |
|---|---|---|---|---|---|---|
| 3*100f | Single | 8.7 (37) | 28.7 (41) | 10.8 | 11.0 | 0.66 |
| | Double | 48.7 (9.5) | 58.7 (11.5) | 21.1 | 11.3 | 0.74 |
| | Single & double | 60 | 20 | / | 47.1 | 1.33 |
| 6*100f | Single | 18.7 (29.5) | 58.7 (38) | 28.8 | 19.5 | 0.59 |
| | Double | 58.7 (14) | 208.7 (24) | 71.4 | 13.6 | 1.13 |
| 9*100f | Single | 18.7 (41) | 108.7 (50.5) | 23.2 | 14.6 | 0.73 |
| | Double | 158.7 (26) | 258.7 (32) | 23.1 | 18.3 | 1.94 |

**4.3.3.3 Effect of load on actuation**

Fabrication load and actuation load can remarkably affect the tensile actuation of thermally powered HCYAs. In order to investigate the effect of load, 3*100f single-level coil actuators were fabricated and actuated under different loads. As shown in Table 4.8, the heavier the fabrication load and actuation load are, the lower extension rate as well as tensile actuation rate can be reached, probably due to the insufficient power of actuators when bearing heavy load. Nevertheless, the specific work capacity rises with increasing actuation load, implying that the heavy actuation load will not

reduce the specific work capacity in certain load range, contrarily may promote the value by realizing more potential power of the actuators.

Table 4. 8 Effect of load on tensile actuation rate and specific work capacity

| PI/PDMS actuator | Fabrication load/g | Actuation load/g | Extension rate/% | ΔT /°C | Tensile actuation rate/% | Specific work capacity /J/(kg·°C) |
|---|---|---|---|---|---|---|
| 1 | 8.77 | 28.7 | 10.8 | 140 | 11.0% | 0.66 |
| 2 | 20 | 30 | 2.31 | 130 | 10.4% | 0.87 |
| 3 | 60 | 80 | 1.35 | 120 | 6.6% | 1.81 |

Note: PI/PDMS single coil actuator, 3*100f, dip-coated with 1:4 coating solution.

**4.3.3.4 Effect of volume fraction on actuation**

Volume fraction of PDMS in the PI/PDMS composite yarn can directly affect the thermal expansion in radial direction, further influencing the effect of actuation. PI/PDMS HCYAs were made by dip-coating (PDMS: solvent = 1:4) or padding method (PDMS: solvent = 1:2, 1:4), achieving volume fraction of 74.6%, 54.0% and 35.9%, respectively. As shown in Table 4.9, the single-level coil actuators with higher volume fraction possess higher tensile actuation rate and specific work capacity, due to larger thermal expansion in radial direction. Double-level coil and single-double-mixed level coil actuators achieve higher tensile actuation and specific work capacity than single-level coil actuators as both of them were actuated through level transition from single-

level to double level state to some extent, not just simply relying on the approach of adjacent coils. Therefore, coil-level has more significant influence than volume fraction within a certain range.

Table 4. 9 Effect of volume fraction on tensile actuation and specific work capacity of 9*100f PI/PDMS HCYAs

| 9*100f PI/PDMS actuator | Volume fraction of PDMS /% | Fabric load /g | Actuation load/g | Extension rate/% | ΔT /°C | Tensile actuation rate/% | Specific work capacity /J/(kg·°C) |
|---|---|---|---|---|---|---|---|
| dip coat 1:4 single | 74.6 | 18.7 | 108.7 | 23.2 | 133 | 14.6 | 0.73 |
| padding 1:2 single | 54.0 | 18.7 | 108.7 | 14.1 | 140 | 8.2 | 0.59 |
| padding 1:4 single | 35.9 | 18.7 | 108.7 | 5.2 | 140 | 5.0 | 0.35 |
| dip coat 1:4 double | 74.6 | 158.7 | 258.7 | 23.1 | 130 | 18.3 | 1.94 |
| padding 1:2 single & double | 54.0 | 108.7 | 108.7 | 0 | 140 | 28.6 | 1.36 |

**4.3.3.5 Low-temperature actuation**

Isotonic tests were carried out for 6*100f PI/PDMS HCYAs under 20g, 85g and 150g (Figure 4.12A~4.12C). It can be seen that the thermally powered HCYA can obtain higher tensile actuation when the load was in medium level compared with the effect under light or heavy load, because light load leads to touch of the coils, while overloading leads to fatigue of the actuator. The linearity of "tensile actuation vs temperature" curve was calculated as 0.99719, 0.99812 and 0.99748 (from -50 °C to100 °C between cycle 2 and cycle 3) for the load of 20g, 85g and 150g, respectively. Therefore, apart from a higher tensile actuation, proper tensile load can also promote the linearity for the thermally powered HCYA, which may have application in the accurate temperature sensor, even in the extremely low temperature range. Moreover, the "tensile actuation vs temperature" curves become similar and overlapped in cycle 2 and cycle 3 in all the load conditions, showing stable performance in short cycles.

The isotonic behaviors of 9*100f PI/PDMS HCYAs were also investigated under 58.8g, 108.8g and 158.8g. As shown in Figure 4.12D and Table 4.10, the tensile actuation of 9*100f PI/PDMS HCYA can reach up to about -17.7% when the load is 58.8g. As the load goes up, the tensile actuation slightly decreases, whereas specific work and specific work capacity (defined as specific work divided by temperature change) increase remarkably. All the HCYAs have higher specific works than mammalian skeleton muscle. Besides, the linearity of actuation curves was better than that of 6*100f

PI/PDMS HCYAs if the loads are higher than 108.8g, due to much even surface of

HCYAs with more filaments.
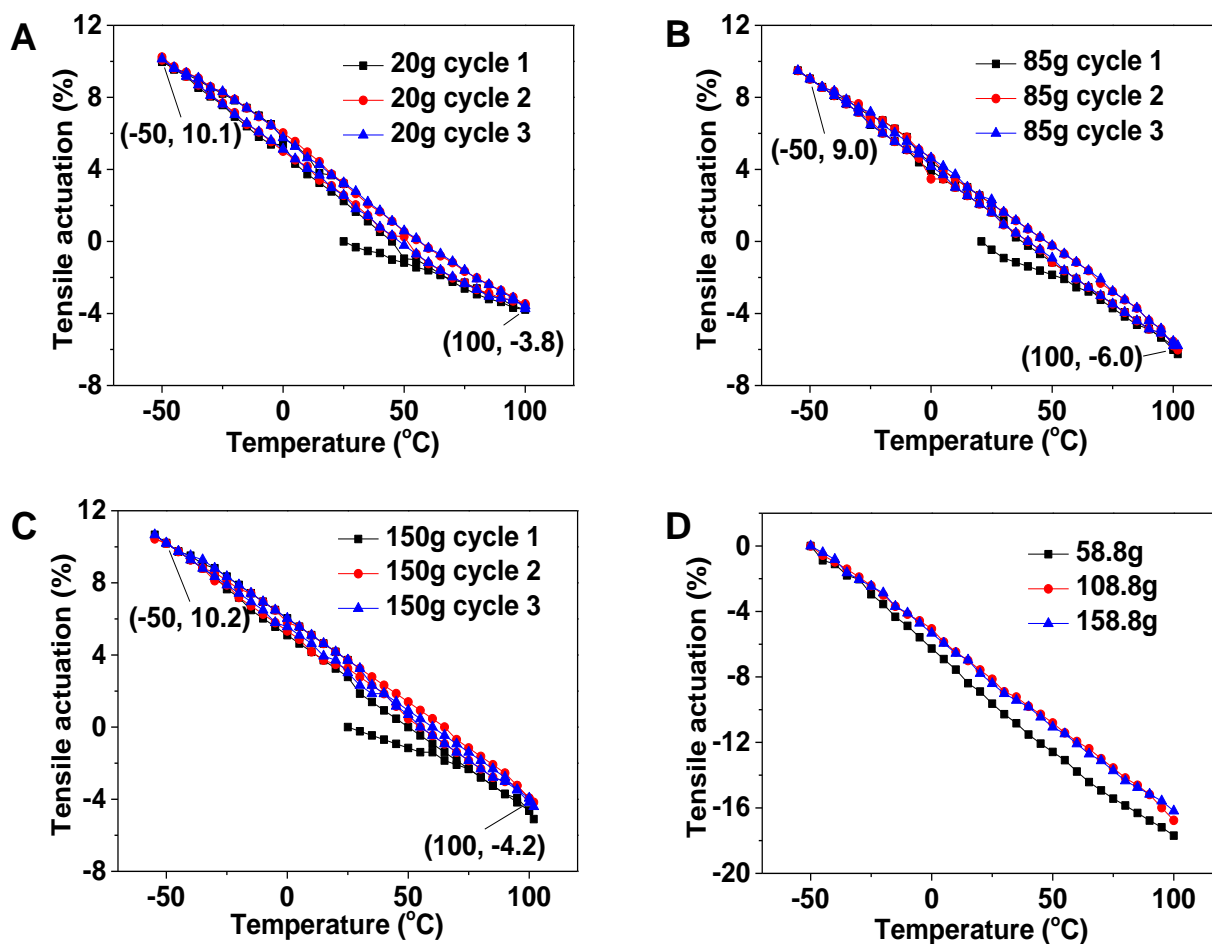


Figure 4. 12 Isotonic tests of 6*100f PI/PDMS HCYAs under load of (A) 20g, (B) 85g

and (C) 150g. (D) Isotonic behaviors of 9*100f PI/PDMS HCYAs under 58.8g

($R^2$=0.99679), 108.8g ($R^2$=0.99927) and 158.8g ($R^2$=0.99900).

Table 4. 10 Isotonic behaviors of 9*100f PI/PDMS HCYAs under different load

| Load for 9*100f PI/PDMS actuator | Tensile actuation (%) | Specific work (J/kg) | Specific work capacity (J/(kg·°C)) |
|---|---|---|---|
| 58.8g | -17.7 | 57.2 | 0.38 |
| 108.8g | -16.8 | 114.1 | 0.76 |
| 158.8g | -16.2 | 158.9 | 1.06 |

Note: Volume fraction of PDMS is 72.6%. Specific work of mammalian muscle is 38.6J/kg.

## 4.3.3.6 Isotonic performance compared with other actuators

For investigating the advantages of PI/PDMS HCYAs, the isotonic performance was compared with other types of actuators. Figure 4.13 clearly shows that the tensile actuation of PI/PDMS HCYA during ordinary temperature range (20~60 °C) is much higher than that of HCYAs made by carbon fiber/PDMS, PET monofilament, CNT/wax, nylon/Ag yarn and nylon filament. This property is attributed to the higher expansion of PDMS ($T_g$ = -123 °C)[2] in the radial direction than that of other fiber/yarn ($T_g$ > 60 °C) under ordinary temperature range, i.e. higher temperature above $T_g$ facilitates the radial thermal expansion and further the tensile actuation. Therefore, PI/PDMS actuators exhibit higher actuations under ambient condition, which facilitate applications in ambient temperature, e.g. wearable and size-adjustable smart textiles. Actually, the HCYAs with large spring index can reach very high tensile actuation through relatively little temperature change, e.g. COCe/PE HCYA[3] and spiral coil nylon actuator[4], but the stresses are rather limited compared with the low spring index HCYAs.
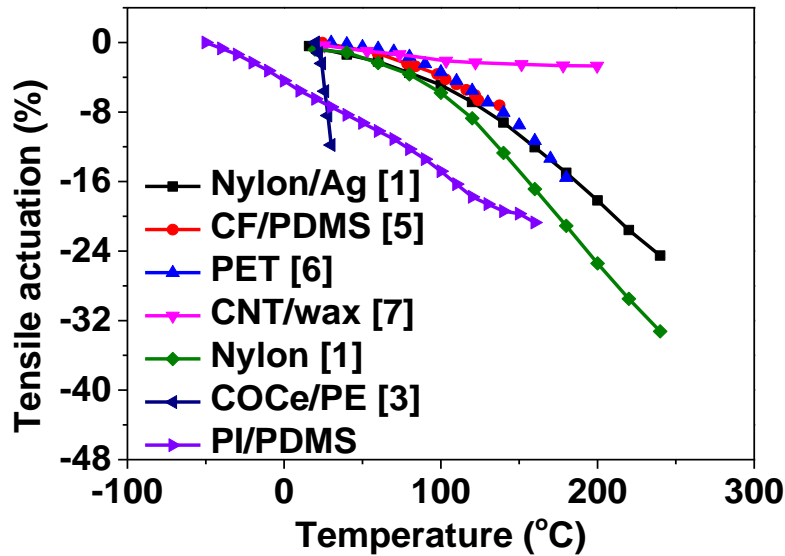
Figure 4. 13 Comparison of isotonic behavior among different fiber-based coiled linear actuators (FCLAs), including nylon6,6 /Ag FCLA with stress of > 17MPa[1], Carbon Fiber/PDMS FCLA with stress of 60MPa[5], PET monofilament FCLA with stress of 6.2MPa[6], CNT/wax FCLA with stress of 6.8MPa[7], nylon monofilament FCLA with stress of 83.6MPa[1], COCe/PE FCLA with stress of 0.07MPa[3] and 6*100f PI/PDMS HCYA with stress of 1.2MPa.

## 4.3.4 Isometric behavior

Investigating isometric behavior of thermally powered actuators has a vital significance on compressive products, e.g. compressive stockings, compressive clothes etc. Isometric behavior was characterized by determining the load change with the increase of temperature on the premise that the total length was fixed.
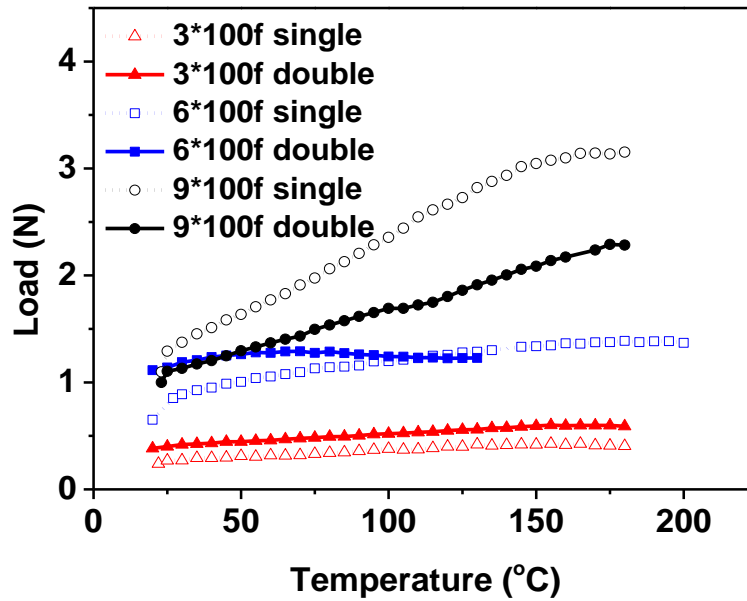
Figure 4. 14 Isometric behaviors of 3*100f, 6*100f and 9*100f thermally powered PI/PDMS HCYAs

As shown in Figure 4.14, the actuating loads gradually go up with increasing temperature until reaching a limitation. Besides, actuating ability became higher when the filament number increased, possibly attributed to higher PDMS volume fraction in the actuators. Besides, the 9*100f single-level coil actuator can achieve nearly three times load as strong as the initial pre-load when heated to 180 °C, which shows the best actuating performance, even better than that of double-level coil actuator. The reason for this might exist in the fixed length which restrained the level change in the double-level coil actuator. To sum up, single-level coil actuator has more advantage than the double-level actuator in terms of isometric test and application.
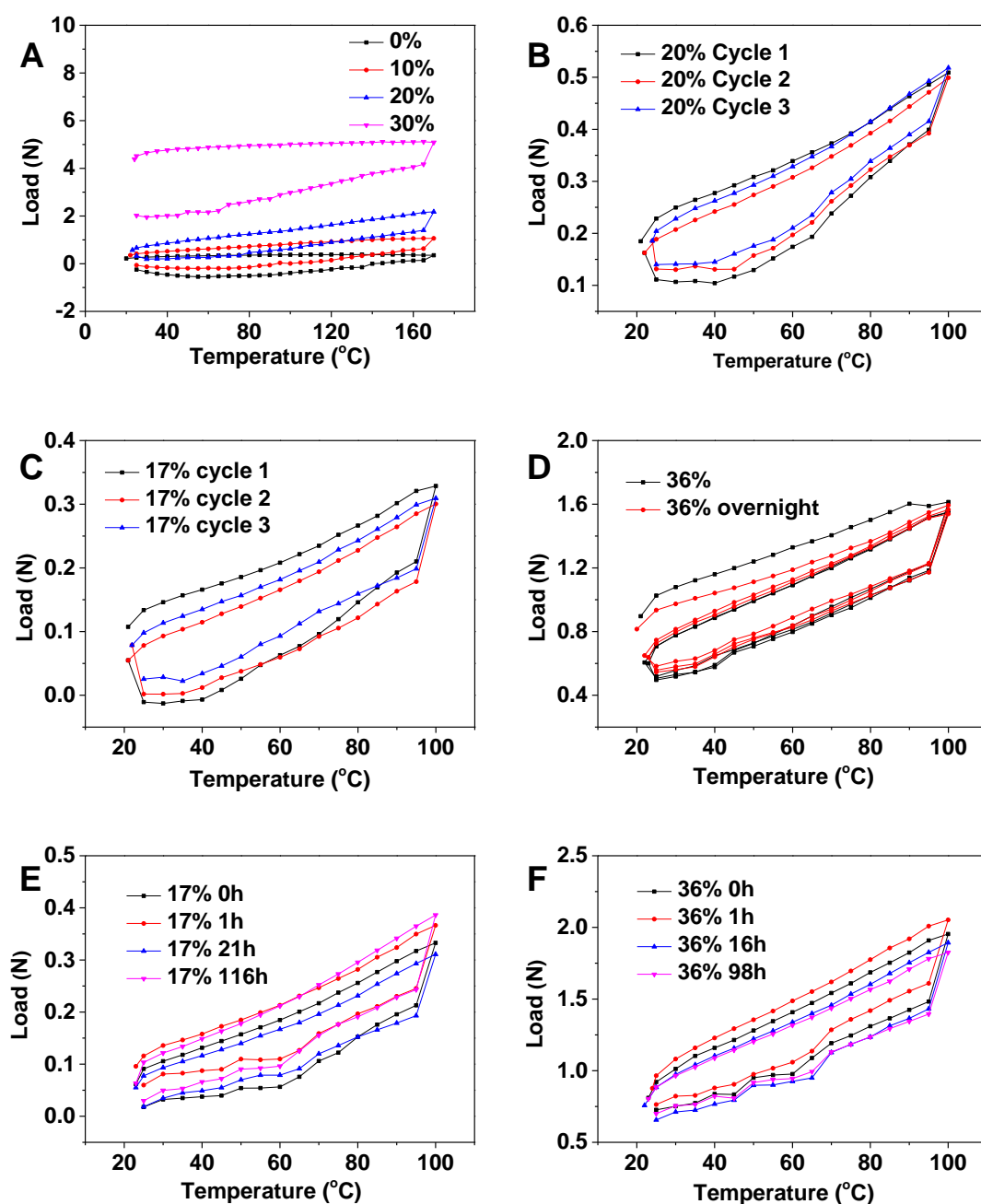
Figure 4. 15 Isometric behaviors of 6*100f PI/PDMS HCYAs. (A) Isometric test of PI/PDMS HCYA with different extension rate; (B) Cyclability of PI/PDMS HCYA with extension rate of 20% in isometric test; (C) Cyclability of PI/PDMS HCYA with extension rate of 17%; (D) Cyclability of 6*100f HCYA with extension rate of 36%; (E) Stability of 6*100f HCYA with extension rate of 17%; (F) Stability of 6*100f HCYA with extension rate of 36%.

The isometric tests of 6*100f PI/PDMS HCYAs were carried out for further investigating the effect of extension rate, cyclability and stability. As shown in Figure 4.15A, extension rate of HCYA has obvious influence on the increased load (difference between initial load and maximum load). The slope of load-temperature curve from 20 °C to 170 °C is highest when the extension rate is 20%, and the load increases nearly three times than that in initial state (from 0.57N to 2.18N). Low extension rate can lose load-enhancing function due to squeezing between coils, while high extension rate directly leads to a limit load for the sample which could overwhelm the radical expansive force of PDMS for contraction. Therefore, extension rate of 20% is the optimal condition to obtain highest enhanced load, thus it was then adopted for heat-setting cycles of PI/PDMS HCYA.
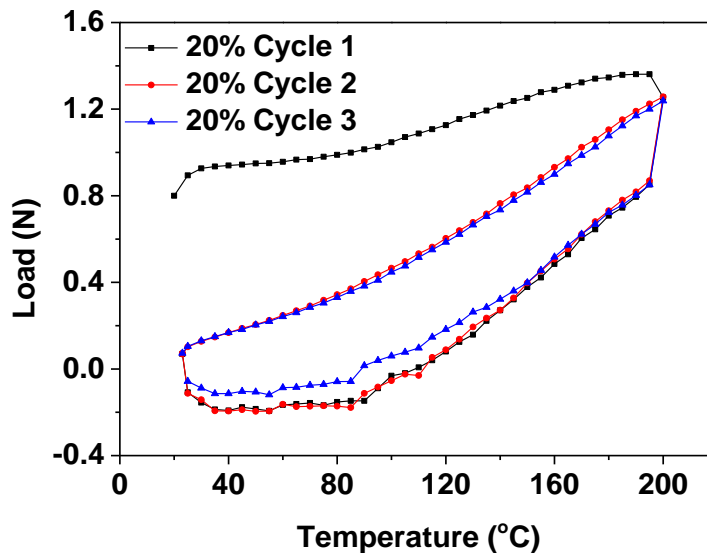


Figure 4. 16 Heat-setting cycles of PI/PDMS HCYA

For eliminating internal stress as much as possible, higher heat-setting temperature (200 °C) was employed (effective working temperature is usually less than 180 °C). Figure 4.16 indicates that the 20% extended 6*100f PI/PDMS actuator become stable after 1

cycle's heat treatment at 200 °C as the curves of cycle 2 and cycle 3 are almost overlapped.

For following isometric test at 20 °C~100 °C, the 20% extended 6*100f PI/PDMS actuator shows good cyclability in 3 cycles. Besides, the load nearly triples from 0.18N to 0.51N (i.e. reactive force is 0.33N) (Figure 4.15B), which is better than the isometric behavior of nylon monofilament HCYA (2.2 times load increase from 32 °C~123 °C)[8], indicating potential applications in controllable compressive products, e.g. functional compressive stocks/garments with adjustable pressure.

After heat-setting under extension rate of 20%, the sample can keep straight only when the extension was more than 17%, whereas too long extension of over 36% would lead to break during heating process. Therefore, these two limit values were chosen for assessing the cyclability and stability. It can be deducted from Figure 4.15C and 4.15D that the 6*100f PI/PDMS HCYAs with extension rates of both 17% and 36% can realize repeatable performance after 1 cycle as approximate cycling curves were exhibited in following cycles. After overnight, the actuator with 36% extension remains its performance as that of previous day, showing its good recovery property. The actuators can bear at least 10 cycles and the cyclability can be improved in terms of even PDMS coating, appropriate training and proper actuating load. Even PDMS coating facilitates the evenness of sample which is important for reversibility. Appropriate training can release the internal stress of sample, thus reducing the instability caused by internal

stress. Proper actuating load avoids the unexpected buckling and curling of sample as well as fatigue, thus keeping the normal operation of actuator.

For further understanding their stabilities, isometric tests were carried out with different time intervals. Figure 4.15E and Figure 4.15F show that the increased loads almost kept constant in approximately 100 hours for the both 6*100f HCYAs (about 0.26N for 17% extended sample and about 1.15N for 36% extended sample), thus illustrating their stable properties during a long period.

**4.3.5 Isothermal behavior**
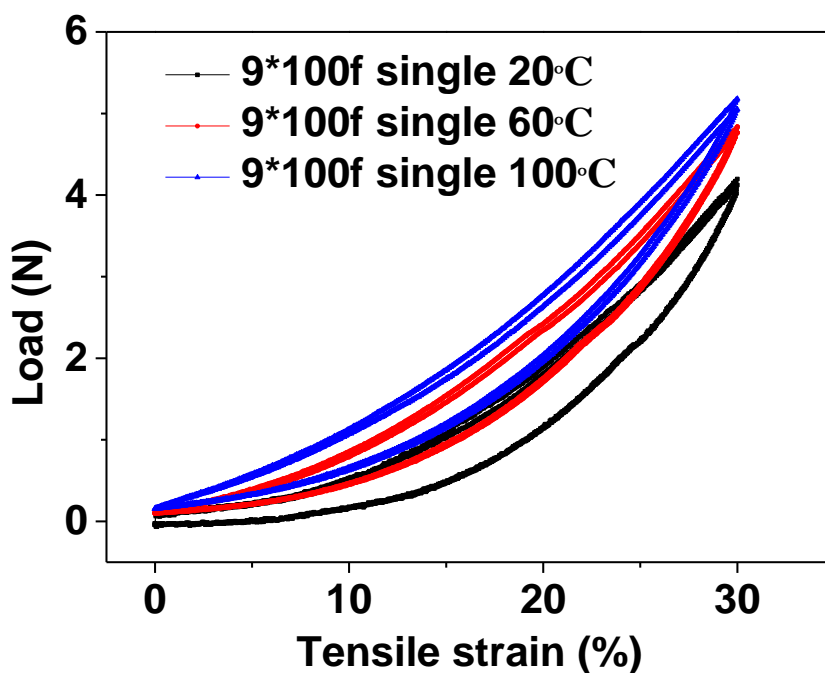


Figure 4. 17 Isothermal behavior of 9*100f single-level coil actuator at different temperature
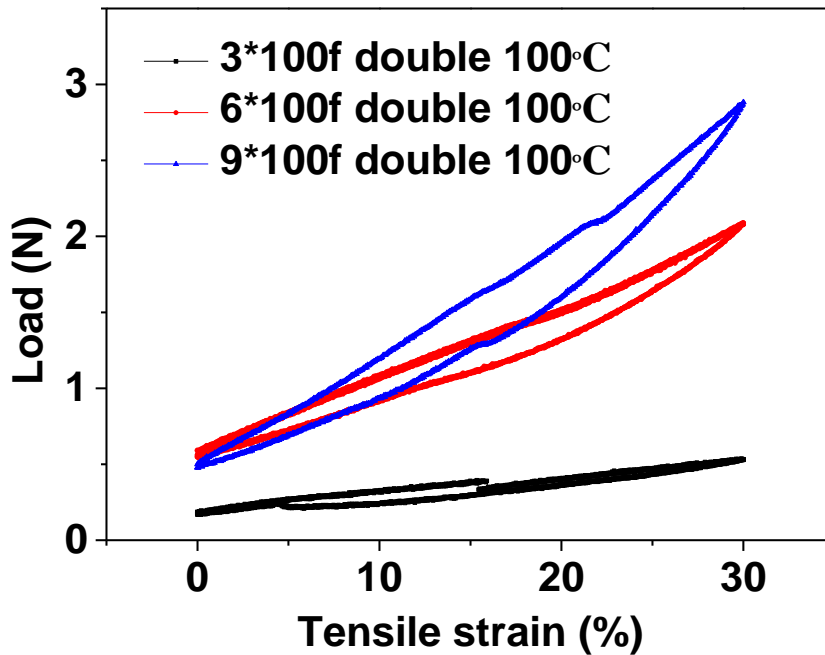
Figure 4. 18 Isothermal behavior of 3*100f, 6*100f and 9*100f double-level coil

actuator at 100 °C

Isothermal behavior reflects the performance of actuators under certain fixed

temperature. Figure 4.17 exhibits the isothermal behavior of 9*100f single-level

actuators at different temperature. It can be seen that the maximum load increases as

the temperature goes up due to the actuation under higher temperature. Besides, the

maximum load grows with more filament number (Figure 4.18) as actuators with more

filament number possess stronger tensile power.

Also, a comparison between 9*100f single-coil HCYA and 9*100f double-coil HCYA

at 100 °C reveals that single-level coil actuator needs stronger force to be stretched

than the double-level coil actuator. This can be explained by the level change in the

double-level coil actuator when stretching, as the transition from double-level to single-

level state can cause relatively more longitudinal change while require lower stretching

load.


The hysteresis of all the actuators above is not large, except 3*100f double-level coil

actuator (Figure 4.18), which is possibly caused by the unevenness of the surface.

Therefore, coating process is important for the performance of actuator, especially for

the double-level coil actuator.
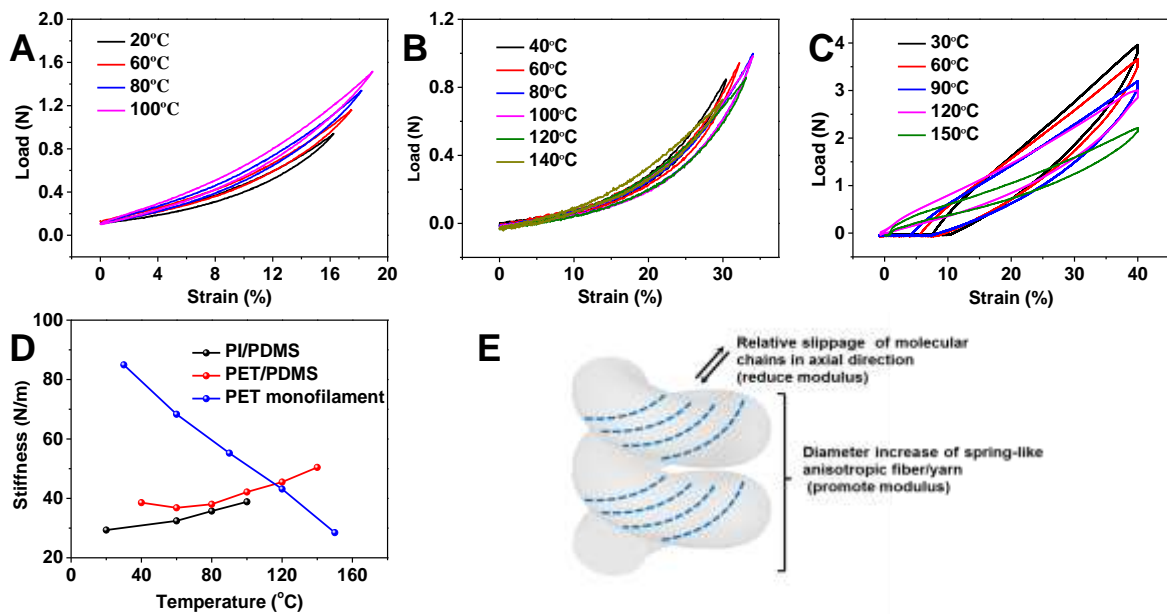


Figure 4. 19 Isothermal behavior of HCYAs. (A) Isothermal behavior of 6*100f

PI/PDMS HCYA (B) Isothermal behavior of PET/PDMS FCLA (C) Isothermal

behavior of PET monofilament FCLA (D) Stiffness vs temperature curve of different

FCLAs at strain of 15% (E) Schematic illustration of different isothermal behaviors of

FCLAs, including PI/PDMS HCYA, PET/PDMS FCLA and PET monofilament FCLA.

Isothermal behavior of 6*100f PI/PDMS HCYA was also investigated under 20 °C, 60 °C, 80 °C and 100 °C. It can be seen from Figure 4.19A and 4.19D that the slope of load-extension curve becomes higher with the increase of temperature from 20 °C to 100 °C, implying an unusual phenomenon that the tensile stiffness increases with the rise of temperature.

The common relationship between modulus and temperature can be formulated as follow:

$$\frac{E}{E_0} = [1 - a\left(\frac{T}{T_m}\right)]$$

where $E$ denotes the modulus of the material at temperature $T$ and $E_0$ is modulus at 0K. $T_m$ and $a$ represent melting temperature and proportional constant of specialized crystalline material ($a$ equals 0.5 for most specialized crystalline materials), respectively[9]. Therefore, the modulus should decrease with growing temperature. Figure 4.19C and 4.19D show an isothermal behavior of PET monofilament FCLA in accordance with this common rule. The slope of load-strain curve, as well as tensile modulus, goes down gradually with increasing temperature from 30 °C to 150 °C. This result is in accord with a nylon monofilament FCLA, which tensile modulus (i.e. slope of stress-strain curve) kept dropping when the temperature ascended from 25 °C to 122 °C[8].

The unusual isothermal behavior of PI/PDMS HCYA can be described as a balance

between diameter increase of spring-like anisotropic fiber (promote modulus) and molecular mobility increase in axial direction (reduce modulus) (Figure 4.19E). When the PI/PDMS HCYA worked under -50 °C~200 °C, which was far below the glass transition temperature ($T_g$) of PI (about 440 °C), the molecular mobility was hardly changed in axial direction, thus the tensile modulus of PI/PDMS composite yarn was reduced very little, whereas the diameter increase of spring-like anisotropic yarn can remarkably raise contractive force[1] and promote the modulus during the rise of temperature, as the thermal expansion of PDMS in radial direction far exceeded that of PI/PDMS composite yarn in axial direction. Apparently, the promoting effect was larger than the reducing effect in this balance system for PI/PDMS HCYA, thus the unusual elevation of tensile modulus under heating was expressed. Therefore, the unusual thermally-hardening property can be achieved by the reasonable composite coiled structure design rather than modifying the materials themselves. This unusual thermomechanical property has potential application in the field where high modulus is needed under high temperature, e.g. heat-resisting materials.

Contrarily, for PET and nylon monofilament FCLA, though their spring-like structure and anisotropic property promote extra contractive force/modulus when heating, the molecular mobility in axial direction raised greatly as the actuating temperature was higher than their $T_g$ ($T_g$ of PET is about 67 °C~81 °C and that of nylon 6 is 47 °C), thus the contractive force/modulus could be reduced by the relative slippage of molecular chains in axial direction. Finally, the tensile modulus of PET and nylon

monofilament FCLA decreased with rising temperature, as the reducing effect was in dominant position.

PET/PDMS FCLA has more complicate isothermal behavior. It can be seen from Figure 4.19B and 4.19D that the stiffness of PET/PDMS FCLA decreased when heated from 40 °C to 60 °C ($< T_g$ of PET) and increase when heated from 80 °C to 180 °C ($> T_g$ of PET). This was because the reducing effect (molecular mobility increase in axial direction) is a little higher than the promoting effect (diameter increase of the spring-like anisotropic PET/PDMS composite yarn) when the temperature approached to $T_g$ of PET while the situation was reversed when the temperature exceeded the $T_g$ of PET, the synergistic expansion of both PDMS and amorphous PET contributed to larger diameter increase which made the promoting effect dominate the tensile property.

## 4.4 Summary

After fabrication and optimization of PI/PDMS composite yarn, this Chapter focuses on the following fabrication of HCYAs and their characterization in terms of morphology and thermomechanical behaviors.

Firstly, the PI/PDMS HCYAs were fabricated by super-twisting process while the twisting curve and coil forming conditions were investigated. It is shown that twist number and load are the main factors that affect the structure of HCYAs. Proper parameters setting can prevent the HCYAs from either buckling or break.

Secondly, the morphology of HCYAs were characterized by electronic microscopy, the influencing factors of morphology include filament number, coil level, coil type and heat-setting temperature. Preferable choices are more filament number, single coil level and lower heat-setting temperature that facilitate evenness of the samples.

Finally, the thermomechanical properties of HCYAs were characterized in terms of isotonic, isometric and isothermal behaviors. In isotonic tests, the actuations are influenced by heat-setting temperature, filament number, coiled level, load, volume fraction and low temperature condition. Lower heat-setting temperature and more filament number facilitate higher volume fraction of PDMS matrix, thus better actuating performance. Double-level coil HCYAs and single-double-mixed-level coil HCYAs realize higher tensile actuation compared with the single-level coil HCYAs, owning to the level change during actuations. Proper loads prevent the squeeze of adjacent coil and fatigue of HCYAs, thus achieving higher actuations. PI/PDMS HCYAs could keep effective actuation under extremely cold condition.

In isometric tests, filament number, coil level and extension rate show most obvious influence on the actuation, i.e. increased load. More filament number can enhance the volume fraction of PDMS and further the effective actuation. Single-level coil HCYA exhibited better load increasing rate than that of double-level coil HCYA which lost the advantage because of coil level change. In the isotonic test, proper extension rate of

sample in isometric tests prevented the compact touch of coils and sample fatigue, thus facilitating higher actuation. Cyclability and stability were good in long period with the verification of time-delay experiments.

An unusual thermally-hardening thermomechanical property was found in the isothermal tests. The relevant mechanism was analyzed through comparing the thermomechanical property of PI/PDMS HCYA, PET/PDMS FCLA and PET monofilament FCLA, as well as their components. The balance between diameter increase of spring-like anisotropic fiber (promote modulus) and molecular mobility increase in axial direction (reduce modulus) was verified as the dominant factor for the unusual behavior. This discovery paves a road to adjust the thermomechanical property of materials by designing composite structure rather than changing the materials themselves.

## Reference

[1] C. S. Haines, M. D. Lima, N. Li, G. M. Spinks, J. Foroughi, J. D. W. Madden, S. H. Kim, S. Fang, M. J. d. Andrade, F. Göktepe, Ö. Göktepe, S. M. Mirvakili, S. Naficy, X. Lepró, J. Oh, M. E. Kozlov, S. J. Kim, X. Xu, B. J. Swedlove, G. G. Wallace, and R. H. Baughman, "Artificial muscles from fishing line and sewing thread," *Science,* vol. 343, no. 6173, pp. 868-872, 2014.

[2] J. E. Mark, *Polymer Data Handbook* (Poly(dimethylsiloxane)). Oxford University Press, 1999.

[3]     M. Kanik, S. Orguc, G. Varnavides, J. Kim, T. Benavides, D. Gonzalez, T. Akintilo, C. C. Tasan, A. P. Chandrakasan, Y. Fink, and P. Anikeeva, "Strain-programmable fiber-based artificial muscle," *Science,* vol. 365, no. 6449, pp. 145–150, 2019.

[4]     C. S. Haines, N. Li, G. M. Spinksb, A. E. Alieva, J. Dia, and R. H. Baughmana, "New twist on artificial muscles," *PNAS,* vol. 115, no. 11, pp. 11709–11716, Mar 13 2018.

[5]     C. Lamuta, S. Messelot, and S. Tawfick, "Theory of the tensile actuation of fiber reinforced coiled muscles," *Smart Materials and Structures,* vol. 27, no. 5, 2018.

[6]     Z. Peng, "Study on thermally activated coiled linear actuators made from polymer fibers," Master, Institute of Textiles and Clothing, The Hong Kong Polytechnic University, Hong Kong, 2018.

[7]     M. D. Lima, N. Li, M. Jung de Andrade, S. Fang, J. Oh, G. M. Spinks, M. E. Kozlov, C. S. Haines, D. Suh, J. Foroughi, S. J. Kim, Y. Chen, T. Ware, M. K. Shin, L. D. Machado, A. F. Fonseca, J. D. Madden, W. E. Voit, D. S. Galvao, and R. H. Baughman, "Electrically, chemically, and photonically powered torsional and tensile actuation of hybrid carbon nanotube yarn muscles," *Science,* vol. 338, no. 6109, pp. 928-32, Nov 16 2012.

[8]     A. Cherubini, G. Moretti, R. Vertechy, and M. Fontana, "Experimental characterization of thermally-activated artificial muscles based on coiled nylon fishing lines," *AIP Advances,* vol. 5, no. 6, p. 067158, 2015.

[9]     T. H. Courtney, *Mechanical Behavior of Materials*, Second ed. (Elastic

Behavior). Long Grove, Illinois: Waveland Press, Inc., 2005, p. 727.

# CHAPTER 5
# ELECTROTHERMALLY POWERED HELICAL COMPOSITE YARN ACTUATORS AND THEIR APPLICATIONS

## 5.1 Introduction

In Chapter 4, thermally powered PI/PDMS helical composite yarn actuators (HCYAs) are fabricated and characterized. These PI/PDMS HCYAs can be actuated by many heating resources, such as air heating, hydrothermal setup, joule-heating etc. Therein, the joule heating method is more feasible for civil and industrial use, compared with other heating sources. Therefore, this chapter presents electrothermally powered PI/Cu/PDMS HCYAs through copper-plating the PI yarn, PDMS coating, prior to a super-twisting process. Influencing factors in copper-plating process are investigated, while both morphology and electrothermal/electrothermomechanical behaviors were characterized for the plated yarns, PDMS-coated plated yarns and electrothermally powered HCYAs. Finally, robotic arm and actuating fabric are designed and fabricated as the practical application of PI/Cu/PDMS HCYA.

## 5.2 Experimental

### 5.2.1 Fabrication and characterization of electrothermally powered HCYAs

For fabricating PI/Cu/PDMS composite yarn, PI yarn was firstly copper-plated by two groups of solutions (A: NaOH, 12g/L; $CuSO_4 \cdot 5H_2O$, 13g/L; $KNaC_4H_4O_6 \cdot 4H_2O$, 29g/L. B: HCHO 9.5mL/L.)[1] after a series of pretreatments, including hydrophilic treatment (2.5mol/L KOH solution), sensitization (11.9 g/L $SnCl_2 \cdot 2H_2O$ and 40mL/L 37% HCl) and activation (0.25g/L $PdCl_2$ and 40mL/L 37% HCl)[2]. Then the two ends of copper-plated PI yarn were protected by two layers of PI film (thickness: 0.05mm) which were stuck together through 3M VHB Tape 4905 for avoiding the reduction of conductivity. Finally, PDMS coating was carried out by padding method as follows. PI/Cu yarns were dipped into PDMS/ethyl acetate solution (w:w=1:2), followed by getting through a padder, in which the gap between two rollers was controlled by a digital level. After dipping and padding once or several times, the PDMS-coated PI/Cu yarns were vulcanized at 80 ℃ for 3h prior to the completion of PI/Cu /PDMS composite yarns. Super-twisting process was adopted to fabricate PI/Cu/PDMS helical composite yarn actuator (HCYA) (Figure 5.1). Silver-plating process was also implemented for comparison with copper-plating process, i.e. treating the PI yarn with silver plating solution (A: $AgNO_3$, 10g/L; $NH_3 \cdot H_2O$ 25%, 80ml/L; B: HCHO 37~40wt%, 20g/L) for 1h at 30 ℃[3].

The morphology was characterized by electrical microscopy while the electrothermomechanical property was characterized by apparatuses composed of DC

power, multimeter, infrared camera and Instron tensile testing machine (Figure 5.2).
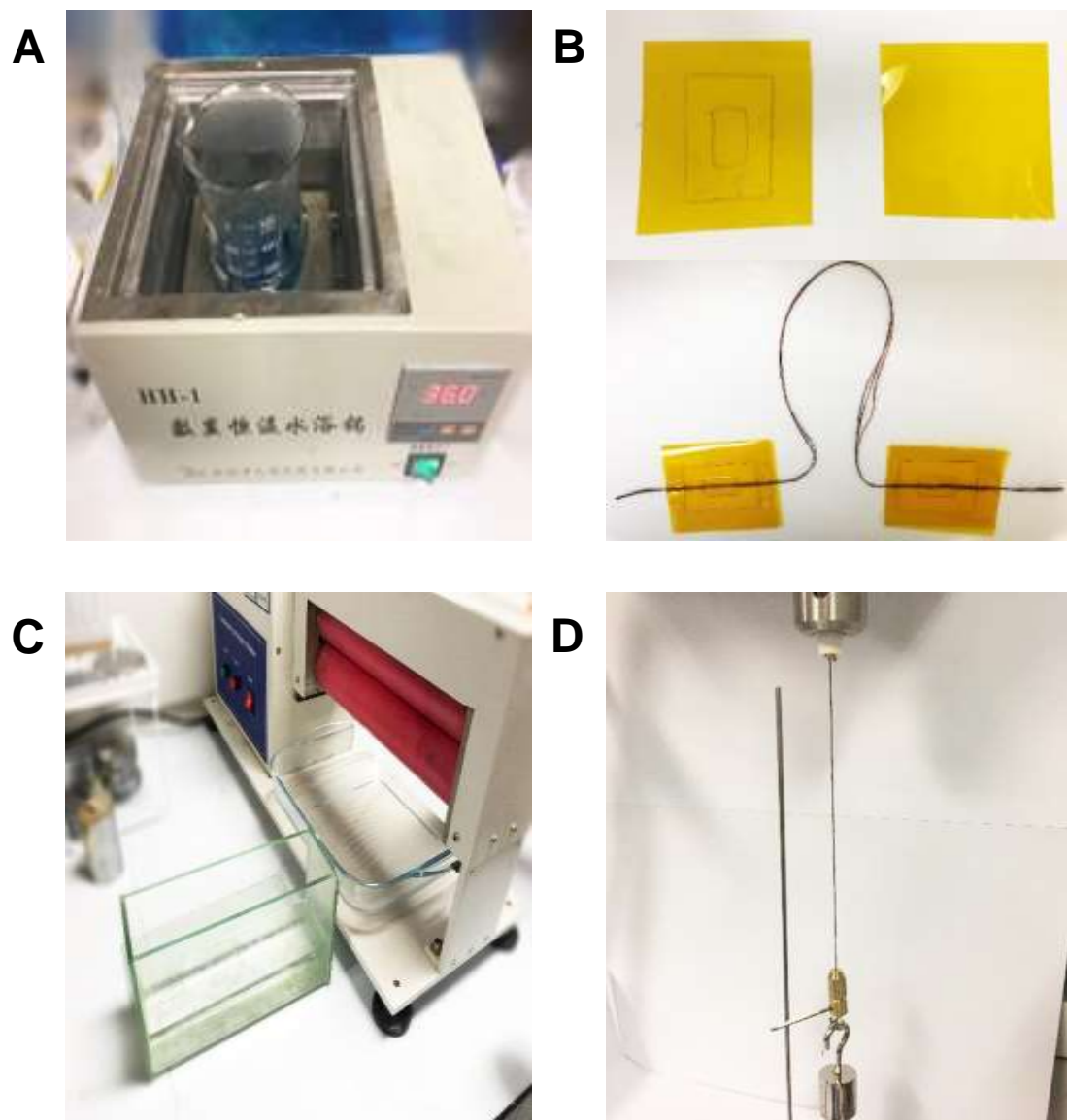


Figure 5. 1 Fabrication of PI/Cu/PDMS electrothermally powered actuators. (A) Copper-plating bath (B) End-protection of PI/Cu yarn (C) PDMS-coating process by a padder (D) Super-twisting PI/Cu/PDMS composite yarn into PI/Cu/PDMS HCYA
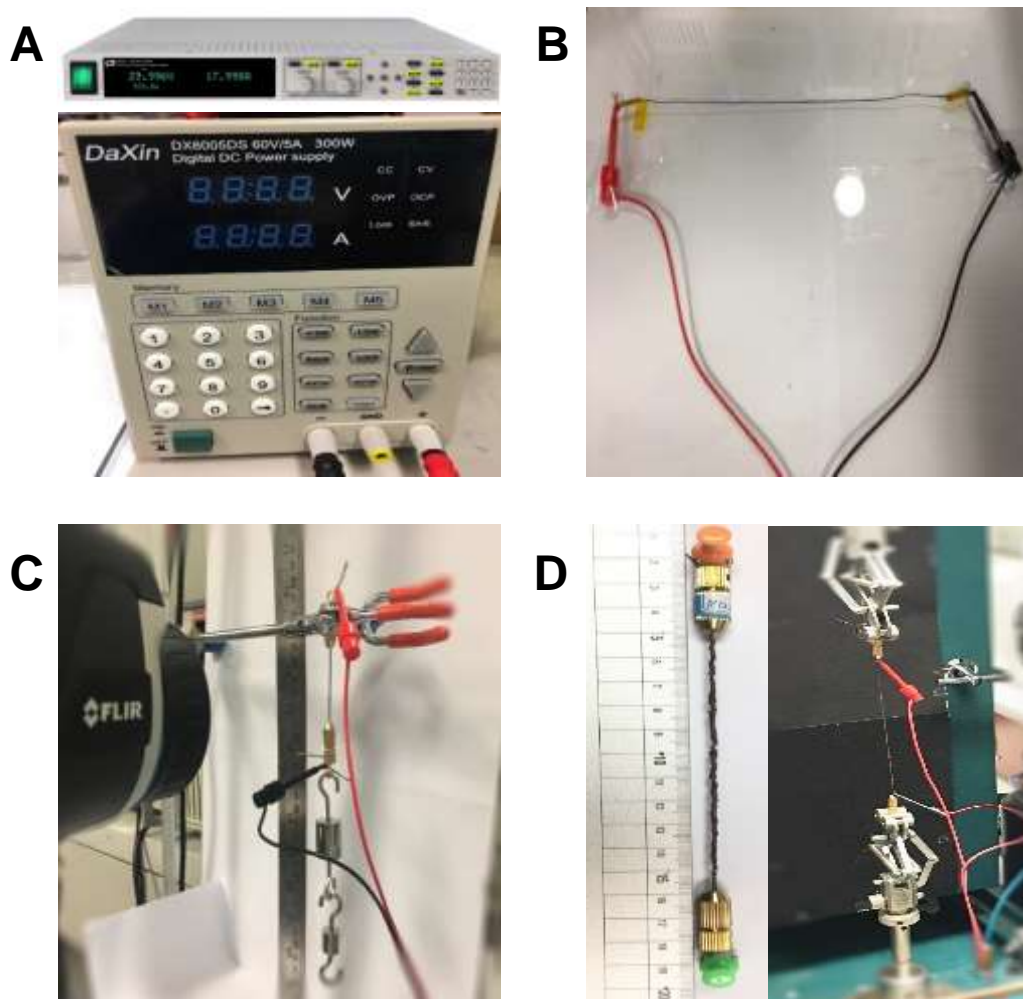
Figure 5. 2 Characterization of PI/Cu/PDMS electrothermally powered actuators. (A) DC electric power with constant power (up) and constant voltage/current (down) (B) Setup for testing resistance and joule-heating PI/Cu/PDMS composite yarn (C) Isotonic test of PI/Cu/PDMS HCYA. (D) Isometric test of PI/Cu/PDMS HCYA

## 5.2.2 Fabrication and characterization of robotic arm

The robotic arm was 3D printed by Polylactic acid (PLA) plastic with Makerbot Replicator 5th Gen 3D Printer. The robotic hand can be made either by 3D printing or cutting proper hand shape from a PI film (Figure 5.3). Spandex was used for stretching fingers back, while nylon monofilaments connected with 2-ply 3*100f PI/Cu/PDMS HCYA were used to offer tensile force for grabbing of the robotic hand. DC power

supply with constant power was used to joule-heat PI/Cu/PDMS HCYA while the resistant, current, power, temperature and tensile actuation were recorded by monitor of electric power, infrared camera and ruler.

Figure 5. 3 Structure of robotic arms. (A) Robotic arm with hand made by 3D printed
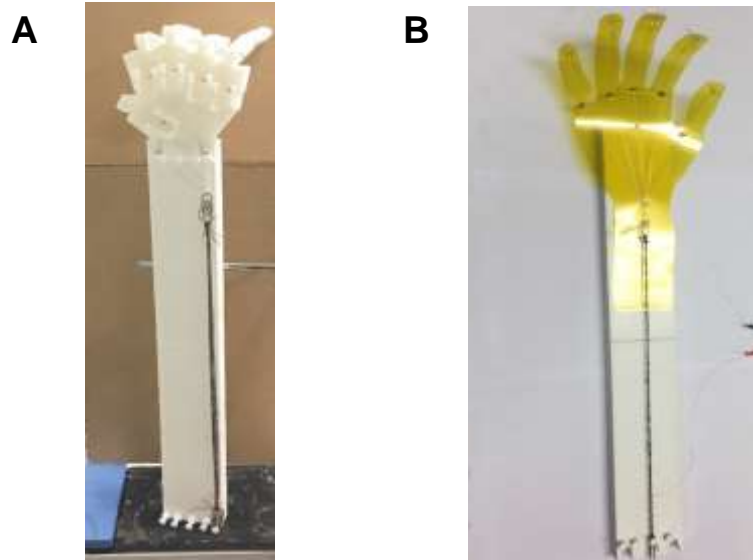


PLA (B) Robotic arm with hand made by PI film

## 5.2.3 Fabrication and characterization of actuating textiles

Actuating fabric was fabricated on a manual weaving machine (Figure 5.4A), applying the 2-ply 3*100f PI/Cu/PDMS HCYA as weft and texture PET yarn as warp (texture: 3 up 1 down, Figure 5.4B). Two groups of wefts made by spandex were weaved beside the 2-ply 3*100f PI/Cu/PDMS HCYA for protecting them from falling off. Iron wires were twined on the two ends of the fabric as electrodes. In isotonic test (Figure 5.4C), proper tensile load was imposed on the actuating fabric, prior to record the change of length, resistance and temperature when joule-heating with constant power. In isometric application (Figure 5.4D), the actuating fabric was tied around the leg for compression (curing varicose vein). Pressure sensor was put under the actuating fabric to record the change of pressure when joule-heating by power supply with constant power.
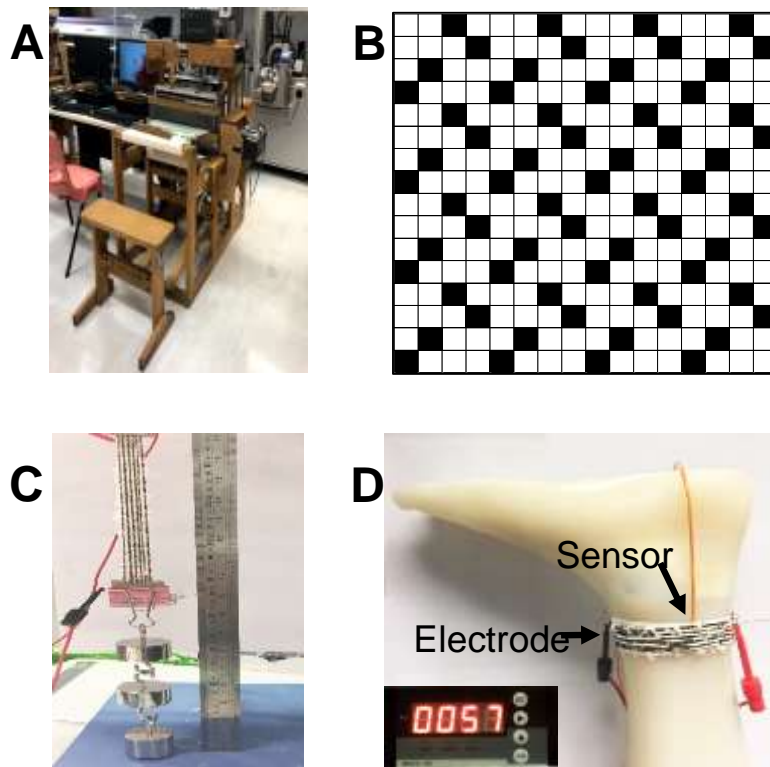
Figure 5. 4 Fabrication and Characterization of actuating textiles. (A) Handloom for weaving PI/Cu/PDMS composite yarns into actuating fabric (B) Weaving texture of actuating fabric (C) Isotonic test of actuating fabric (D) Isometric application of actuating fabric as a compressive band.

## 5.3 Results and discussions

### 5.3.1 Morphology of electrothermally powered HCYAs
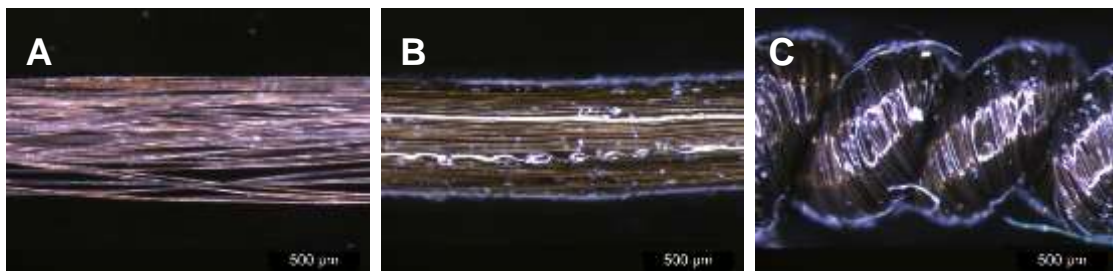


Figure 5. 5 Forming process of PI/Cu/PDMS electrothermally powered actuator. (A) 100f PI/Cu yarn (B) 3*100f PI/Cu/PDMS yarn (C) 3*100f PI/Cu/PDMS HCYA.

The morphologies of forming process of PI/Cu/PDMS electrothermally powered actuator are shown in Figure 5.5. The PI/Cu yarn becomes much looser than the raw yarn due to hydrogen bubble formed on fiber surface during the plating process (Figure 5.5A). The looser morphology obviously facilitated higher volume fraction of PDMS in composite yarn as more coating solution can penetrate the inside of the plated yarn. After PDMS coating, the prepared 3*100f PI/Cu/PDMS yarn achieves smooth surface (Figure 5.5B) and high volume fraction of PDMS (67.1%). After twisting the PI/Cu/PDMS composite yarn into spring-like structure (Figure 5.5C), the electrothermally powered HCYA is completed with regular and even surface, as well as a low resistance of about 1 ohm/cm.

## 5.3.2 Influence factors on resistance and strength of metal-plated yarns

Copper plating is an important process for fabricating electrothermally powered HCYAs, as a continuous and conductive metal layer could ensure effective joule heating to actuate HCYAs. Many factors can influent the copper plating effect, including hydrophilic pretreatment (plasma, alkali solution), plating time, filament number, moisture state, PDMS coating and end protection.

### 5.3.2.1 Effect of plasma on electroless Cu plating

Plasma can improve the surface hydrophilic property of the polymer and other materials[4, 5], thus can be used to promote the affinity of activated metal ion onto the surface of polyimide yarn, form more activated position for deposition of copper and further obtain effective and conductive layer. Table 5.1 presents the effect of plasma on copper plating of PI yarns of different filament number. It can be seen that longer plasma treating time facilitates lower resistance and higher conductivity. Besides, PI yarns with more filament number only get higher resistance and lower conductivity.

Therefore, it can be deducted that longer plasma treatment time can create more hydrophilic group for better copper plating, while more filament number impedes the penetration of plasma to inside of yarn, thus resulting in relatively low conductivity.

Table 5. 1 Effect of plasma on electroless Cu plating

| Filament No. | Plasma treatment time (min) | Plating time (min) | Resistance with tension (Ω/cm) | Resistance without tension (Ω/cm) |
|---|---|---|---|---|
| 6*100f | 5 | 30 | 1.8 | 1.8 |
| 6*100f | 10 | 30 | 1.1 | 1.1 |
| 6*100f | 15 | 30 | 0.36 | 0.36 |
| 9*100f | 8 | 15 | 7.5 | 37.5k |
| 9*100f | 8 | 30 | 7.5 | 20k |

Note: Air plasma is used to improve the hydrophilic property of PI yarn.

## 5.3.2.2 Effect of KOH solution on electroless Cu plating

KOH aqueous solution can react with polyimide and form hydrophilic carboxylic group[6], thus facilitate copper plating on the surface of PI yarn. Table 5.2 shows the effect of concentration, treating method and treating time on the PI yarn copper-plated for different time. 3*1*100f yarn means each 100f yarn was copper-plated prior to be combined for resistance test, while 3*100f yarn means three 100f yarns were combined and copper-plated simultaneously. It seems independent yarn treatment is not better than those of yarn combined, as independent 1*100f yarn only can absorb limited activating solution and 3*100f yarn can pick up more activating solution owning to more internal space. Appropriate higher concentration can improve treatment effect and

reduce the resistance, whereas too high concentration leads to the strength loss and break. The optimal treating parameter is 15min of treatment by concentration of 2.5mol/L to achieve low and stable resistance of 0.23Ω/cm. As a whole, KOH solution can improve the hydrophilic property of PI yarn better than air plasma in terms of evenness and appearance, due to treatment of full direction in the solution, even covering the core of the yarns.
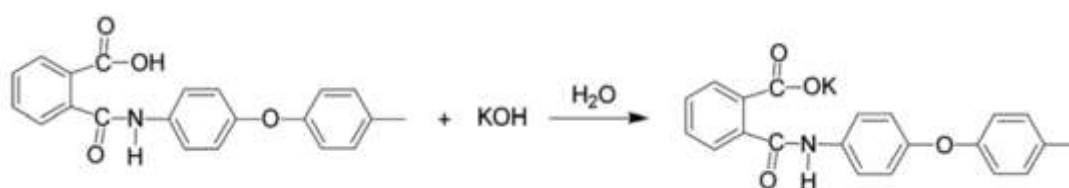


Figure 5. 6 Imide ring opening after treatment of KOH solution[6]

Table 5. 2 Effect of KOH solution on electroless Cu plating

| Filament No. | Concentration (mol/L) | treating time (min) | Plating time (min) | Resistance (Ω/cm) | Resistance after 24h (Ω/cm) |
|---|---|---|---|---|---|
| 3*1*100f | 1 | 15 | 30 | 1.02 | 1.16 |
| 3*100f | 1 | 15 | 30 | 0.70 | 0.77 |
| 3*100f | 1 | 15 | 60 | 0.29 | 0.50 |
| 3*100f | 1 | 30 | 30 | 0.68 | 0.75 |
| 3*100f | 2.5 | 15 | 60 | 0.23 | 0.23 |
| 3*100f | 5 | 15 | 30 | 2.42 | 3.01 |
| 3*100f | 5 | 30 | 30 | break | break |

### 5.3.2.3 Effect of plating time

The control of plating time is rather vital for achieving effective conductive layer. Appropriate parameter control can realize a balance between resistance and yarn strength, i.e. low resistance and sufficient strength should be obtained simultaneously. The relationship between resistance and plating time is shown in Figure 5.7. The resistance reduces sharply when the plating time prolongs from 20min to 30min, then slightly goes down with prolonged time. Considering the factor of consumption of time and energy, as well as strength loss of yarn, 45min~75min can be acceptable as shorter time leads to high resistance and unevenness, while longer time results in too much strength loss of the yarns.
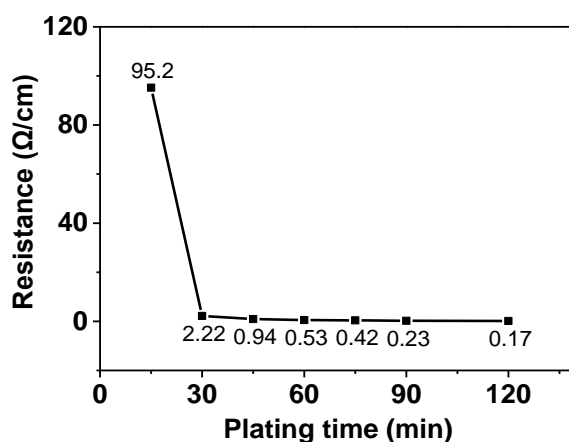


Figure 5. 7 Resistance change with plating time for 3*100f PI yarns pretreated by 2.5mol/L KOH solution for 15min

### 5.3.2.4 Effect of filament number and moisture state

During the copper plating process, it seems that effective surface area exposed to copper ion was closely related to the filament number, as more filament number means more core filament could not sufficiently absorb copper ion, thereby reducing the

127

conductivity of plating layer. It can be seen from Table 5.3 that 6*100f PI yarn obtains

a bit higher resistance than 3*100f PI yarn under the same condition.

Besides, the moisture state of PI yarn can also affect the plating effect. In Table 5.3,

"Wet" means the PI yarn was rinsed with DI water after each step of KOH pretreatment,

sensitization and activation, while "dry" means the PI yarn was dried after above rinse.

After drying PI yarn with hot air, the previous absorbed catalytic ions were removed

off with treating solution, thus the number of activated positions for metal deposition

decreased and the resistance increased.

Table 5. 3 Effect of filament number and moisture state on resistance

| Filament No. | Plating time (min) | Resistance ($\Omega$/cm) |
|--------------|--------------------|--------------------------|
| 3*100f | 60 | 0.23 |
| 6*100f | 60 | 0.27 |
| 3*100f (wet) | 30 | 2.8 |
| 3*100f (dry) | 30 | 6.3 |

Note: PI yarns were pretreated by 2.5mol/L KOH solution for 15min;

### 5.3.2.5 Effect of PDMS coating on resistance

As PDMS is an insulator material, PDMS coating process can reduce the conductivity

of copper-plated PI yarn to some extent. Table 5.4 shows the resistance change of four

PI/Cu yarn samples with and without tension, as well as before and after PDMS coating.

Tension can make individual plated yarns more compact to each other, thus creating

more continuous conductive layer of low resistance, which effect is more vivid for the

samples with higher resistance, i.e. sample with insufficient continuous conductivity. The variation of resistance is rather large after PDMS coating, as the thickness of coating layer was hard to control due to the variation of diameters of each PI/Cu yarn, i.e. uneven yarn surface. This process should be further improved through controlling the yarn state after the accomplishment of copper plating. If the surface of PI/Cu yarn is even enough, the evenness of coating layer can be effectively controlled, and variation of yarn resistance could be reduced, too.

Table 5. 4 Effect of PDMS coating on resistance

| 3*100f PI/Cu yarn | Resistance with tension (Ω/cm) | Resistance without tension (Ω/cm) | Resistance after PDMS coating (Ω/cm) |
|---|---|---|---|
| 1 | 1.15 | 1.69 | 4.91 |
| 2 | 0.60 | 1.02 | 1.92 |
| 3 | 0.40 | 0.40 | 5.43 |
| 4 | 0.50 | 0.50 | ∞ |

Note: Coating solution: PDMS/Ethyl acetate=1:2; Padding method

### 5.3.2.6 End protection of PI/Cu yarn

As the PDMS coating process has an obvious negative effect for the conductivity of plated PI yarn, end protection before PDMS coating was adopted for avoiding the resistance increase. Three end protection methods are listed in Table 5.5. If the conductive fabric was used for end protection, the PDMS coating solution could penetrate PI/Cu yarn for the gaps on the surface of fabric. For the second method, in

which PI/acrylic tape/PI sandwich structure and thermoplastic sealing glue were applied, the penetration of coating solution was avoided successfully, whereas the sealing glue was hard to be removed. Only when the sealing glue was substituted to PDMS, as method 3, the protecting effect was still good while almost all the protecting materials can be removed. Table 5.6 presents the resistance of PI/Cu yarn before and after end protection (method 3). It can be seen that end protection can successfully ensure stable resistance for PI/Cu yarns, compared with those without end protection.

Table 5. 5 End protection of PI/Cu yarn
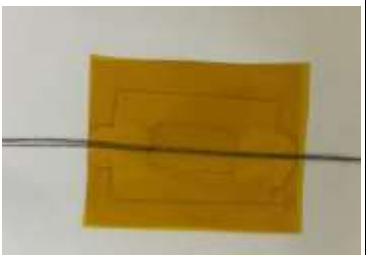
| Protecting method | | Inner protecting layer | Outer protecting layer | Sealing glue | Effect |
|---|---|---|---|---|---|
| 1 |  | Conductive fabric | PP tape | None | Penetration of coating solution |
| 2 |  | Acrylic tape | PI film | Thermo plastic glue | Hard to remove the glue |
| 3 |  | Acrylic tape | PI film | PDMS | Almost all the protecting materials can be removed |

Table 5. 6 Resistance after end protection

| PI/Cu yarn | Plating time (min) | Initial resistance ($\Omega$/cm) | Resistance after end protection ($\Omega$/cm) |
|---|---|---|---|
| 3*100f | 60 | 0.22 | 0.28 |
| 6*100f | 60 | 0.31 | 0.31 |
| 3*100f | 30 | 1.54 | 2.24 |

### 5.3.3 Joule heating tests for conductive yarns

### 5.3.3.1 Joule heating of metal-plated yarns without PDMS coating

For testing the conductive and joule heating effect of metal-plated yarns, a DC power was applied to electrify the metal-plated yarns until the maximum temperature of joule-heated sample had been reached (samples can be fused when exceeding maximum temperature). Table 5.7 shows the joule heating test results of PI/Cu yarn and PI/Ag yarn. For the PI/Cu yarn, it was difficult to obtain high temperature as the heat exchange between yarn and air was so fast due to large specific surface area of the yarn. The samples with high resistance, e.g. $> 3\Omega$/cm, cannot afford high current ($> 0.2A$), owning to fusing caused by local overheating. Compared with PI/Cu yarn, PI/Ag yarn made by sputtering can reach higher temperature due to more filament number, lower resistance and more continuous conductive layer. PI/Ag yarn was prepared by silver plating process rather than coating silver nanowire as the affinity of silver nanowire on polyimide fiber was low due to lack of chemical bond and sufficient contact on fiber surface for forming Van der Waal's force.

Table 5. 7 Joule heating of PI/Cu yarns

| Sample | Length (cm) | Maximum Voltage (V) | Maximum Current (A) | Resistance (Ω/cm) | Maximum Temperature (℃) |
|---|---|---|---|---|---|
| 3*100f PI/Cu | 27.5 | 6 | 0.550 | 0.4 | 28.7 |
| 3*100f PI/Cu | 35 | 9.0 | 0.2 | 1.3 | 28.8 |
| 3*100f PI/Cu | 34 | 18 | 0.150 | 3.5 | 30.8 |
| 3*100f PI/Cu | 30 | 10 | 0.060 | 5.5 | 30.0 |
| 9*100f PI/Cu | 5.4 | 1.25 | 1.3 | 0.2 | 42 |
| 6*100f PI/Ag | 30 | 20 | 0.169 | 3.9 | 64.0 |
| 9*100f PI/Ag | 5 | 2 | 3.5 | 0.1 | 170 |

## 5.3.3.2 Joule heating of PDMS-coated plated yarn

Table 5. 8 Joule heating of PDMS-coated plated yarn

| Sample | Length (cm) | Maximum Voltage (V) | Maximum Current (A) | Resistance (Ω/cm) | Maximum Temperature (℃) |
|---|---|---|---|---|---|
| 3*100f PI/Cu/PDMS yarn | 27 | 7.8 | 0.55 | 0.5 | 80 |
| | 19 | 15.9 | 0.45 | 1.9 | 140 |
| | 30 | 36 | 0.18 | 6.7 | 150 |

After PDMS coating process, as shown in Table 5.8, the prepared PI/Cu/PDMS yarn can achieve higher maximum temperature compared with the uncoated PI/Cu yarn, owing to smaller specific surface area. Higher resistance facilitates obtaining higher maximum temperature for the PI/Cu/PDMS yarn. These results are opposite to that of metal plated yarns without PDMS coating, as higher resistance means thicker PDMS coating which helps to resist heating damage to the yarns.

### 5.3.4 Isotonic behavior of electrothermally powered HCYAs

To apply electrothermally powered HCYAs as artificial muscle or size-adjustable textiles, the investigation in their isotonic behaviors is essential. The isotonic test results of 3*100f and 6*100f PI/Cu/PDMS HCYAs are compared in Table 5.9. The volume fractions of these HCYAs are about 70%. For 3*100f PI/Cu/PDMS HCYA, a tensile actuation of -4.2% can be achieved with a low power, voltage and temperature of 0.6W, 3.87V and 63.1 ℃, respectively. This actuation effect is fit for wearable device which require relatively low temperature (20~60 ℃). When the power and temperature are increased to 1.27W and 118 ℃, the tensile actuation of 3*100f PI/Cu/PDMS HCYA can reach -7.4%. This higher temperature of over 100 ℃ requires the actuator should be applied in robotic or industrial field rather than wearable device. The 6*100f PI/Cu/PDMS HCYA can bear higher temperature (162 ℃) and thus achieve larger tensile actuation (-17.9%) due to larger radial size than the 3*100f PI/Cu/PDMS HCYA, while even much higher tensile actuation of -25.4% can be obtained for the partially coiled HCYA, as the coil-level change from partially coiled state to fully coiled state generated significant length change. The obvious disadvantages existed in the long actuation time of about 30s, which lead to low energy conversion efficiency. This may be caused by the low thermal conductivity of PDMS (0.15~0.2)[7], which impedes the prompt heat conduction from copper layer to the whole HCYA.

Table 5. 9 Isotonic tests of 3*100f and 6*100f PI/Cu/PDMS HCYA

| PI/Cu/PDMS HCYA | 3*100f | 3*100f | 6*100f | 6*100f partially coiled |
|---|---|---|---|---|
| Volume fraction of PDMS/% | 73.5 | 73.5 | 70.1 | 70.1 |
| Load/g | 78.7 | 78.7 | 100 | 100 |
| length L/mm | 94 | 68 | 62 | 55 |
| Length change $\Delta$ L/mm | 3.95 | 5 | 11.1 | 14 |
| Power P/W | 0.60 | 1.27 | 1.90 | 2.06 |
| Voltage U/V | 3.87 | 6.35 | 5.95 | 10.30 |
| Current I/A | 0.15 | 0.20 | 0.32 | 0.20 |
| Tensile actuation/% | -4.2 | -7.4 | -17.9 | -25.4 |
| Max. Actuation time/s | 30 | 30 | 33 | 30 |
| Max. Average Temperature/℃ | 63.1 | 118 | 162 | 149 |
| Energy conversion efficiency $\eta = mg \Delta L / UIt$ | 0.0175% | 0.0101% | 0.0173% | 0.0222% |
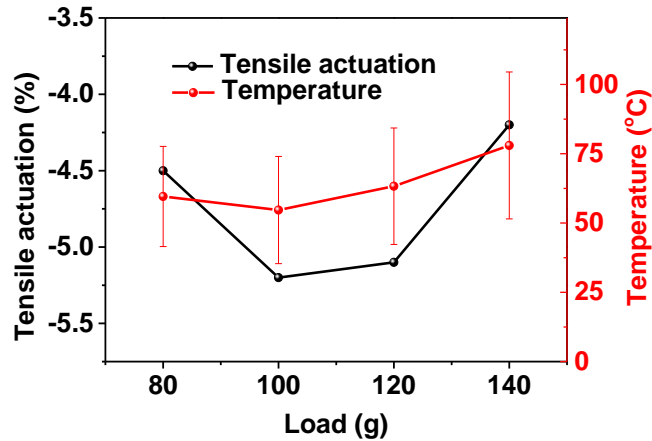
Figure 5. 8 Variation of tensile actuation and temperature of 2-ply 3*100f PI/Cu/PDMS

HCYA with different actuating load under electric power of 1.5W

The conductivity of PI/Cu/PDMS composite yarn is not constant for each segment,

owing to the uneven copper plating layer through the whole yarn. Therefore, 2-ply

3*100f PI/Cu/PDMS HCYA was fabricated for improving the constant conductivity

and evenness of the copper plating layer, then the HCYA with different actuating load

was joule-heated by electric power of 1.5W. Figure 5.8 shows that the tensile actuation

of PI/Cu/PDMS HCYA increases to -5.2% when actuating load raises from 80g to 100g,

then drops down with heavier actuating load. The reason exists in a balance between

touch of the adjacent coils (caused by light load) and fatigue of the HCYA (caused by

heavy load). Under the optimal load of 100g, the temperature is about 60 ℃, which is

an acceptable temperature for wearable materials, denoting its potential application in

wearable functional device, e.g. exoskeleton muscle, deformable textile etc.

## 5.3.5 Isometric behavior of electrothermally powered HCYA
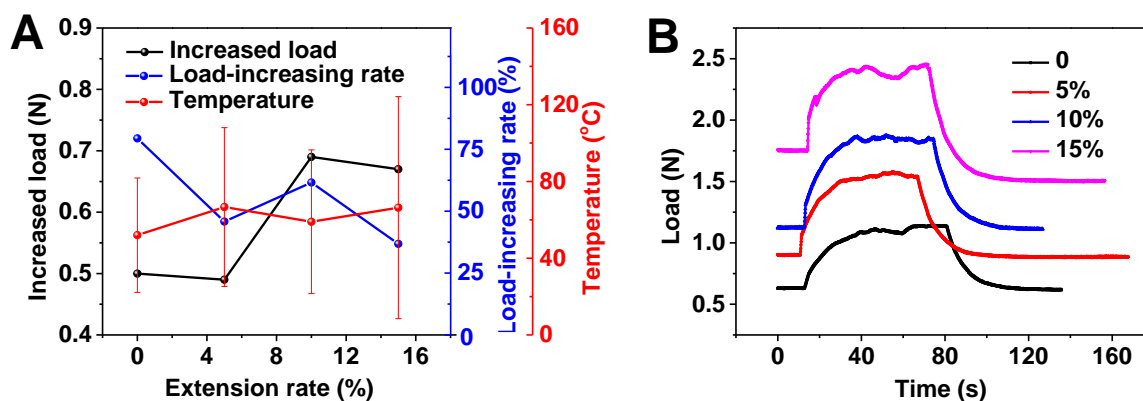


Figure 5. 9 Isometric test of 2-ply PI/Cu/PDMS 3*100f HCYA. (A) Effect of extension rate on increased load and load increasing rate under electric power of 1.5W (B) Increased load-time curve of 2-ply PI/Cu/PDMS 3*100f HCYA with different extension rate.

Isometric tests of 2-ply 3*100f PI/Cu/PDMS HCYA with different extension rate were implemented with electric power of 1.5W (Figure 5.9A). The increased load is low and load increasing rate is high when the extension rate is 0, whereas the increased load becomes high and load increasing rate becomes low when the extension rate is 15%. The optimal extension rate is 10% which can achieve high increased load (from 1.12N to 1.81N) and load increasing rate (61.6%) simultaneously. Low extension leads to mutual squeezes of adjacent coils and the consequent low increased load, whereas the low initial pre-load (denominator during calculation) contributes to the high load increasing rate.

The load reaches peak within 20 seconds when heating with 1.5W and goes back to the

initial load within about 20s after switching off the power for the extension rate of 5%, 10% and 15% while it takes longer time for the HCYA with extension rate of 0 to peak due to compact coils (Figure 5.9B). The significant load enhancement and satisfactory response time facilitate its pressurizing or strengthening application in many fields, e.g. controllable compressive stockings or massage bandages.

Actually, thermally or electrothermally powered actuators based on polymer yarn have relatively slow response time compared with the pneumatic actuator, electromagnetic actuator etc, owing to their instinct property, especially for the thermal conductivity. For shortening the response time and improving the performance, the transmission of thermal energy should be promoted, e.g. adopting fiber/yarn with smaller diameter, larger specific area and higher thermal conductivity (e.g. polyethylene fiber with high crystallinity and degree of orientation)[8, 9].

### 5.3.6 Performance of robotic arm
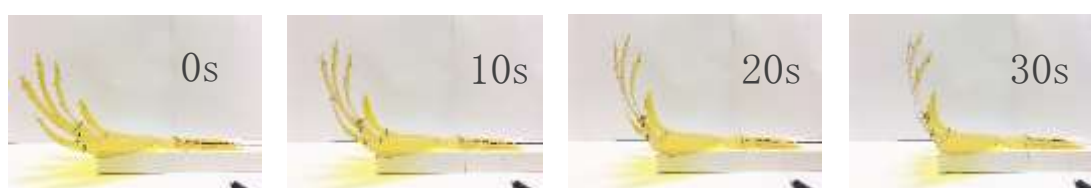


Figure 5. 10 Robotic arm actuated by 2-ply 3*100f PI/Cu/PDMS HCYA.

For demonstrating the application, a robotic arm was 3D printed by polylactic acid (PLA). Spandex was used for stretching fingers back, while nylon monofilaments

connected with 2-ply 3*100f PI/Cu/PDMS HCYA were used to offer tensile force for grabbing of the robotic hand. A tensile actuation of -2.9% was obtained with electric power of 4.8W, thus effectively realized the grabbing action (Figure 5.10). Moreover, the robotic arm can also be actuated in an extremely cold environment of -50 ℃, achieving same tensile actuation with doubled electric power (9.2W). The cold resistance of each component, including PI, copper and PDMS, had contributed to the stable performance of the actuator.

**5.3.7 Performance of actuating fabric**
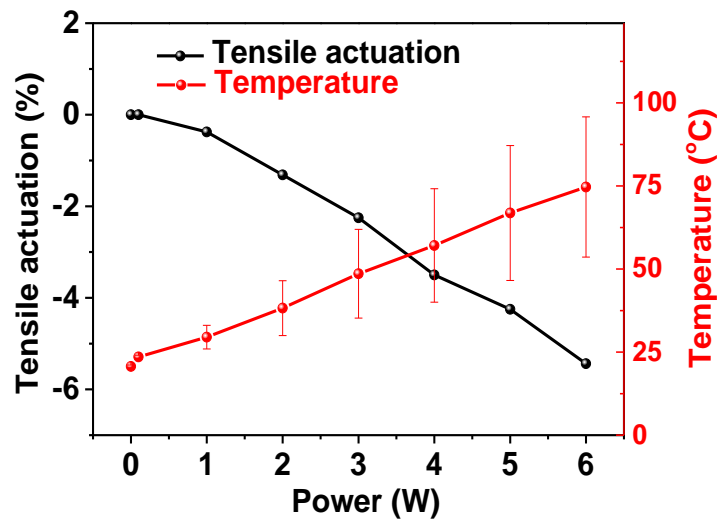


Figure 5. 11 Tensile actuation and temperature under different electric power in the isotonic test of PI/Cu/PDMS actuating fabric.

An actuating fabric was fabricated by a handloom machine, applying the 2-ply 3*100f PI/Cu/PDMS HCYA as weft and cotton yarn as warp (texture: 3 up 1 down). Braided PET textured yarns and the PI/Cu/PDMS HCYAs were weaved alternatively for ensuring effective contraction. Iron wires were twined on the two ends of the fabric as

electrodes. A DC power was employed to joule heat the actuating fabric, which was loaded with 600g. Both temperature and tensile actuation increased with the rise of electric power. A tensile actuation of about -5.4% is achieved as the temperature reached 75 ℃ approximately (Figure 5.11). This result is comparative with that of 2-ply 3*100f PI/Cu/PDMS HCYA which has not been weaved into fabric (-5.2% under 54.7 ℃).
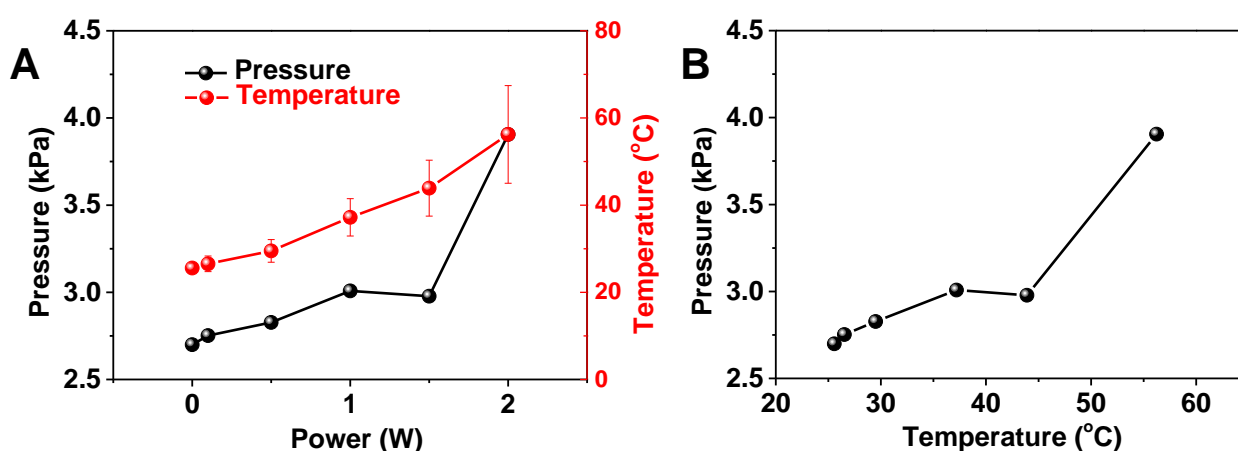


Figure 5. 12 PI/Cu/PDMS actuating fabric applied as compressive bandage. (A) Change of pressure and temperature with increasing electric power (B) Change of pressure with increasing temperature

The actuating fabric was also demonstrated as a compressive bandage for the adjunctive therapy of varicose vein, which could offer pressure when joule-heating. Figure 5.12 shows that both temperature and the pressure exerted by the compressive bandage increased with higher electric power. As the pressure sensor could be affected by the temperature, a baseline was established through recording the value change caused only by temperature. The actual pressure increases by about 44.7% (2.699 kPa ~ 3.905 kPa)

when the temperature rises from 25.6 ℃ to 56.2 ℃, illustrating an effective compression exerted by the actuating fabric. The pressure of actuating fabric can also be adjusted by many parameters benefiting from the composite yarn structure design, including volume fraction of PDMS, filament number, fabric density etc.

## 5.4 Summary

Electrothermally powered PI/Cu/PDMS HCYAs were fabricated through copper-plating the PI yarn, PDMS coating, prior to a super-twisting process. For the copper-plating process, influencing factors on resistance and strength of metal-plated yarns were investigated, including hydrophilic pretreatment (plasma, alkali solution), plating time, filament number, moisture state, PDMS coating and end protection. The typical process parameters are: KOH solution treatment (2.5mol/L, 15min), plating 45~75min, 3*100f, wet state during whole process, end protection by PI film/acrylic tape/PI film structure glued with PDMS.

Besides, both morphology and electrothermal/electrothermomechanical properties were characterized for the plated yarns, PDMS-coated plated yarns and electrothermally powered HCYAs. The unevenness of metal-plated layer on the surface of yarn led to uneven PDMS coating and variation of resistance from part to part, which needed to be further improved in term of evenness control during plating process. PI/Cu/PDMS yarns could reach higher maximum temperature than PI/Cu yarns when joule heated, because PDMS prevented the partial overheating of yarn. 3*100f, 6*100f

and 2-ply 3*100f PI/Cu/PDMS HCYAs could realize effective tensile actuation in isotonic tests, wherein 2-ply 3*100f PI/Cu/PDMS HCYA can achieve tensile actuation of -5.2% when joule heated to about 60 ℃ (suitable for wearable device use), while 6*100f PI/Cu/PDMS HCYAs can achieve tensile actuations of 17.9% (single level coil) and 25.4% (partially coil) under temperature of over 100 ℃ (suitable for industrial applications). In isometric test, the actuating load of 2-ply 3*100f PI/Cu/PDMS HCYA increased 61.6% within 20s when the temperature was elevated to about 60 ℃, showing its potential actuating function in compressive textiles.

Finally, robotic arm and actuating fabric were designed and fabricated for demonstrating the practical application of PI/Cu/PDMS HCYA. The robotic arm can be actuated (tensile actuation of -2.9%) under both ambient condition and extremely cold condition (-50 ℃), realizing effective grabbing of robotic hand. Actuating fabric could be applied as integrated artificial muscle (isotonic application) and compressive bandage (isometric application). As artificial muscle, the actuating fabric realized a tensile actuation of -5.2% under 54.7 ℃, while as a compressive bandage, 44.7% of load increasing rate was achieved when the temperature rose from 25.4 ℃ to 56.2 ℃.

## References

[1]    R. Guo, Y. Yu, Z. Xie, X. Liu, X. Zhou, Y. Gao, Z. Liu, F. Zhou, Y. Yang, and Z. Zheng, "Matrix‐assisted catalytic printing for the fabrication of multiscale, flexible, foldable, and stretchable metal conductors," *Advanced Materials,* vol.

25, no. 24, pp. 3343-3350, 2013.

[2] L. Gao, J. U. Surjadi, K. Cao, H. Zhang, P. Li, S. Xu, C. Jiang, J. Song, D. Sun, and Y. Lu, "Flexible fiber-shaped supercapacitor based on nickel–cobalt double hydroxide and pen ink electrodes on metallized carbon fiber," *ACS applied materials & interfaces,* vol. 9, no. 6, pp. 5409-5418, 2017.

[3] C. Xu, R. Zhou, H. Chen, X. Hou, G. Liu, and Y. Liu, "Silver-coated glass fibers prepared by a simple electroless plating technique," *Journal of Materials Science: Materials in Electronics,* vol. 25, no. 10, pp. 4638-4642, 2014.

[4] A. E. Wiącek, K. Terpiłowski, M. Jurak, and M. Worzakowska, "Low-temperature air plasma modification of chitosan-coated PEEK biomaterials," *Polymer Testing,* vol. 50, pp. 325-334, 2016.

[5] G. A. Arolkar, M. J. Salgo, V. Kelkar-Mane, and R. R. Deshmukh, "The study of air-plasma treatment on corn starch/poly(ε-caprolactone) films," *Polymer Degradation and Stability,* vol. 120, pp. 262-272, 2015.

[6] S.-J. Park, E.-J. Lee, and S.-H. Kwon, "Influence of surface treatment of polyimide film on adhesion enhancement between polyimide and metal films," *Bulletin of the Korean Chemical Society,* vol. 28, no. 2, pp. 188-192, 2007.

[7] A. C. M. Kuo, *Polymer Data Handbook*. Oxford University Press, Inc. , 1999

[8] B. Zhu, J. Liu, T. Wang, M. Han, S. Valloppilly, S. Xu, and X. Wang, "Novel Polyethylene Fibers of Very High Thermal Conductivity Enabled by Amorphous Restructuring," *ACS Omega,* vol. 2, no. 7, pp. 3931-3944, Jul 31 2017.

[9]    S. Shen, A. Henry, J. Tong, R. Zheng, and G. Chen, "Polyethylene nanofibres with very high thermal conductivities," *Nat Nanotechnol,* vol. 5, no. 4, pp. 251-5, Apr 2010.

# CHAPTER 6
# CONCLUSIONS AND
# RECOMMENDATIONS FOR FUTURE
# WORK

## 6.1 Conclusions

As inflexible structure design and limited range of working temperature restricts the

performance and application of many actuators, this project has fabricated and

systematically studied helical composite yarn actuators (HCYAs) for achieving

simple/flexible/portable/programmable structure, high strain, high stress, high energy

density, long-time cyclability, wide working temperature range, low hysteresis, low

operating voltage, low cost and simple fabricating process. The whole study consists of

materials selection, fabrication and characterization of composite yarns, fabrication and

characterization of thermally powered HCYAs, as well as fabrication, characterization

and application of electrothermally powered HCYAs.


Primary conclusions that contribute to this scientific field are listed as follows:

1. Polyimide (PI) and polydimethylsiloxane (PDMS) were selected from many fiber

   substrates and polymer matrixes to fabricate the composite yarn, owning to their

   temperature resistance, ductile physical property under extremely cold condition,

   different thermal expansion coefficient and biological safety. Influencing factors of

   fabricating composite yarn have been investigated for optimizing the morphology

144

and property, e.g. concentration of coating solution, volume fraction of PDMS, coating method, filament number etc. The typical processing parameters that can obtain even appearance and good anisotropy were: padding method, PDMS: ethyl acetate=1:2, padding 3 times, 6*100 filaments, without tension, 260μm coating gap, pre-squeeze and non-vacuum vulcanization.

2. Thermally powered PI/PDMS HCYAs based on composite structure were fabricated by super-twisting process, while the morphology of HCYAs have been optimized in terms of filament number, coil level, coil type and heat-setting temperature. The thermomechanical properties of HCYAs were then characterized in terms of isotonic, isometric and isothermal behaviors. In isotonic tests, the actuations were influenced by heat-setting temperature, filament number, coiled level, load, volume fraction and low temperature condition. Lower heat-setting temperature and more filament number facilitated higher volume fraction of PDMS matrix, thus further better actuating performance. Double-level coil HCYAs and single-double-mixed-level coil HCYAs can realize higher tensile actuation compared with the single-level coil HCYAs, owning to the level change during actuations. The typical 6*100f PI/PDMS HCYA can achieve tensile actuation of 20.7% under 1.2MPa among a wide temperature range from -50 °C to 160 °C, while high linearity ($R^2$=0.99927), competitive specific work (158.9J/kg, 4 times of natural muscle) and low hysteresis (6.7%) can be realized. Relatively high tensile actuation (-4.0%) among temperature range from 20 °C to 60 °C shows its

advantage in application as wearable device (Table 6.1).

Table 6. 1 Tensile actuating performances of fiber-based coil actuators made by different materials.

| Actuators made by different materials | Temperature range (°C) | Tensile actuation from 20 °C to 60 °C (%) | Total Tensile actuation (%) | Stress (MPa) |
|---|---|---|---|---|
| Nylon 6,6/Ag yarn | 16~240 | -1.6 | -24.5 | >17 |
| CF/PDMS | 24~138 | -1.4 | -7.2 | 60 |
| PET | 30~180 | -1.0 | -15.6 | 6.2 |
| CNT/wax | 26~200 | -0.9 | -2.7 | 6.8 |
| Nylon 6,6 monofilament | 20~240 | -1.6 | -33.2 | 83.6 |
| COCe/PE | 20~30 | - | -11.8 | 0.07 |
| PI/PDMS | -50~160 | -4.0 | -20.7 | 1.2 |

3. In isometric tests, filament number, coil level and extension rate showed most obvious influence on the actuation, i.e. increase of load. More filament number enhanced the volume fraction of PDMS and further the effective actuation. Proper extension rate of sample in isometric tests prevented the compact touch of coils and sample fatigue, thus facilitating higher actuation. Typical 20% extended 6*100f PI/PDMS HCYA can realize nearly tripled stress (from 0.38MPa to 1.07MPa) when temperature changed from 20 °C to 100 °C, with good cyclability and stability in

long period time-delay experiments.

4.  An unusual thermally-hardening thermomechanical property was found in the isothermal tests. The relevant mechanism was analyzed through comparing the physical property of PI/PDMS HCYA, PET/PDMS HCYA and PET monofilament HCYA, as well as their components. The balance between diameter increase of spring-like anisotropic fiber (promote modulus) and molecular mobility increase in axial direction (reduce modulus) was verified as the dominant factor for the unusual behavior. This discovery paves a road to adjust the thermomechanical property of materials by designing composite structure rather than changing the materials themselves.

5.  Electrothermally powered HCYAs were fabricated by adding conductive layer, thus the actuators can be triggered conveniently by joule heating. The process of electroless deposition of copper and silver has been optimized in terms of solution concentration, processing temperature, processing time, filament number, yarn state. The resistance, strength and evenness are used to assess the qualities of conductive composite yarns and electrothermally powered HCYAs. Functional devices adopting electrothermally powered HCYAs were fabricated for practical applications, such as electrothermally powered artificial muscle for robotic arm, actuating strips and actuating fabrics for smart compressive stockings. The combination methods and weaving/braiding processes are developed through

optimizing relevant parameters, including tension, filament/yarn number, end-fixing method, texture design.

## 6.2 Limitation and recommendations for future work

Despite this project has achieved many valuable and significant contribution for the field of actuators, several limitations still could not be neglected. Main limitations are listed as follows:

1. PDMS coating of constant thickness through the whole yarn has not been realized, as the middle part of yarn is usually slightly thicker than other segments after hanging vulcanization due to gravity.

2. Easy untwisting of the HCYAs as the heat-setting temperature is lower than the glass transition temperature of PI.

3. Slow cooling speed caused by low thermal conductivity of PDMS ($0.16\ \mathrm{W\cdot m^{-1}\cdot K^{-1}}$) and relatively large diameter of composite yarn.

4. Low energy conversion efficiency from thermal energy to mechanical energy.

5. Relatively long response time to achieve maximum actuation.

6. Large change of temperature for achieving high tensile actuation.

7. Super-twisting process is not a continuous process.

8. Unevenness of copper plating layer as the copper plating solution cannot be stirred during the process (prevent the twining of yarn).

9. Parameters of actuating fabric have not been optimized for better pressure control and application as compressive bandage/stocking, such as diameter of composite

yarn, density of textile, texture and integrating method with stockings.

For improving and pushing this project forward, several recommendations for future work are listed as follows:

1.  Constant-speed coating machine, together with vulcanizing apparatus, could be adopted for realizing even matrix polymer coating on the substrate yarn.

2.  The substrate yarn with high $T_g$ (e.g. PI yarn) could be super-twisted and heat-set in advance, prior to coat matrix polymer, so that the fabricated FCYAs will not untwist easily.

3.  For solving the slow cooling problem, matrix polymer of high thermal conductivity (e.g. polyethylene fibers after amorphous restructuring) could be applied for improving the cooling efficiency and response time. Besides, preparing composite yarns and FCYAs of smaller diameter can be another way to promote cooling.

4.  For improving the energy conversion efficiency, shortening the response time, miniaturizing the device and increasing heat transfer efficiency, smart coating materials could be explored, which possess high thermal resistance when electrified and high thermal conductivity when electrification is removed, thus realizing high energy conversion efficiency and low energy loss simultaneously.

5.  For achieving higher tensile actuation with less change of temperature, the spring index of HCYAs could be adjusted to higher value, e.g. heat-setting the PI yarn twined around a mandrel at temperature of above $T_g$, prior to PDMS coating process. Alternatively, exploring an electrochemical actuating methodology for

avoiding the generation of heat as much as possible.

6. For producing HCYAs in industrial scale, continuous process is essential. This requires the development of new machines that can super-twisting composite yarn continuously, as well as rolling up and collection simultaneously.

7. Improvement of the evenness of copper plating layer. Fixing setup should be developed for substrate yarn in the copper plating solution, so that the solution can be stirred to become more homogeneous. Besides, the state of yarn should be investigated during plating process, for avoiding uneven penetration of solution caused by compact arrangement of yarn and saving processing space at the same time.

8. Optimization and integration the actuating fabric. The parameters of fabrication actuating fabric, including diameter of composite yarn, density of textile, texture, resistance, actuating voltage etc, should be optimized to achieve appropriate pressure/temperature for certain compressive wearable devices. Besides, as the actuating fabric is woven fabric whereas compressive stocking is knitted fabric, integrating method between them should be explored in terms of sewing, sticking, attaching etc.